

Stony Brook University



OFFICIAL COPY

The official electronic file of this thesis or dissertation is maintained by the University Libraries on behalf of The Graduate School at Stony Brook University.

© All Rights Reserved by Author.

**Development of novel gene therapy vectors via metabolic labeling and chemoselective
modification of adenovirus capsid**

A Dissertation Presented

by

Partha Sarathi Banerjee

to

The Graduate School

in Partial Fulfillment of the

Requirements

for the Degree of

Doctor of Philosophy

in

Chemistry

Stony Brook University

August 2011

Stony Brook University

The Graduate School

Partha Sarathi Banerjee

We, the dissertation committee for the above candidate for the
Doctor of Philosophy degree, hereby recommend
acceptance of this dissertation.

Isaac S. Carrico – Dissertation Advisor

Assistant Professor of Chemistry

Nicole S. Sampson – Chairperson of Defense

Professor of Chemistry

Kathlyn A. Parker – Third member of Defense

Professor of Chemistry

Markus A. Seeliger – Outside member of Defense

Assistant Professor of Pharmacological Sciences

This dissertation is accepted by the Graduate School

Lawrence Martin
Dean of the Graduate School

Abstract of the Dissertation

**Development of novel gene therapy vectors via metabolic labeling and chemoselective
modification of adenovirus capsid**

by

Partha Sarathi Banerjee

Doctor of Philosophy

in

Chemistry

Stony Brook University

2011

Surface modification of adenovirus vectors can improve tissue selective targeting, attenuate immunogenicity, and enable imaging of particle bio-distribution; thus significantly improving therapeutic potential. Currently, surface engineering is constrained by a combination of factors including impact on viral fitness, limited access to functionality, or incomplete control over the site of modification. In order to alleviate this complication, our aim was to “prelabel” the virions metabolically with unnatural residues, which allow access to highly chemoselective reactions. Due to their small size, permissibility within biosynthetic pathways, and access to reactions with high specificity, azides and alkynes act as excellent bio-orthogonal handles.

We utilized two different classes of unnatural residues, sugars and amino acids to metabolically label the capsid of adenovirus particles. The introduced substrates contain a chemical handle that can subsequently be modified with suitable probes. *O*-N-acetylglucosamine (GlcNAc) surrogate Ac₄GalNAz affords specific incorporation of azide tag on the virus capsid while amino acids Azidohomoalanine and Homopropargylglycine make available a high concentration of modifiable substrates on the viral surface. Copper catalyzed bio-conjugation and Staudinger ligation reactions were used to decorate the particles with small molecules, peptides and even proteins. Incorporation of the unnatural substrates and the subsequent chemistries were characterized by western, fluorescence, enzymatic and mass spectrometry based assays. Analysis of viral infectivity by plaque forming assays showed substrate incorporations to have minimal effects on viral fitness.

Targeted gene delivery capacities of the modified particles were analyzed by chemically attaching a targeting ligand on the virion surface. For this we initially utilized a folic acid based targeting system. After chemoselective attachment of this ligand onto virions containing GFP or Luciferase transgenes, the virions were targeted to breast cancer cell line, where we observed 20-fold higher levels of transgene expression compared to non-targeted particles. We also produced a new dual functional virus that contains 2 different bio-orthogonal tags and utilizing this system to probe applications into chemo and gene therapy based combination effects on tumor cell viability.

Dedicated to my parents and jethumoni

Table of Contents

List of Figures	x
List of Schemes	xiii
List of Tables	xiv
List of Abbreviations	xv
Acknowledgments	xviii

Chapter 1

Introduction

1.1. Engineering Biomolecules	2
1.2. Oncolytic Virotherapy	11
1.3. Adenovirus based vectors	16
1.4. Specific Aims	23

Chapter 2

Specific labeling of adenovirus capsid with an unnatural azido sugar

2.1. Introduction	28
2.2. Results	33
2.2.1. Synthesis of per- <i>O</i> -acetylated GlcNAz and GalNAz	33

2.2.2. Production of <i>O</i> -GlcNAz labeled adenovirus	34
2.2.3. Chemical modification and characterization of <i>O</i> -GlcNAz labeled Ad5	35
2.2.4. Targeting of <i>O</i> -GlcNAz labeled virions	42
2.2.4.1. Synthesis of alkyne-PEG-folate	43
2.2.4.2. Targeting of murine breast cancer cells	44
2.3. Discussion	47
2.4. Summary	48

Chapter 3

Metabolic incorporation of an unnatural amino acid onto adenovirus capsid

3.1. Introduction	51
3.2. Results	55
3.2.1. Synthesis of Azidohomoalanine (Aha)	55
3.2.2. Production and characterization of Aha labeled ad5 particles	56
3.2.3. Chemical modification of Aha labeled virus	62
3.2.4. Assessment of viral fitness	64
3.2.5. Quantification of chemical labeling of Aha-enabled hAd5	69
3.2.6. Targeting of Aha enabled virions	73
3.2.7. Dye labeled Ad5 for cell imaging	77
3.3. Discussion	78
3.4. Summary	85

Chapter 4

Introduction of labeling specificity within unnatural amino acid enabled adenovirus

4.1. Introduction	87
4.2. Results	91
4.3. Summary	93

Chapter 5

Dual surface modification of adenovirus particles

5.1. Introduction	96
5.2. Results	100
5.2.1. Synthesis of homopropargylglycine (HPG)	100
5.2.2. Production and characterization of Ad5 particle labeled with Ac ₄ GalNAz and HPG	101
5.2.3. Toxicity and targeting of chemically armed dual modified adenovirus	106
5.3. Discussion	110
5.4. Summary	112

Chapter 6

6.1. Future Directions	114
------------------------	-----

Chapter 7

Experimental methods

7.1. Synthetic methods	118
7.2. Adenovirus production using unnatural substrates	130
7.3. Chemical modification and characterization of substrate labeled virions	133
7.4. Targeting, imaging, cytotoxicity	141
7.5. Cloning	144
References and notes	146
Appendix	178

List of Figures

Figure		Page
Chapter 1		
1-1.	Bio-orthogonal chemical reporter system	5
1-2.	Use of residue specific incorporation of amino acid analogs	7
1-3.	Azides incorporated into glycoconjugates using glycan biosynthesis	9
1-4.	Phases of gene therapy clinical trials	12
1-5.	Indications addressed by gene therapy clinical trials	13
1-6.	An adenovirus structure	15
1-7.	Early events in adenoviral infection	19
1-8.	Viral surface modification	21
Chapter 2		
2-1.	GlcNAc and GalNAc salvage pathways	29
2-2.	<i>O</i> -GlcNAz labeling sites on adenovirus fiber	31
2-3.	Reactions of azide enabled virions	32
2-4.	Qualitative analysis of azido sugar incorporation into the fiber protein	36
2-5.	Hexosaminidase treatment of fiber protein	37
2-6.	Azide enabled adenoviral fitness	39
2-7.	Determination of labeling of azido sugar enabled virus	40
2-8.	Fluorescence imaging of 4T1 cells infected with retargeted Ad5	45
2-9.	Quantification of gene transduction within 4T1 cells	46

Chapter 3

3-1.	Cartoon of Aha incorporation onto Ad5 particles	52
3-2.	Production of adenoviral type 5 proteins hours after infection	54
3-3.	Mass spectrometry characterization of Aha labeled adenovirus particles	58
3-4.	Chemical labeling of Aha incorporated into adenovirus particles	61
3-5.	Particle count of virus produced in the presence of Aha	63
3-6.	Determination of adenoviral protein production during labeling with Aha	64
3-7.	Shelf life and thermo-stability of Aha labeled adenovirus	66
3-8.	Increasing concentrations of Aha on Ad5 particles	67
3-9.	Effect of chemical labeling on adenovirus infectivity	69
3-10.	Determination of labeling of Aha enabled virus	71
3-11.	Fluorescent imaging of Aha labeled Ad5 targeting towards 4T1 cells	74
3-12.	Quantification of infection towards 4T1 cells	75
3-13.	Con-focal imaging of cells infected with TAMRA labeled Ad5 particles	78
3-14.	Azide incorporation pattern of Aha labeling at different times	80
3-15.	Concentration dependent “click” labeling of Aha enabled virus	83

Chapter 4

4-1.	Structure adenovirus type 5 fiber	88
4-2.	Cloning approach taken to generate virus fiber mutants	90
4-3.	Vector map of pTG3602 showing restriction sites for fiber	92
4-4.	DNA agarose gel showing production of fiber shuttle plasmid pBADfib5	93

Chapter 5

5-1.	Dual modified adenovirus particles chemically modified	98
5-2.	Chemoselective modification of GalNAz and HPG labeled adenovirus	102
5-3.	Determination of labeling of HPG enabled virus	103
5-4.	Dual modified viral fitness analysis	105
5-5.	MTT assay to determine cytotoxicity of TRAIL-Ad5	108
5-6.	Targeting analysis of SB-T-1214 and folate modified AdLuc	110

Chapter 7

7-1.	HPLC purification of alkyne-PEG-folate	125
7-2.	HPLC purification of folate-PEG	129
7-3.	HPLC purification of folate-PEG-phosphine	129

List of Schemes

Scheme	Page
Chapter 2	
2-1. Synthesis of per acetylated <i>N</i> -azidoacetylgalactosamine	34
2-2. Synthesis of Alk-PEG-Folate	43
Chapter 3	
3-1. Synthesis of L-azidohomoalanine	56
Chapter 5	
5-1. Synthesis of homopropargylglycine	100
5.2. Structures of az-SBT1214 and phosphine-folate	106
Chapter 7	
7.1. Synthesis of per acetylated <i>N</i> -azidoacetylgalactosamine	118
7.2. Synthesis of L-azidohomoalanine	121
7.3. Synthesis of Alk-PEG-Folate	124
7.4. Synthesis of homopropargylglycine	126

List of Tables

Table		Page
Chapter 2		
2-1.	Concentration of dye observed on viral fiber	41
Chapter 3		
3-1.	List of the peptides on Aha labeled adenovirus particles	59
5-2.	Number of Aha residues incorporated in Ad5 particles	72
Chapter 5		
5-3.	Number of HPG residues incorporated in Ad5	106

List of Abbreviations

Ad	Adenovirus
Ad5	Adenovirus type 5
Ad2	Adenovirus type 2
Aha	Azidohomoalanine
BBN	Borabicyclo nonane
BCA	Bicinchoninic acid
BCS	Bovine calf serum
BONCAT	Bio-orthogonal non-canonical amino acid tagging
CAR	Coxsackie adenovirus receptor
CMV	Cytomegalovirus
CRAd	Conditionally replicative adenovirus
CuAAC	Copper assisted azide-alkyne cycloaddition
DCC	N,N'-Dicyclohexylcarbodiimide
DMSO	Dimethylsulphoxide
DNA	Deoxyribonucleic acid
DIGE	Difference gel electrophoresis
EDTA	Ethylene diamino tetra acetic acid
EGFR	Epidermal growth factor receptor
EM	Electron microscope
FDA	Food and drug administration

FRET	Förster resonance energy transfer
GFP	Green fluorescent protein
GalNAc	<i>N</i> -acetylgalactosamine
GalNAz	<i>N</i> -azidoacetylgalactosamine
GlcNAc	<i>N</i> -acetylglucosamine
GlcNAz	<i>N</i> -azidoacetylgalactosamine
HEK	Human embryonic kidney
HPG	Homopropargylglycine
HOBt	Hydroxybenzotriazole
HVR	Hyper variable region
iTRAQ	Isobaric tag for relative and absolute quantitation
LSM	Laser scanning microscope
MBP	Maltose binding protein
Met	Methionine
MOI	Multiplicity of infection
MMP	Matrix metalloproteinase
MTT	3-(4,5-Dimethylthiazol-2-yl)-2,5-diphenyltetrazolium bromide
NHS	<i>N</i> -hydroxy succinamide
OD	Optical density
PDB	Protein data bank
PEG	Poly ethylene glycol
PFP	Pentafluoro phosphine
PTM	Post translational modification

RNA	Ribonucleic acid
SBT	Stony Brook Taxoid
SCID	Severe combined immunodeficiency
SDS-PAGE	Sodium dodecyl sulphate polyacrylamide gel electrophoresis
TAMRA	Tetramethylrhodamine
TEA	Triethylamine
TFA	Trifluoroacetic acid
TLC	Thin layer chromatography
TMZ	Temozolomide
TRAIL	Tumor necrosis factor- α related apoptosis inducing ligand
UDP	Uridine diphosphate

Acknowledgments

In the fall of 2006 when I was travelling half the globe to arrive at Stony Brook for my PhD, a Caltech graduate made his journey across America – all the way from sunny California, to start his own research lab here. Little did I know that within a few months I would be working with him to produce “designer virions”. Isaac, thank you for the new directions of science to which you have opened my doors and which I never knew existed. I shall always remember your guidance, your support, your passion and your expectations. None of what has been described in the next few pages would ever be possible without you.

I want to acknowledge the guidance and support of Prof Patrick Hearing and Philomena Ostapchuk in our research. I am also grateful to Prof Orlando Schärer and Prof Nicole Sampson for their guidance and support during my time at Stony Brook. I would also like to thank Toni Koller in the proteomics facility, Dr. Guo-Hui Tian at the microscopy facility, Bela Ruzsicska at ICBDD.

The other member of my research group Lakshmi, Yoon and Yanjie, thank you guys for all your help and support and I hope you will forgive my obsessive rants. I shall always cherish the sheer agony and ecstasy of research that I have experienced in the lab working with you. To the members of the Boon lab - Bernadette, Zhou, Dhruv, Tanaya, Niu and everybody else – you really made working in lab and my PhD experience extraordinary!

To my friend Debasish – I’m blessed to find a friend in you here who stuck with me for these five years. Get ready I’m coming over to visit you in Cali!!!!

To all my other friends in the fifth, sixth and the seventh floors – my sincere thanks.

I would like to thank my parents for their tremendous love and support and their constant encouragement towards my education, I am forever grateful to them.

Finally to my best friend and wife, thank you for believing in me when I wouldn't, for walking with me when I needed and for everything else.

Chapter 1

Introduction

1.1. Engineering Biomolecules

1.2. Oncolytic Virotherapy

1.3. Adenovirus based vectors

1.4. Specific Aims

1.1. Engineering biomolecules

Through the process of evolution, a set of molecules, amino acids, sugars, bases, lipids *etc.* have developed different families of bio-polymers that generate the natural basis of cellular life. These molecules represent a small subset of the available chemical space. Yet by their capabilities of self organization they have achieved astounding feats of complex activities and structures, selective catalyses to specific molecular assemblies. Despite their accessibility to an array of functions, there remain reactions and structures that these bio-molecules are unable to access and such limitations provide opportunity to the chemical biologist to study and understand their structures, activities or environment and also to modify them for different clinical applications.

Synthetic and bio-chemical techniques developed to engineer bio-molecules, specifically proteins, have had a myriad of applications. Starting from studying their structure and function to using them as therapeutics, every aspect of protein biology has benefited from such new developments. Site directed mutagenesis has been used by enzymologists for a long time to understand protein activity.(77) Developments of His-6 and MBP tags have assisted in protein purification by affinity chromatography.(36, 57) N-terminal or lysine residue modifications have assisted in protein quantitation and identification with commercially available iTRAQ or DIGE reagents.(67, 164) Cystein modification via maleimide or acetamide linked dyes have furthered understanding of protein structure and folding via fluorescence or FRET based assays.(186) Expressed protein ligation techniques have allowed for site specific insertions of fluorophores, post-

translational modifications, unnatural amino acids *etc.* thereby allowing greater understanding of protein structure, activity and interactions.(56, 129) Gradually the need for *in vivo* labels/ tags has increased because it is within the dynamic systems of the organism that complete characterization of different biopolymers, from proteins to nucleic acids, is possible. In this regard GFP chimeras have been widely used to monitor cellular systems.(124) An interesting approach towards such bio-chemical goals has been co-opting the cellular biosynthetic machinery for bioengineering. An early development in this area was the use of “dideoxy” nucleotides as substrates for DNA polymerases – this forms the basis of all current DNA sequencing techniques.(174) In a similar vein studies have been made to challenge the synthetic capabilities and fidelity of the protein synthesis machinery. Protein engineering by expanding the natural set of amino acids, i.e. by use of non-canonical amino acids, has advanced substantially over the past few years. The discriminatory nature of the aminoacyl-tRNA synthetase limits the use of random amino acids. As such, in the beginning, changes using non-natural amino acids were done mostly either by solid phase peptide synthesis or native chemical ligation *etc.* Presently the most efficient means rely on exploiting the unnatural substrate tolerance of the cellular translational apparatus.

Cowie and Cohen in the 1950's used selenomethionine(35) as a methionine surrogate, which was later championed by Hendrickson to revolutionize the field of protein X-ray crystallography. Over the years a number of different methods have been used to incorporate non-natural amino acids within proteins. Currently there are 2 broad techniques by which this procedure is attempted.

A) Residue-specific incorporation(82, 98) involves the replacement of all or a fraction of a particular natural amino acid with an unnatural surrogate. This can be used to alter the physical and chemical properties of the target protein and said protein can also be specifically targeted for subsequent bio-orthogonal chemical modifications. Generally this method is one of metabolic labeling where a structurally similar unnatural analog is fed to the growth media of the microbe/ cell and this gets charged onto the cognate tRNA. Increased efficiency of amino acid incorporation can be obtained by over expressing additional plasmid copies of the aminoacyl tRNA synthetase or by engineering the synthetase with a modified active site – to better accommodate the incoming non-canonical substrate.(78) All such studies have mostly been undertaken within auxotrophic expression hosts, for the target amino acid, to aid in the metabolic incorporation of the substrate analog and generate high levels of modified protein.(95, 187, 189) Residue specific incorporation of unnatural amino acids allow for global analysis of protein expression. Beatty *et al.* used this technique to label two temporally defined protein populations in mammalian cells while Schuman *et al.* studied protein synthesis and localization dynamics within rat neurons.(16, 44)

B) The above method though useful, has the major drawback of limited specificity. To replace only a single residue at a particular position of interest with an unnatural amino acid while retaining all other natural sites, site-specific incorporation via the amber nonsense codon (TAG) was championed by Schultz(138) in 1989. This method relies upon chemically mischarging a suppressor tRNA by the unnatural amino acid. It was further advanced in 1998 when a yeast tRNA and tRNA synthetase pair were used to specifically attach an unnatural amino acid - development of the heterologous 21st pair.(59,

198) Though the incorporation of multiple substrates within a single protein is highly limited by this codon suppressor technique. Also low protein expression as a result of 21st pair usage and inability to suitably develop within mammalian cells are some of its other drawbacks. Recent reports using the ocher suppressor codon along with the amber codon attempted to overcome some of these issues.(91, 172) Also development of degenerate sense codons and an orthogonal ribosome-tRNA pair have looked to increase suppression efficiency.(39) Expanding codon size to four and use of non-natural base pairs are potential ideas advancing this technique, though they are currently too inefficient for practical applications.(74, 137, 204)

Substitutions of natural amino acids by their corresponding unnatural surrogates have developed greatly to incorporate a large number of unnatural amino acids into different target proteins. This has been used to study catalytic properties of proteins, assist protein purification, study protein folding, delve into post translational modifications, and a number of other applications.(34, 38, 149) One of the major achievements of the metabolic labeling technique is the ability to incorporate residues that have reactive functional groups like azides, alkynes, olefins or ketones for specific protein labeling.

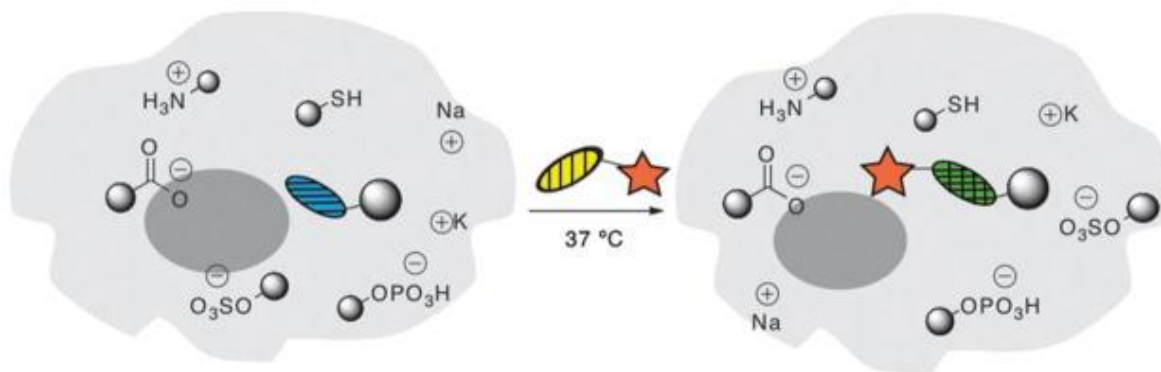


Figure 1-1. Representation of bio-orthogonal chemical reporter system within *in vivo* systems.(28)

Subsequent use of bio-orthogonal chemistry on these functional groups has afforded a host of different applications, from *in vivo* visualization to identification of newly synthesized proteins (Figure 1-1).(5) A number of different amino acids with different chemical handles and corresponding labeling probes have hence been developed.(211) Azidohomoalanine (Aha) and Homopropargylglycine (HPG), two methionine surrogates that are amenable to azide-alkyne cycloaddition have been extensively utilized. Amine reactive keto-and thio ether phenylalanine analogs have also been developed.(198)

The need for chemical tagging within biological systems has spawned research in the field of chemoselective bio-orthogonal reactions – with two conjugation techniques, the “click” based and the Staudinger ligation reactions finding detailed applications. Recently Diels Alder based couplings and Mannich-type conjugations have been developed. Braun *et al.* utilized the Diels Alder based tetrazine coupling reaction to develop a drug transport system for TMZ delivery to prostate cancer cells;(153) while, the Francis lab developed a bio-conjugation protocol by using formaldehyde to activate an aniline label

for condensation with a tyrosine residue of interest – a Mannich condensation reaction.(163)

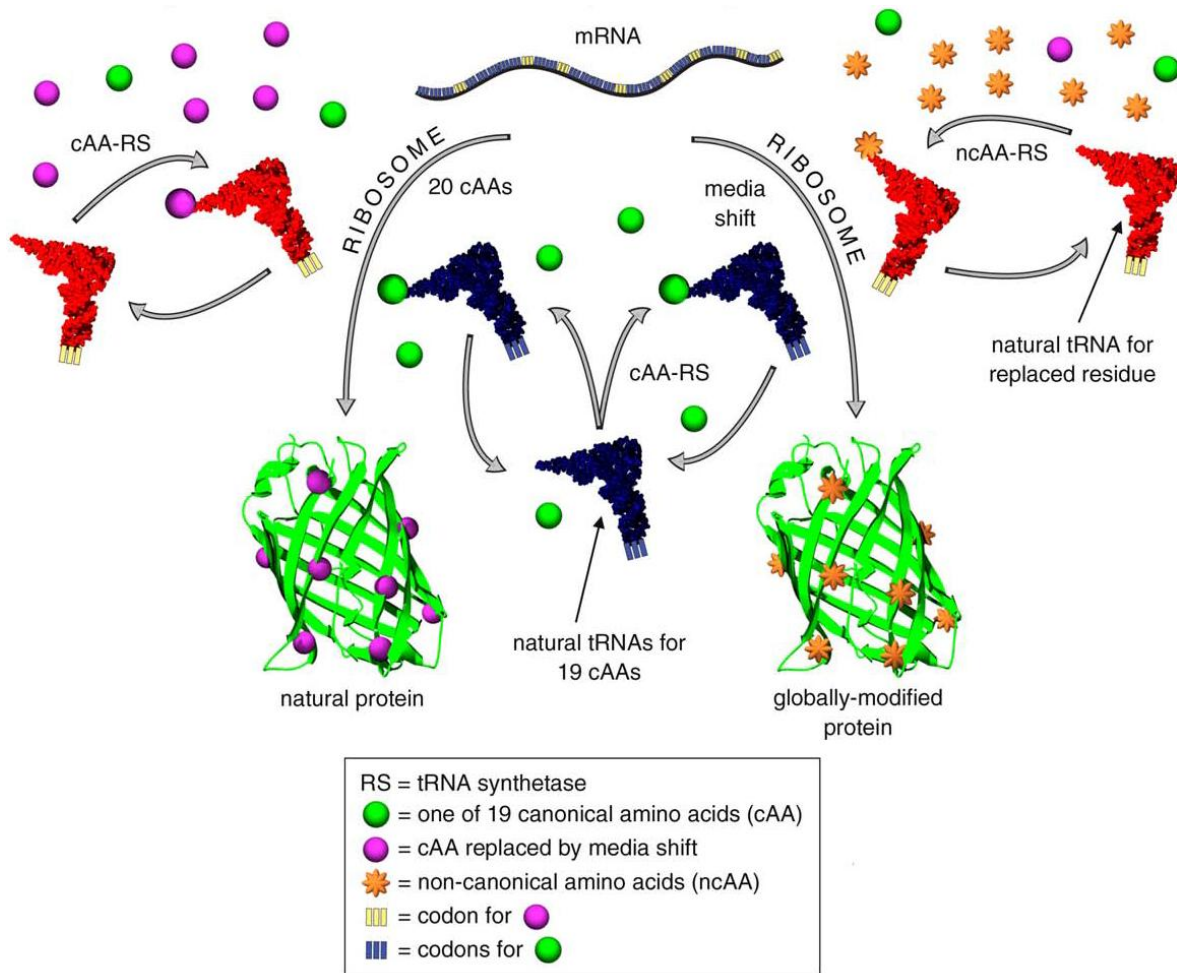


Figure 1-2. Animated representation of residue specific incorporation of non-canonical amino acid analogs onto cellular proteins.(82)

Traditionally, bacterial or yeast systems have been used to incorporate the unnatural amino acids within proteins. Schuman and coworkers for the first time in 2006 used

residue specific unnatural amino acid incorporation within mammalian HEK 293 cells (cell line derived from human endothelial kidney cells). They used a methionine surrogate, Azidohomoalanine to identify expression of newly synthesized proteins. Azidohomoalanine on the metabolically labeled proteins were chemically labeled with an alkyne-FLAG tag by copper assisted [3+2] electrocyclization chemistry.(196) Using a 2 hour labeling window they reported the identification of 195 metabolically labeled proteins. This new BONCAT (bio-orthogonal non-canonical amino acid tagging) system could thus be used to selectively label proteins being synthesized after a particular impulse, e.g. heat shock, viral infection *etc.* The BONCAT system has since been used to look at protein expression within neurons, visualize temporally defined protein populations in complex mammalian cell populations, determine protein functions in vivo, and co-relate protein syntheses with post translational modifications.(15, 44)

Use of small molecules that are natural analogs of biological monomers have also been extended to sugars for labeling proteins.(33) Glycans are proteins that have post-translational modifications on them in the form of sugar moieties. Most glycans that are exposed on the cell surface have large oligosaccharide modifications on them.(51) These are used as receptors for cell signaling, anti-body/ antigen interactions, cell-cell adhesion *etc.* Their structures are reported to change from normal to diseased cell states.(50) Bertozzi and coworkers have targeted these oligosaccharides for labeling with unnatural sugars.(68, 86, 154) Using azide(177) or ketone(210) labeled sialic acid residues they have been able to modify these cell surface glycans. Subsequent chemistry on the azido labeled sugars with either “click” chemistry or Staudinger ligation reaction affords visualization and identification of these proteins.(3, 14, 102, 176) Alkyne-sugars have

recently been used for similar purposes with modifications being carried out via various azide probes. This technique is currently being pursued for identifying changes in cell surface glycans as a response to different diseases, especially cancer and to study embryonic development and morphogenesis.(13, 40) In these labeling studies it is important for the enzymes that are necessary for donor sugar synthesis to tolerate modifications of the unnatural substrates. The kinetics and properties of the enzymes responsible in most of these cases have been worked out.(80, 112, 115) In many cases the biosynthetic machinery accepts subtle modifications on the incoming small molecule. Figure 1-3 illustrates the underlying concepts for such labeling techniques.

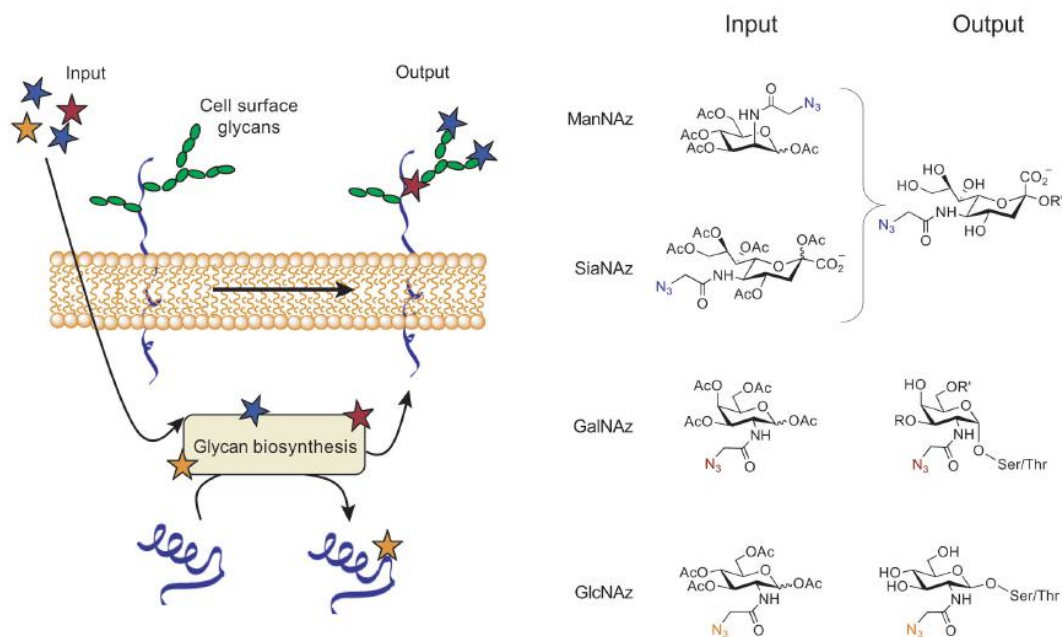


Figure 1-3. Use of unnatural sugar monomers, containing the azide functional group, within glycoconjugates through the cellular glycan biosynthetic machinery.(155)

There occurs a similar type of post translational modification within nuclear and cytosolic proteins, where *N*-acetylglucosamine residues are added on to serine or threonine moieties on the protein chain. But subsequent modification of these sugars does not take place. The end result being that these proteins contain only a single monosaccharide as an O-linked glycan.(69) The *O*-GlcNAc post translational modification has emerged as a major player in regulation of transcription and translation, in protein trafficking and turnover, is involved in neurodegenerative diseases and underlies diabetes and glucose toxicity.(22, 43, 199, 214) It is a highly dynamic modification that is seems to interact closely with protein phosphorylation.(201) Identification of *O*-GlcNAcylation within proteins has traditionally been difficult due to sub-stoichiometric labeling at specific protein sites and its inability to be detected by standard proteomic techniques.(200) Vocadlo(194) *et al.* first reported that this PTM could be labeled with unnatural *N*-acetylglucosamine surrogates. These sugar residues are not only biosynthesized from a couple of different pathways; they are also uptaken via certain salvage pathways – thus accepting sugar moieties from an external source. Thus adding non-canonical sugars onto growth media containing cells afforded labeling via the hexosamine salvage pathway. The substrate used in these experiments was an *N*-azidoacetylglucosamine moiety that was subsequently treated with either an alkyne tag for [3+2] cycloaddition or by a Staudinger reagent. It was recently reported that using an *N*-azidoacetylgalactosamine moiety offers higher levels of substitution of the *O*-GlcNAc residue within proteins compared to the *N*-azidoglucosamine analog.(20) Specifically, an epimerase present within the galactosamine salvage pathway is responsible for increasing the cellular concentrations of *N*-azidoacetylglucosamine. Incidentally not only azido

sugar analogs, but alkynyl analogs are reportedly tolerated in this aforementioned pathway.(213)

1.2. Oncolytic virotherapy

The concept of gene therapy follows logically from the observation that certain diseases are caused by the inheritance of a functionally defective gene/s. Hence theoretically, the insertion and expression of a therapeutic gene can potentially alleviate the genetic defect.(58, 119) In late 2000 a clinical trial of two patients suffering from SCID-X1 with a retrovirus expressing the defective cytokine receptor gene was carried out. After ex-vivo infection of CD34⁺ cells and a 10 month follow up period, the patients expressed T, B and NK cells comparable to age matched controls.(27) Thus, the employment of gene delivery as a therapeutic molecular intervention to selectively correct or eradicate defective genes can be defined as gene therapy.(165) In the past 30 years tremendous research has focused in utilizing gene therapy to treat a number of diseases. Data from the journal of gene medicine shows that since 1989 more than 1700 clinical trials have been approved for gene therapy applications. In spite of such attempts, only about 3.5% of all trials have gone on to phase III; indicating that current gene delivery techniques suffer heavy drawbacks. In contrast about 50% of all clinical trials carried out on small molecules proceed to phase III.(8) A number of problems seem to arise from the type of vector used in gene transfer. Non-specific gene delivery and high

immunogenicity are two of the main reasons why traditional gene therapy has somewhat fallen out of favor amongst researchers and administrators alike.

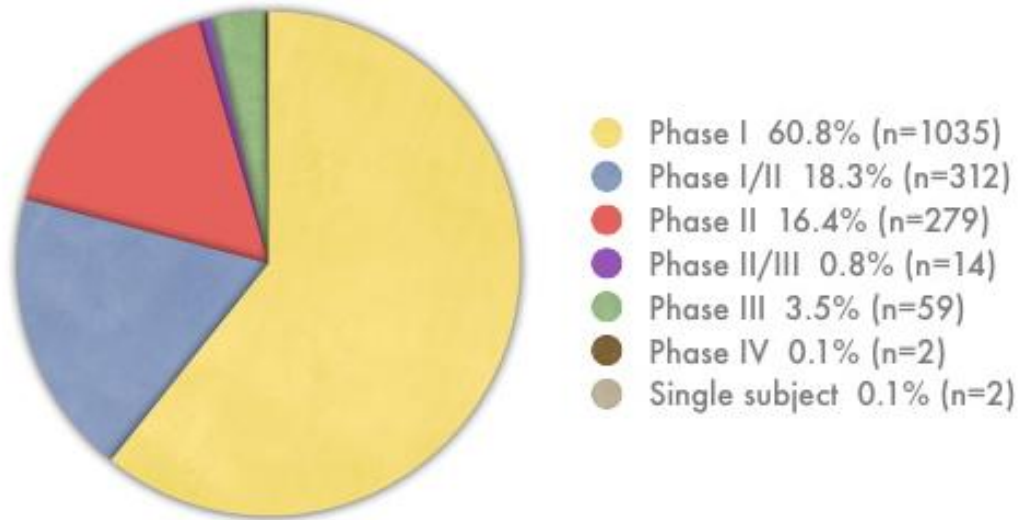


Figure 1-4. Data showing the number of gene therapy clinical trials completing either phase I, II or III. From the database of the journal of Gene Medicine within the years 1989 to 2010.

Whereas traditional gene therapy looked to deliver genetic material to overcome defective protein expressions, a more recent variation utilizes the same idea for cell toxicity purposes – to target cancerous tissue. The majority of current clinical trials using gene therapy are now targeted towards cancer (Figure 1-5). The use of viral vectors to target tumorous tissue, a recent development in cancer therapeutics, is classified as oncolytic virotherapy.(45) Initial reports leading to the development of virotherapy for cancer go back to the beginnings of the 20th century. A paper from 1904 reported the transient remission of cancer within patients who had been vaccinated for rabies.(46)

Subsequently it was observed that patients suffering from viral infections like mumps, adenovirus, west nile virus *etc.* showed reduced cancer growth and in some cases tumor shrinkage.(9, 76, 180) In recent years researchers have focused on developing genetically modified virions with anti-tumor activity – honing in on the ability of viruses to replicate selectively within cancer cells. Currently adenoviruses, adeno-associated viruses, poxviruses, lentiviruses, herpes viruses *etc.* are being studied for tumor selective infection and propagation. Thus viruses have emerged as pre-eminent gene transfer agents for use in virotherapy.

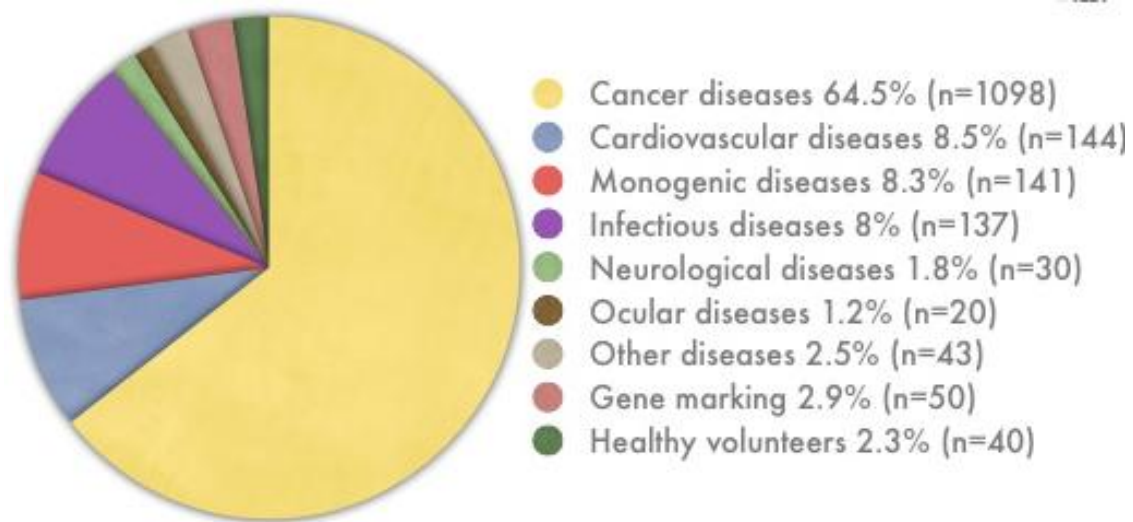


Figure 1-5. Indications addressed by gene therapy clinical trials worldwide from 1989 to 2010. Data from the database of the journal of Gene Medicine.

Viruses have been used as delivery vectors for gene therapy for a long time due to their inherent capabilities to transfer and express genes within various tissues.(203) These are obligate particles that are dynamically active only within a host system. Their overall

make up consists of a protein coat or capsid that encapsulates their DNA or RNA. Though many different viruses have been tested for virotherapy applications,(62, 84, 104, 152) adenoviruses (Ad) (24% of all gene therapy clinical trials use adenovirus) have become the most heavily relied upon for therapeutic delivery applications. This is because of a number of key factors: better *in vivo* stability, superior gene transfer efficiency to a great number of dividing and non-dividing cells, and well established production parameters for clinical grade vectors.(37) Also adenoviruses have rarely been linked to any severe disease in humans. Hence a tremendous amount of research has been done to develop these virions for targeted oncolytic therapy, gene therapy, for vaccine development and for tumor imaging purposes.(49, 121, 123) Use of Ad as oncolytic agents is dependent on two pathways utilized to make these particles transcriptionally tumor specific.

One is the pathways use of tumor specific promoters – thus enabling the virus to replicate within cancerous tissue.(109, 161) One of the earliest tumor specific promoter used was directed against prostate cancer – the widely used prostate specific antigen.(147) Later virions were produced that were controlled by two different promoter elements - the E2F-1 and hTERT promoters.(169) But engineering of viral genetic elements via this technique can upset the coordinated expression of virion proteins. Also, virus host interactions can have serious impact on performance of such tumor specific promoters.(90)

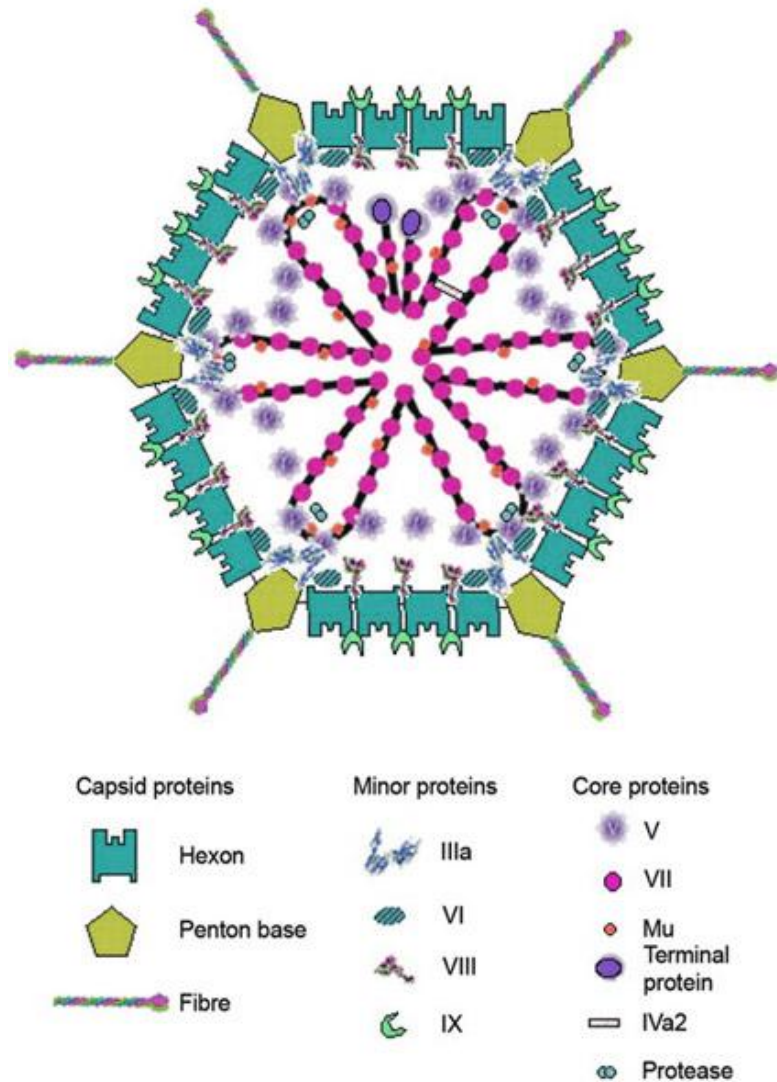


Figure 1-6. Schematic representation of an adenovirus structure showing all major structural proteins.(167)

The second pathway towards tumor specificity is *via* a method of selective gene deletion that allows Ad gene expression only within cells that have bypassed apoptotic signals – cells with low p53, reduced retinoblastoma activity *etc.*(100, 127) The success of this technique allowed the Chinese FDA to allow the use of an oncolytic Ad ONYX-15, which specifically works within p53 negative cells.(131)

In spite of such progress, there have been increasing recent reports about non-specific infection of such transcriptionally targeted Ad. Infection within kidney and lungs due to non-specific initial infections caused the US FDA to reject a variant on ONYX-15 for clinical use. The only current conditionally replicative adenovirus in clinical trial is AdD24-RGD; which contains retinoblastoma deficient cell specificity with targeting achieved via integrins.(99) Hence development of specific transductional targeting modalities for adenoviruses to cancerous issue is an important area of developing research.(107) Along with this, due to a high level of humoral immune response to Ad infections, using such particles for repetitive use becomes impossible. Also understanding bio-distribution of infecting virions is necessary to efficiently evaluate vectors. Thus there is a need to develop virus engineering techniques to overcome not only the targeting drawbacks of Ad, but also to reduce immunogenicity and for the development of multi-functional platforms for use in coupled targeting / tissue tracking experiments.

Thus with considerable interest in generating better gene therapy and / or virotherapy vectors, it is becoming more important to better understand the molecular aspects of virus-cell interaction and infection and host responses towards it.

1.3. Adenovirus based vectors

The adenovirus (Ad), shown in Figure 1-6, is a non-enveloped icosohedral dsDNA containing virus with sizes between 90-100nm. There are more than 50 different Ad serotypes which cause illness such as respiratory infection, conjunctivitis, gastroenteritis,

cystitis and rashes. Ad serotypes are classified based on their ability to be neutralized by specific animal anti-sera. These 50 serotypes can be further subdivided into 6 sub groups (A to F) based on their agglutination with erythrocytes. The hexon, penton and the fiber are the three main structural proteins of Ad.(118) The fiber protein of adenovirus, consisting of a rod and knob domain, attaches it to the Coxsackie Adenovirus Receptor (CAR) on mammalian cells through its knob domain.(88) Different Ad serotypes have varying lengths and flexibility of their fiber proteins. Though most of the subgroup Ads are known to bind CAR, there does occur some differences in the molecular interactions based on fiber structure and length.(89) Only type B virions are known to bind CD46 receptors on cell surfaces.(183) Initial interaction of the fiber with CAR induces conformational changes that allow it to bend and induce penton base interactions with integrin receptors on cell surface. RGD motif on the variable loop of the penton binds to integrins $\alpha_v\beta_3$ and $\alpha_v\beta_5$ allowing virus internalization within endosomes. Changes in pH within endosomes result in fiber and penton proteins to being released from the core virus structure. Subsequently the virus escapes the endosome by protease mediated cleavage and travels over microtubules to the nuclear pore where it delivers its DNA into the nucleus.

Generation of adenovirus based retargeting vectors focus on biochemical modification of the viral surface to redirect virus infection towards desired tissue types. Given its broad tissue tropism, adenovirus needs specifically to be de-targeted from the natural receptor, CAR and subsequently retargeted.(125) Modifications to the coat proteins are thus necessary for generation of effective gene delivery vehicles. So far most of the alterations that have been attempted are either genetic changes to alter the capsid

proteins or chemical attachments of different polymer chains for better targeting. In adenoviruses the CAR binding site within the fiber knob has been the focus with either deleted or modified knob domains used for vector retargeting to other cellular receptors. This approach not only detargets the virus from native coxsackie adenovirus receptor but also assists in retargeting it towards other diseased tissue types. One of the first attempts at retargeting Adenovirus was de-knobbing the virus and inserting an artificial trimerization motif to retain virus assembly.(116) This virion was retargeted using an RGD peptide insert into the fiber. Peptide based targeting of Ad virions was also assessed using MMP targeted peptides on the viral fiber, epidermal growth factor receptor targeted ligands, laminin derived peptides for alpha-6 integrin targeting and muscle binding peptides using phage display libraries.(1, 60, 83, 182) Retargeting has more recently been based on single chain antibodies fused to viral capsid proteins and bi-specific molecules that contain anti-body based targeting approaches. In this regard targeting has been achieved using EGFR specific antibodies e.g. cetuximab, melanoma associated antigens, vascular proteins, e.g. endoglin and neuronal targeted proteins, e.g. tetanus toxin.(66, 128, 136, 161)

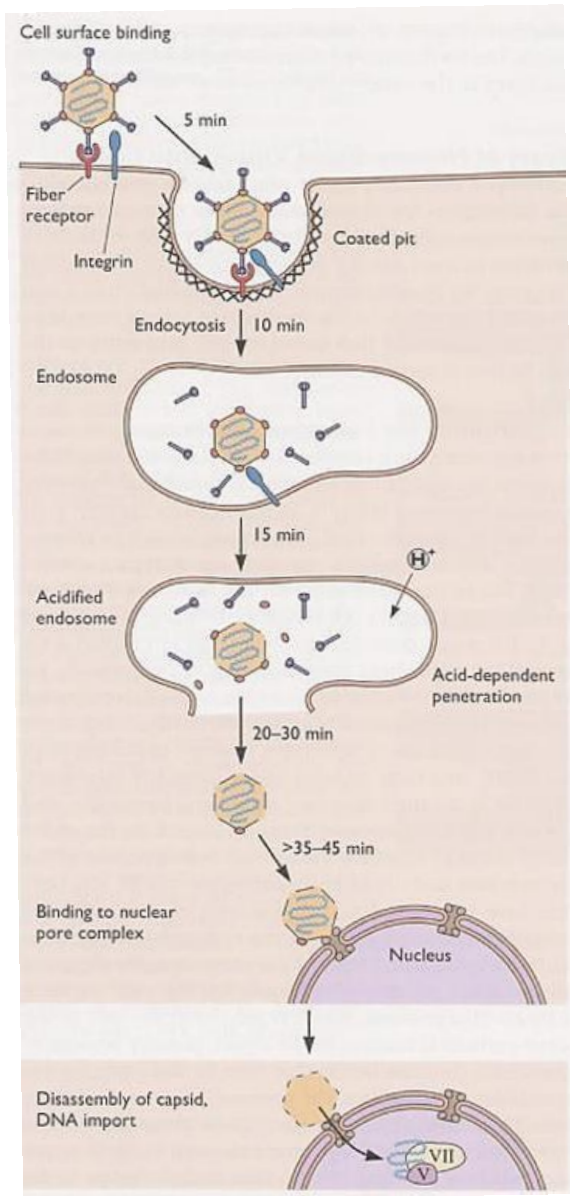


Figure 1-7. Early events in adenoviral infection – cell entry and viral translocation to nucleus(126)

Genetic modification of the coat proteins is the most prevalent and has been explored at numerous positions on the adenoviral surface, however due to impact on viral stability and infectivity most studies focus on the HI loop or C-terminus of the fiber protein, the HVR domain within the hexon and the carboxyl terminus of pIX.(61, 206) Despite being

relatively permissive, genetic alteration of these sites often challenges viral fitness, as evidenced by losses in particle production and infectivity, with such issues determined by the nature and size of modification.(73, 117) The fiber C-terminus showed promising results at retargeting the virion with RGD motifs while other similar sized peptides failed to produce substantial effects.(148, 202) Incorporation of large targeting peptide sequences, 63 to 83 amino acids in length, on the fiber HI loop has a relatively modest effect on viral fitness, 3-fold and 7-fold reduction effect on virus production and infectivity respectively. While incorporation of smaller 13 to 43 amino acid peptides at the same site has virtually no effect on particle production and only a 20% reduction in infectivity.(17, 92) Compare this to any of the hyper variable loop regions of the hexon, where increasing insertion ligands from 6 to 43 residues results in a precipitous drop of infectivity from zero negligible effect to a 1000 fold reduction.(122) The length and nature of peptides displayed probably determines their ability to form stable domains, with respect to protein folding and assembly, within the viral capsid protein being modified. On the other hand pIX seems well suited for incorporations of large peptide domains, *e.g.* biotin acceptor peptide, and even proteins, *e.g.* GFP.(23, 120) The modified vectors generated by genetic modifications suffer from defects such as low particle production and ineffective transductional efficiencies. This is because virus packaging and fusion is a delicate process and is easily offset by alterations in its protein structure. Thus it is important to affect subtle changes in these vector systems that would be malleable to modification yet not hamper the overall physiology. It is thus important to be able to concomitantly de-target them from their natural tissues and re-target them towards diseased cell lines.

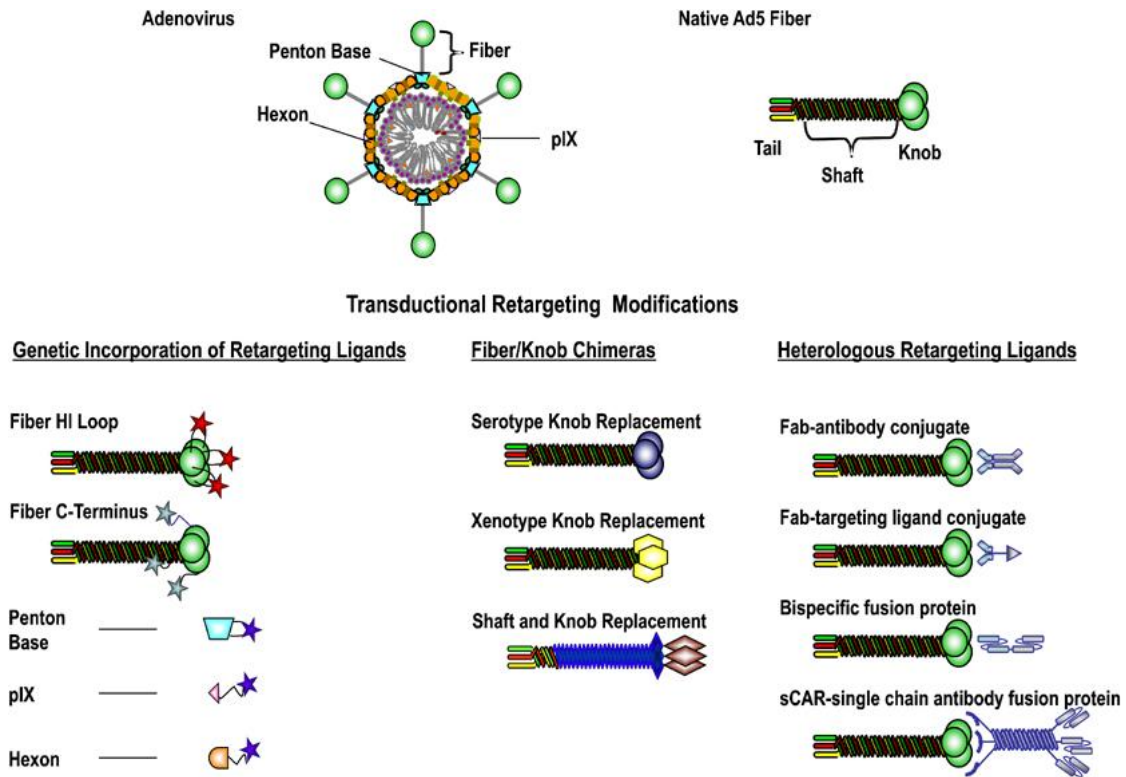


Figure 1-8. Viral surface modification based on genetic, chimeric and bispecific ligand systems.(121)

Another form of generating capsid modified Ad, using genetic technique, involves deriving chimeric viruses.(108, 188) This involves switching between fiber proteins of different Ad serotype to change virus tropism.(85) Specifically using the sub-group B serotypes within type 5 fibers, retargets them from CAR receptors to CD 46 receptors. But the assembly of chimeras is difficult and often generates mixed fiber virions, greatly reducing assembly and particle production.

Non-covalent adenoviral decoration was first demonstrated with chemically modified anti-CAR antibodies. Advantageously, this strategy allows for both de-targeting, from

CAR mediated infection, and retargeting in a single step.(49) Such “molecular bridges” between the vector and the cell specific receptor consist of two domains, often the first binds specifically to the primary targeting motif in the knob region, effectively masking it, while the second contains receptor specific antibodies, small molecules or peptides.(197) However, antibody-ligand conjugation is non-trivial and, more importantly, *in vivo* stability of the modified adenoviral particle remains a significant question.(133) A conceptually similar technique incorporates the biotin acceptor peptide on the adenoviral fiber as shown by Campos *et. al.* providing a potentially powerful merging of genetic and adapter based approaches.(23, 148) Here the biotin acceptor peptide acts as the binding site for one part of the molecular bridge on the virus while keeping the other part available for efficient retargeting ligand insertion.(151) A final variation of this example with a fiber mosaic viral capsid was also developed to show effective transgene delivery *in vivo*.

To broaden the range of accessible functionality, chemical modification of solvent accessible natural residues has been explored. Lysine modification allows a high degree of functionalization with immunosuppressive polymers, targeting polypeptides and imaging reagents.(139) Conjugation of polyethylene glycol (PEG) polymers allows production of “stealth” vectors, which are both protected from immune recognition and effectively detargeted.(83, 94, 140) In addition, PEG polymers can be armed with targeting moieties, allowing the vector to be efficiently retargeted in a single step.(48) However, due to the nature of lysine conjugation, control is limited and modification changes the surface charge of the virus. Accessible functionality is inherently constrained by the nature of amide-bond formation. As a result, modification with proteins, nucleic

acids and other nucleophile containing ligands is limited. Alternatively, cysteines have been genetically introduced at exposed locations on the fiber HI loop allowing selective chemical modification (93) by taking advantage of disulphide based conjugating ligands. Thus introduction of new chemically accessible sites for decorating viral vector surface would not only increase the repertoire of attachable probes but also introduce additional sites for modification with direct able ligand systems, providing further control to the retargeting capabilities of vectors.

Ideally chemical modification of adenoviral particles would allow access to any effector functionality, demonstrate specificity akin to genetics, and not diminish viral fitness. In addition effects on viral infectivity and fitness needs to be minimal and should have the potential to be extended to the development of multifunctional vector systems.

1.4. Project Aim

1.4.1. Capsid modification of adenoviral particles with unnatural sugar

Efficient development of adenoviral particles for tumor targeting applications necessitates the ability to selectively target the virions towards specific tissues. Moreover, such selective tissue tropism requires engineering techniques that should ideally be easy to access and produce minimal impact on virus production and infectivity. Exploiting the metabolic pathways of the mammalian cellular system, this project aims to introduce

otherwise harmless changes into adenoviral particles in the form of unnatural amino acids and sugars. These unnatural substrates distinguish themselves from their natural surrogates in containing specific chemical handles. Such functionality embedded within the bio-molecules allows access to highly chemoselective bio-orthogonal reactions. Such reactions facilitate the labeling of fully intact virions with small molecules, peptides and even proteins. The adenovirus does not contain complex poly-saccharides on its coat proteins except for a single *N*-acetylglucosamine (*O*-GlcNAc) residue on the fiber. We aimed to utilize two azido sugar analogs, *N*-azidoacetylglucosamine (GlcNAz) and *N*-azidoacetylgalactosamine (GalNAz) to specifically label the virus capsid at a single site. Staudinger ligation with phosphine probes and copper catalyzed [3+2] electrocyclozation with alkyne probes were utilized to chemically modify the virions after metabolic unnatural monosaccharide incorporation. We demonstrate efficient metabolic incorporation and subsequent chemical modification of the intact adenovirus particles. Metabolic attachment produces minimal impact on virus production and infectivity. Quantification of the amount of modifiable azides being incorporated within the intact particles was attempted. Finally we aimed to develop a small molecule based targeting approach for the modified viruses. Since different types of cancerous cells are reported to have over expressed folic acid receptor, our aim was to re-target the unnatural substrate enabled virions towards folic acid based tissue targeting approaches. Thus, we designed a folate-alkyne ligand containing small polyethylene glycol linker to effectively modify our azido virions. Targeting based on these small molecules was utilized on murine breast cancer cells; with the virions expressing a GFP or a Luciferase transgene – allowing for quantification of vector infection.

1.4.2. Capsid modification of adenoviral particles with unnatural amino acid

For facile generation of surface modified adenoviruses we aimed to utilize a residue specific unnatural amino acid incorporation technique to label the virions. While monosaccharide incorporation of the virus particles were aimed to be site specific, metabolic amino acid incorporation was expected to produce global protein modification. By employing subsequent bio-orthogonal chemistries only surface exposed amino acid side chains were expected to be modified. Towards this aim we utilized a methionine surrogate, Azidohomoalanine to label adenovirus coat proteins. Subsequent modification of this azide amino acid via phosphine and alkyne dependent chemistries produced efficient virions suitably decorated with small molecules, peptides and even proteins. Mass spectra and other bio-physical techniques were used to effectively characterize the unnatural amino acid incorporated viruses. Successful quantification of azide incorporation was also carried out. Our metabolically labeled and chemically modified virions possess strong potential to be utilized for specific targeting towards tumor tissues. And similar to our azido sugar modified virions we show efficient cancer cell targeting of Aha modified virions with folic acid based ligands. Targeting was also characterized via GFP imaging of infected cells on a confocal fluorescent microscopy system. Effective dose dependent inhibition also showed targeting was mediated by folate receptors. Modified virions were also utilized for preliminary cell trafficking experiments.

Since Aha incorporation within the viruses is not site specific, we are currently attempting to engineer a system that can utilize residue specific amino acid incorporation in a site directed manner. Here we also report the initial steps towards designing a mutated adenovirus fiber, which has its surface exposed methionine residues mutated such that further chemoselective attachment would be accessible.

1.4.3. Dual modified virus to study combination therapy

One of the drawbacks of oncolytic virotherapy is its efficacy, especially within clinical trial settings. In trials less than 15% of tumor targeted adenovirus shows effective efficacious cancer cell toxicity.(96) Thus it is becoming important to study chemo and virotherapy combination effects that can show higher tumor cell toxicity. Also, to better understand vector biology, imaging cell trafficking of vectors or bio-distribution within tumor tissue needs addressing. All such applications demand development of multifunctional platforms based on adenovirus particles. Traditional routes for multivalent platforms using genetic modifications or generation of chimeric virions by use different serotype capsid proteins fail to produce effective infectious particles. We aimed to progress our unnatural substrate incorporation technique towards development of a dual substrate modified adenovirus – these could be chemically derivatized with two different ligand systems. Towards this end, utilizing both our unnatural sugar and amino acid monomers to effectively label virions seemed most promising. This system will be developed to study combination therapy of TRAIL encoding oncolytic Ad covalently

modified with a Taxol derivative (SBT-1214) – developed by Prof. Ojima, on a number of different tumor cells.

Chapter 2

Specific labeling of adenovirus capsid with an unnatural azido sugar

2.1. Introduction

2.2. Results

2.3. Discussion

2.4. Summary

Note: The material in this chapter has been published (Banerjee, P. S.; Ostapchuk, P.; Hearing, P.; Carrico, I. *J. Am. Chem. Soc.* **2010**, *132*, 13615). The chapter contains direct excerpts from the manuscript that was written by me with suggestions and revisions by Prof. Carrico.

2.1. Introduction

Viral surface engineering has significant potential to tune the virus-host-interface enabling oncolytic therapy, gene delivery and vaccine development.(72, 122, 197) Despite being a long-standing objective, targeting therapeutically relevant tissues remains a significant hurdle. A contributing factor is the lack of general, effective methods to introduce targeting ligands onto viral surfaces that do not compromise fitness. The vast majority of retargeting efforts rely upon genetic manipulation of virus surface proteins.(197) However, due to the delicate nature of viral protein assembly and infection, such changes often offset particle production and cellular transduction.(73, 117) To overcome limitations in targeting functionality inherent to genetic approaches, chemical modification has been explored. As these approaches are largely dependent on exposed lysine residues, they lack the precision and control of genetic manipulation.(94) Some attempts have also been made to use thiol linkages with genetically incorporated cysteine residues at solvent accessible sites on the viral capsid(93). In order to combine the flexibility and robust nature of chemical modifications with the specificity obtained through genetics, we demonstrate the metabolic labeling of adenoviral capsid with an unnatural azido sugar, *N*-azidoacetylglucosamine (GlcNAz).

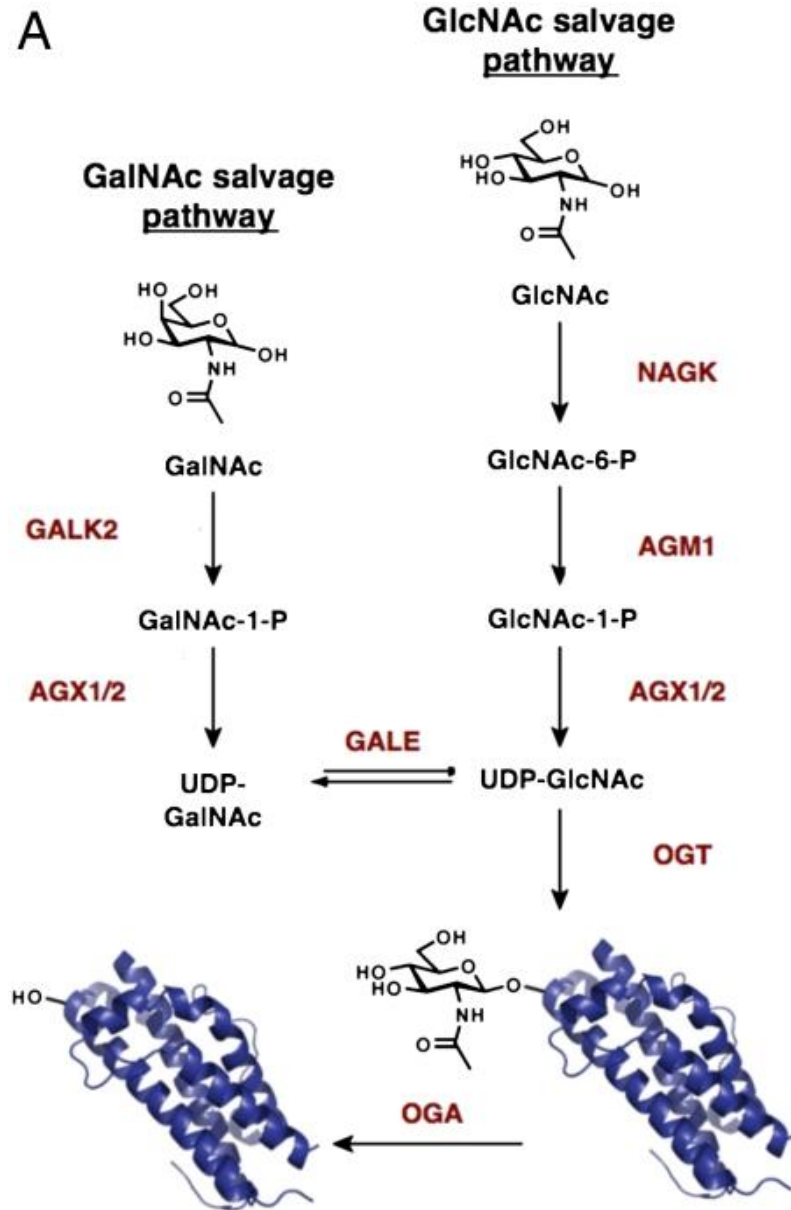


Figure 2-1. GlcNAc and GalNAc salvage pathways showing uptake of these residues, their conversion to the UDP-donor sugar, UDP-GlcNAc or UDP-GalNAc and the epimerase dependent interconversion of the donor sugars.

Metabolic incorporation of non-canonical hexose sugars bearing azide, alkyne or keto groups have been used to effectively label mammalian cell surface proteins – using them for identification, functional analysis and imaging purposes.(4) These sugar monomers are known to label the more abundant *N*-linked oligosaccharides or mucin type *O*-linked structures on cell surface.

There also occurs a very well known *O*-linked GlcNAc modification of serine/threonine residues within intra-cellular proteins. In 2003, Vocadlo et al. showed that these intracellular monosaccharide units could be metabolically labeled via the use of per acetyl *N*-azidoacetylglucosamine (GlcNAz) derivatives.(194) But the incorporation of this unnatural unit within *O*-GlcNAcylated proteins was relatively low and large amounts of protein were necessary to demonstrate sufficient labeling.

Recently an epimer of GlcNAz, *N*-azidoacetylgalactosamine (GalNAz) has been shown to act as an effective surrogate for intercellular *O*-GlcNAc residues.(20) Uptake of this unnatural sugar derivative has been shown to occur through the glucosamine/galactosamine salvage pathways and finally get converted to the *O*-GlcNAc donor substrate – UDP-GlcNAz (Figure 2-1). Detailed analysis of the enzymes associated with the salvage pathways show that an epimerase converts the GalNAc derivative to its GlcNAc counterpart. Data suggests that the initial phosphorylation step in glucosamine salvage pathway catalyzed by NAGK (Figure 2-1) is rate limiting. Due to altered substrate tolerance of NAGK, derivatives of acetylglucosamine uptake via this pathway are compromised – not so for acetylgalactosamine. This accounts for increased availability of the UDP-GlcNAz donor when utilizing unnatural GalNAc surrogates (in

this case Ac₄GalNAz). Recent reports also suggest that alkyne based sugars can also act as effective *O*-GlcNAc surrogates.(213)

Of the different non-canonical monosaccharide units used, azide/ alkyne bearing sugars have been most widely used and developed due to their ability to act as bio-orthogonal reaction centers. These surface exposed azides can subsequently be modified with peptides, fluorophores and small molecule targeting ligands.

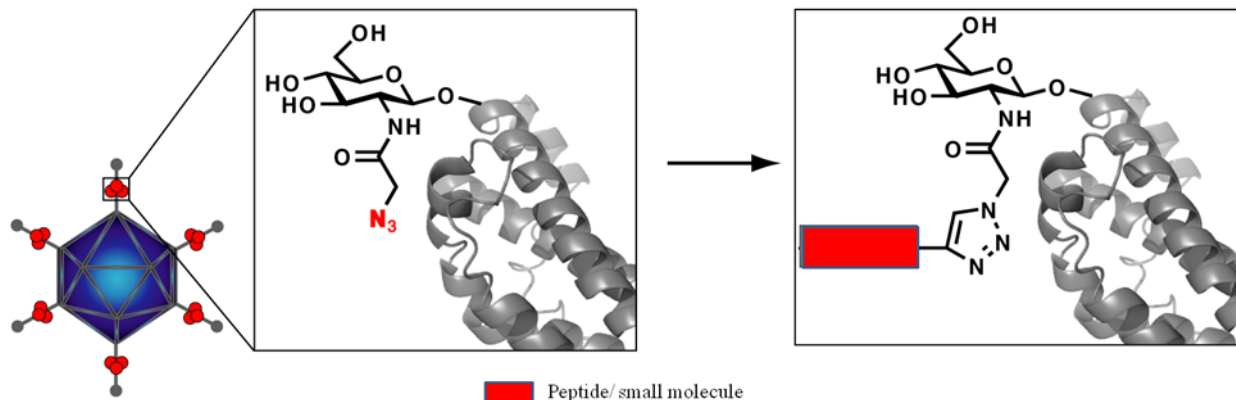


Figure 2-2. Cartoon representation of *O*-GlcNAz labeling sites on adenovirus fiber protein. Subsequent chemical modification with “click” chemistry affords attachment of peptides and/ or small molecules.

Advantageously, type 5 adenovirus is reported to have a single *O*-GlcNAc residue on Ser-109 of the fiber protein (Fig. 2-2), which exists as a homotrimer on twelve vertices of the virus capsid.(26, 130) Replacing this residue with an azido analog would allow for specific placement of an azide on the viral coat. Ser-109 is located proximal to the natural primary targeting motif on the fiber knob. The sugar is expected to specifically decorate a single adenoviral capsid protein, and present a bio-orthogonal reaction site poised for

efficient and selective chemistry. As a result, chemoselective placement of targeting moieties at this site is expected to be effective in re-targeting the viral particles.

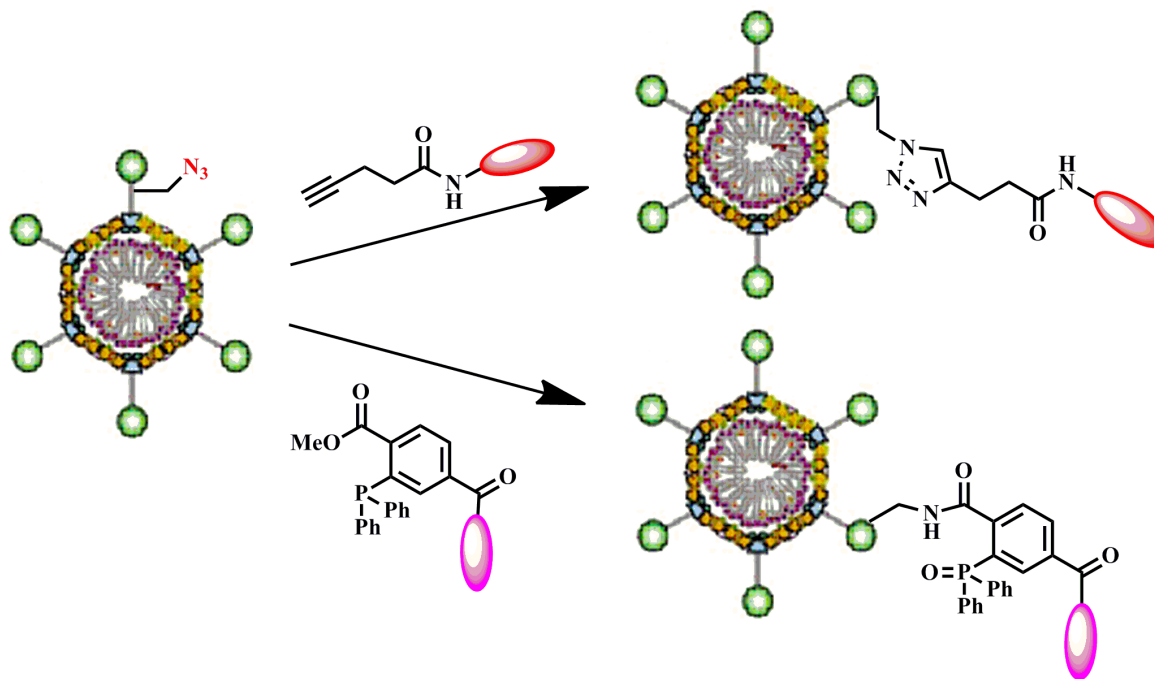


Figure 2-3. Reactions of azide enabled virions with either alkyne- or phosphine- based probes to generate corresponding triazole or amide linked virus-ligand attachments.

As a result of low pathogenic potential, ease of production and established safety protocols, human adenovirus has been developed extensively as vectors for gene delivery applications. In addition, conditionally replicative adenoviruses are currently gaining focus as oncolytic agents to infect and lyse cancerous cells specifically.(32) Since, adenoviruses produced for therapeutic applications are propagated on eukaryotic cell lines; use of unnatural sugars during the propagation cycle was expected to potentially

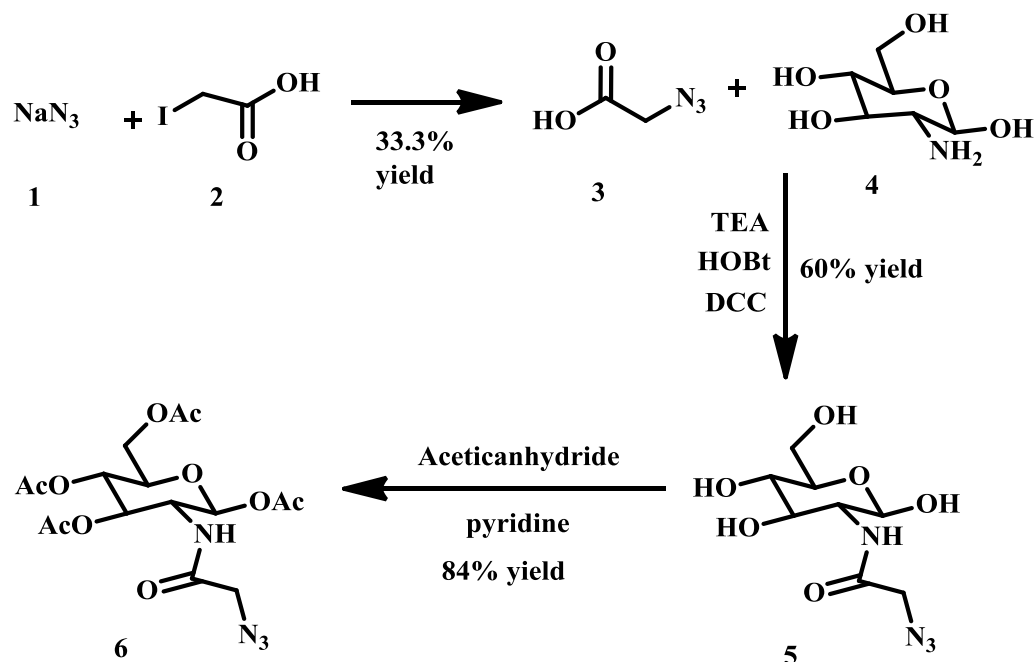
substitute for monosaccharide within viral glycoprotein. Hence, both Ac₄GlcNAz and Ac₄GalNAz were used to supplement growth media of human adenovirus. The peracetylation of the GlcNAc surrogates increases their cell permeability – once inside, these are converted to the free sugars via the action of deacetylases. Concentrations of per acetylated sugar were controlled at 50 μM levels. This was based on literature reports of higher sugar analog concentrations being cytotoxic. Two very well known bio-orthogonal reactions were used to exploit these azido sugar incorporations – the copper (I) catalyzed azide-alkyne electrocyclization (click) chemistry and the Staudinger ligation technique (Figure 2-3).

2.2. Results

2.2.1. Synthesis of per-*O*-acetylated GlcNAz and GalNAz

Per acetylated azido sugars were synthesized as reported by Bertozzi *et al.* and as shown in scheme 2-1.(101) Substitution of iodoacetic acid with sodium azide generated azidoacetic acid as light yellow oil. The synthesis of azido- glucosamine or galactosamine was performed in methanol via treatment of glucose/ galactosamine with azido acetic acid and triethyl amine (TEA). The coupling agent for the synthesis was N-hydroxybenzotriazole (HOBt) and N, N'-dicyclohexyl carbodiimide (DCC). The azido

sugars were per-acetylated with excess pyridine and acetic anhydride to finally generate the per-O-acetylated GlcNAz or GalNAz.



Scheme 2-1. Synthesis of per acetylated N-azidoacetylgalactosamine

Synthesized compounds were purified by flash chromatography and characterized by ^1H -NMR spectroscopy and ESI mass spectroscopy.

2.2.2. Production of *O*-GlcNAz labeled adenovirus

Metabolic incorporation of GlcNAz was accomplished by production of adenovirus particles in the presence of either Ac₄GlcNAz or Ac₄GalNAz. Specifically, HEK 293 cells were infected with Ad5 particles at an MOI of 5. The cell growth media was supplemented with 50 μM of either per acetylated azido sugar during virus growth phase. Both precursor sugars are metabolic precursors of UDP-GlcNAz, a known substrate for *O*-GlcNAc Transferase. The viruses were allowed to grow for 42 to 46 hours. After which the cells were lysed by repeated freeze thaw cycles, and the resultant cell extract – which contained fully formed virions, were loaded onto a cesium chloride step gradient. Ultracentrifugation of the soluble protein solution afforded density dependent separation of the fully formed virions from empty virions and other cellular and viral proteins. The virus band was collected and re-purified on another CsCl continuous gradient. The resultant virions were collected and stored in a Phosphate buffered saline solution containing CaCl₂, MgCl₂ and 10% glycerol. Particle production was assayed based on absorbance of virus containing solution at 260 nm (1 OD = 10¹² particles/ mL).

2.2.3. Chemical modification and characterization of *O*-GlcNAz labeled Ad5

To determine azido sugar labeling of viral fiber protein, Ad5 particles produced in the presence of per acetylated sugar were treated with alkyne- peptides and small molecules.

For this we used an alkyne-FLAG probe, which is an eight amino acid peptide (DYKDDDDK) epitope containing an N-terminal alkyne. We also used an alkyne-dye, tetramethyl rhodamine (TAMRA-alk) to chemically label virions. Both these reactions used the Cu (I) catalyzed “click” chemistry under deoxygenating conditions and in the presence of bathophenanthroline disodium disulphonic acid salt to form a triazole linked virus-peptide/ dye conjugate.

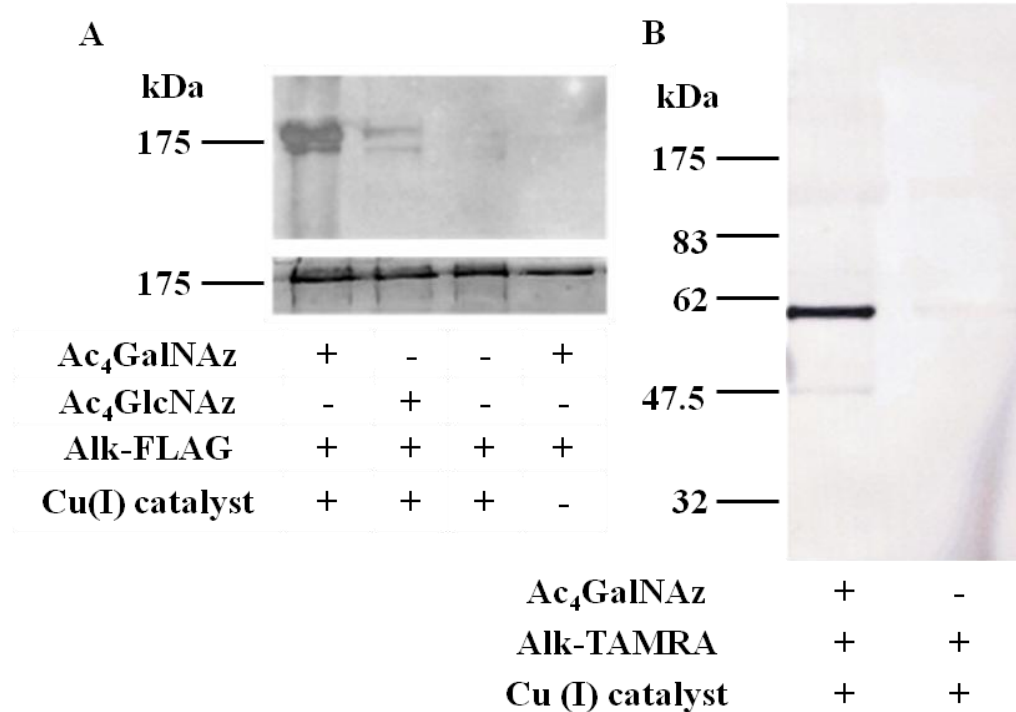


Figure 2-4. Qualitative analysis of azido sugar incorporation into the fiber protein of hAd5. A) Anti-FLAG Western of non-denatured viral particles treated with alkyne-FLAG under CuAAC conditions (100 mM Tris pH = 8; 1 mM CuBr; 3 mM Bathophenanthroline disulphonic acid disodium salt; 400 μ M alk-FLAG; 12 hr; RT). Top: anti-FLAG Western. Bottom: Coomassie. B) Fluorescent analysis of denatured *O*-GlcNAz-enabled viral particles treated with alkyne-TAMRA under CuAAC conditions (ex: 532; em: 580 BP 30).

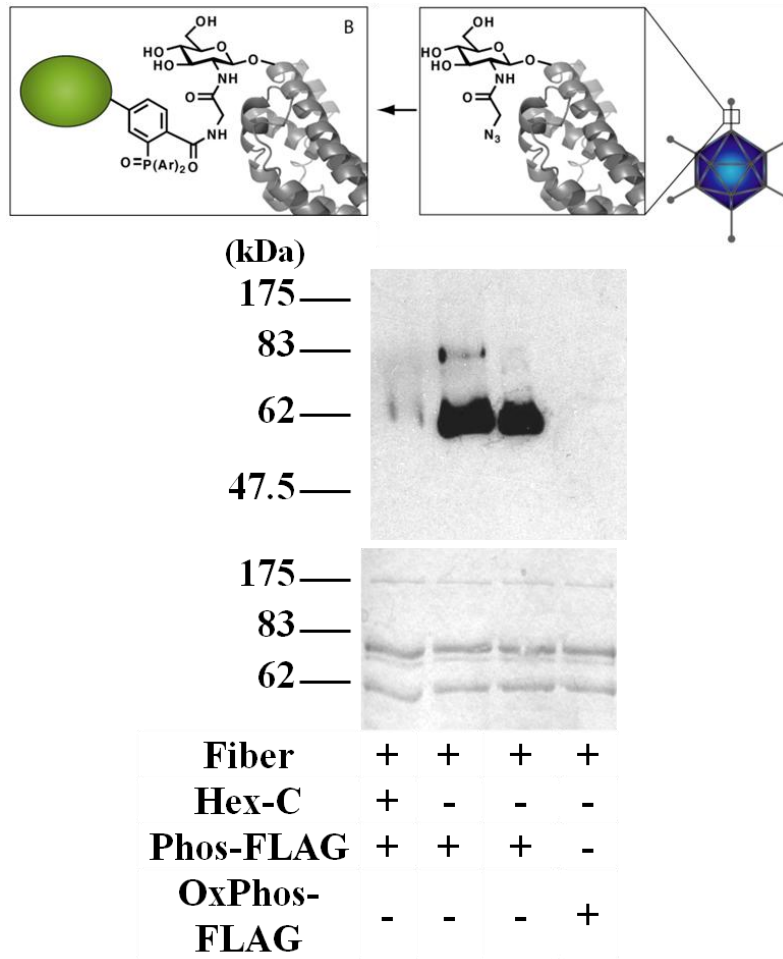


Figure 2-5. Hexosaminidase treatment (5 $\mu\text{g}/\mu\text{L}$ Hex-C; 37°C overnight) and subsequent Staudinger modification of partially purified *O*-GlcNAz labeled fiber protein (100 mM Tris pH = 8; 400 μM phos-FLAG; 2 hr; RT). Top: anti-FLAG Western. Bottom: Coomassie

Initial characterization of the *O*-GlcNAc site of hAd5 indicated that it was enzymatically inaccessible in complete virion. In order to determine if an installed *O*-GlcNAz was chemically accessible, whole viruses were chemically treated, and not denatured, prior to analysis. After chemistry, the particles were purified from the ligand,

copper and excess probe by gel filtration and stored at -20 °C in virion storage solution. We used western blot analysis and fluorescent gel scanning to determine modification of Ad5 (Figure 2-4). While western analysis of viruses grown with either Ac₄GalNAz or Ac₄GlcNAz sugar demonstrated effective labeling of the fiber protein (MW 61.5 kD) with *O*-GlcNAz (Figure 2-4), Ac₄GalNAz mediated labeling was markedly higher.

In order to confirm both the identity and placement of the installed azide, modification analysis of both denatured virus and partially purified fiber was carried out. Modification of the denatured virus with a fluorescent probe under click conditions demonstrated exclusive labeling of a protein at 62 kD (Figure 2-4). This corresponds to either fiber or protein IIIa, which co-migrate. To categorically determine labeling of a single adenoviral protein with an *O*-GlcNAz residue, fiber protein was partially purified from complete virus by simple pH change and centrifugation. Reduction of solution pH to 6.4 affords loss of Ad5 fiber from fully formed virions. After centrifugation, the icosahedral particles, now without fiber, aggregate and settle at the bottom of the tube with only the virus fiber and penton base in supernatant.

Fiber samples obtained from such metabolically labeled virions were denatured in guanidinium hydrochloride and then resuspended in PBS. The protein was treated with a hexosaminidase known to remove both *O*-GlcNAc and *O*-GlcNAz.(194) Subsequent chemical modification using Staundinger ligation with a phosphine-FLAG probe demonstrated almost a complete loss of azide-dependent signal (Figure 2-5) in the anti-FLAG western blots. Cumulatively, these results strongly indicate the fiber bears an *O*-GlcNAz modification, which is the exclusive source of virus labeling.

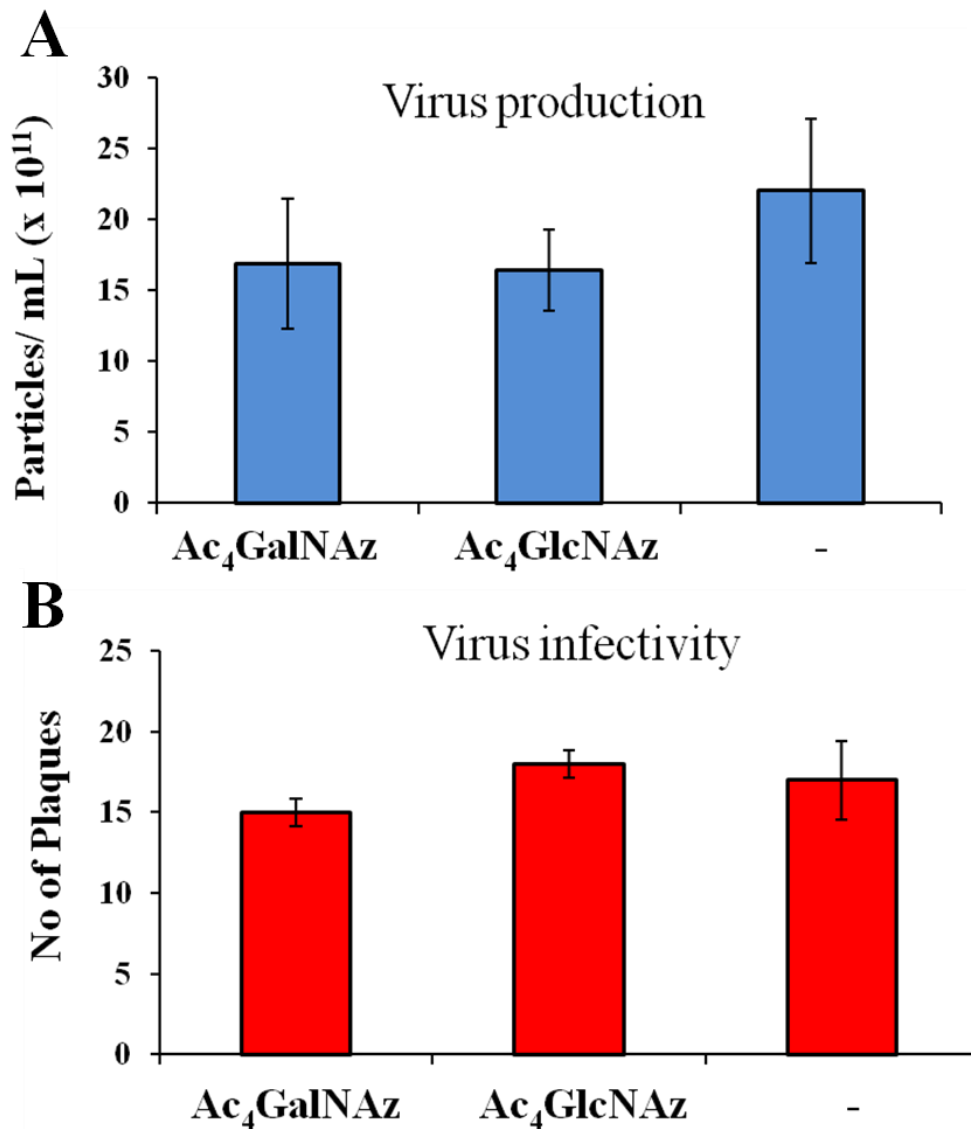
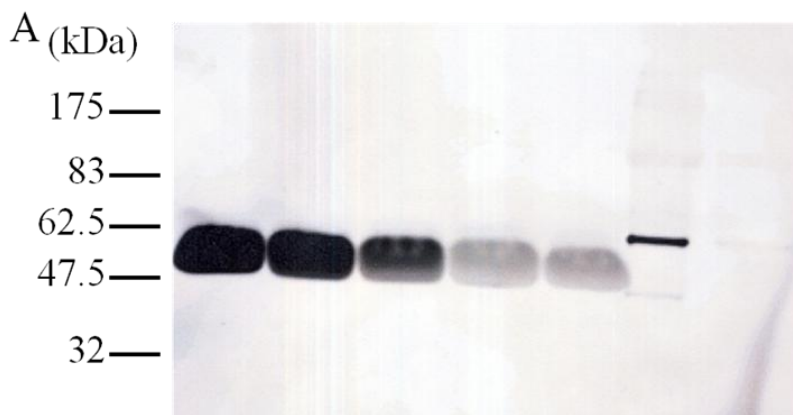


Figure 2-6. Azido sugar enabled adenoviral fitness determined by viral particle production and infectivity.

A) Number of adenoviral particles obtained by labeling growth media with Ac₄GalNAz, Ac₄GlcNAz or no exogenous sugar. Viral particle count is obtained by measuring absorbance at 260nm with 1OD = 1 x 10¹² particles/mL. B) Plaque assay comparing infectivity of Ad5 labeled by Ac₄GalNAz, Ac₄GlcNAz or no exogenous sugar in the growth media. Infectivity was assessed by counting no of plaques produced upon infection of 293 cells with labeled virus.



Alk-TAMRA(nM)	200	150	100	50	40		
GalNAz labeled Ad5						+	-

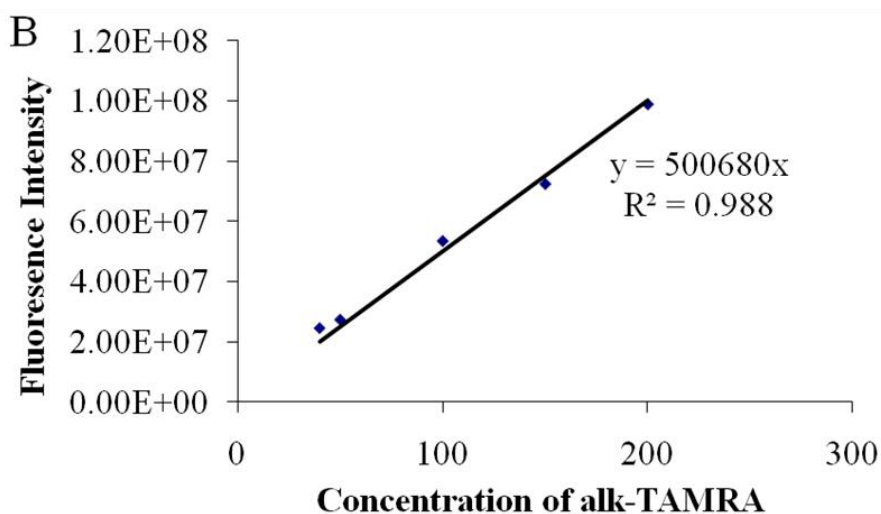


Figure 2-7. Determination of azido sugar incorporation and subsequent chemical modification of *O*-GlcNAz enabled virions with alkyne-fluorophore by Cu catalyzed “click” chemistry. A) Fluorescent gel scanned image of azido sugar enabled virus reacted with alkyne-TAMRA (well 6) and unlabeled virus reacted with alkyne-TAMRA (well 7). The “click” reaction was run overnight in a deoxygenated glove bag. Well 1-5: Decreasing concentrations of standard dye (TAMRA) for determining the concentration of label. The gel was run at 200V for 1 hour at 4°C and scanned within 10 minutes of the end of run. B) Standard curve drawn between fluorescence intensity and concentration of dye loaded on gel. Slope of graph was used to determine concentration of labeled protein.

	Concentration of Dye on 10^{12} viral Fiber (nM)	Dye/ viral particle	Average dye/viral particle
O-GlcNAz labeled	37.2	22.3	21.9 ±1.5
virus	33.2	19.9	
	39.2	23.5	

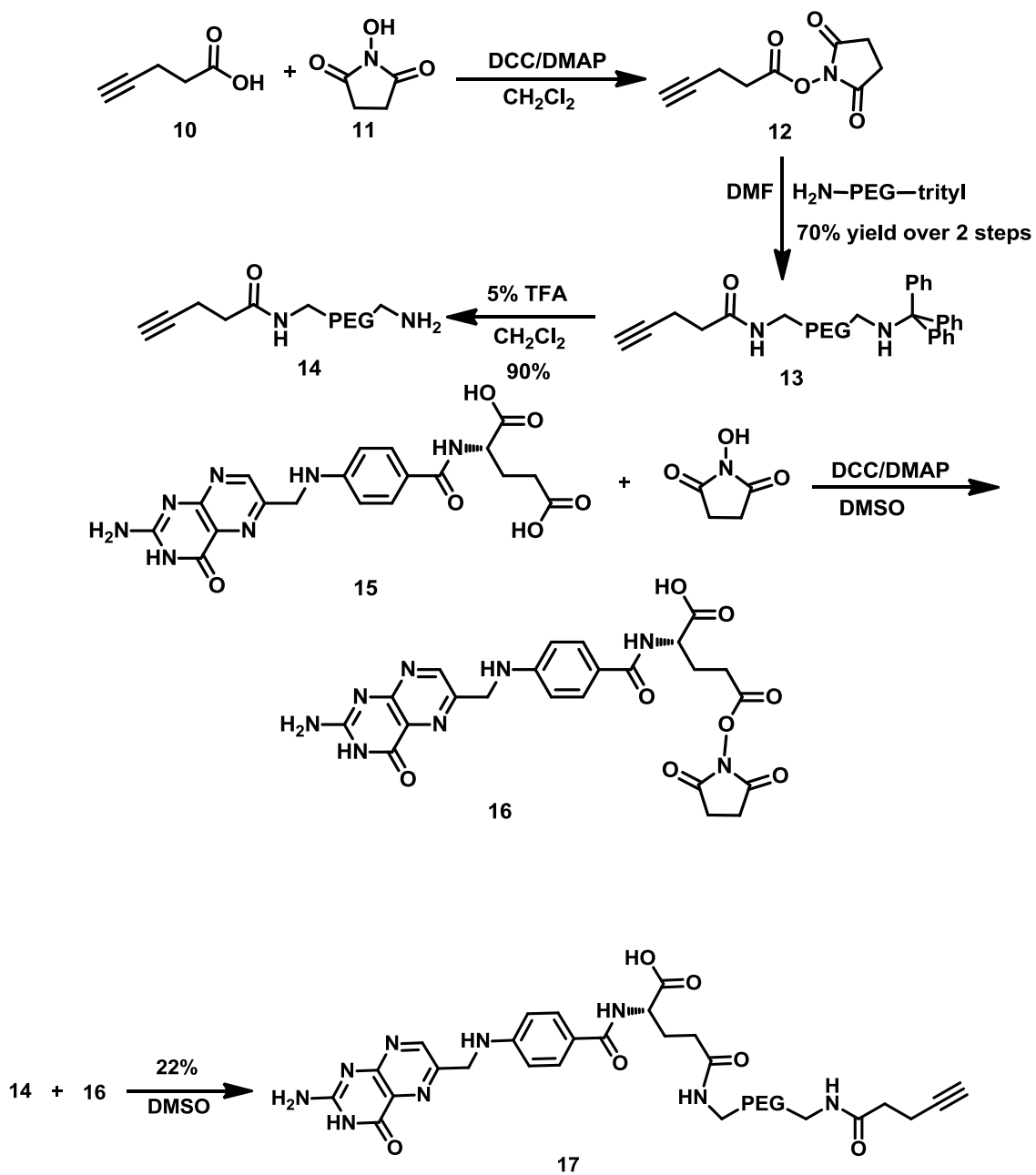
Table 2-1. Summary of viral surface modification using metabolic labeling and chemical modification. Column 1 shows the concentration of dye observed on viral fiber labeled with alkyne-TAMRA (from gel) from three independent experiments. Column 2 shows the corresponding number of dye molecules per virus labeled by Cu catalyzed “click” chemistry with a concentration of 1×10^{12} viral particles/ml loaded on gel. Column 3 is the average of the independent three experiments.

In contrast to genetic engineering, we expected the introduction of *O*-GlcNAz to have little impact on adenoviral physiology. Virus production in the presence of either azido sugar demonstrated no difference on producer cell viability. In addition, no reduction in particle production was apparent as a result of azide incorporation (Figure 2-6). Similarly, infectivity of *O*-GlcNAz labeled virus particles as assessed via standard plaque forming assay, remained unaffected (Figure 2-6). Fluorescently labeled particles (with alkyne-TAMRA) were analyzed to determine the number of chemically addressable azides on

the viral surface. Quantification of the number of azides on each virus by fluorescent gel scanning demonstrated exclusive fiber labeling in agreement with Western analysis (Figure 2-7) and an average attachment of 21.9 ± 1.5 dyes per particle (Table 2-1), consistent with previous *O*-GlcNAc characterization indicating ~50% occupancy at Ser109.(26)

2.2.4. Targeting of *O*-GlcNAz labeled virions

Low CAR expression is exhibited in a number of cancers, including ovarian, pancreatic and gastrointestinal cancers, generally limiting the effectiveness of hAd5 for oncolysis.(61, 81, 178, 209) As a result of tumor associated overexpression and limited abundance in normal tissues, the folate receptor has become an appealing target for cancer therapy.(111, 140) Folic acid is a vitamin essential for cell proliferation and maintenance, it is also essential in the synthesis of nucleotide bases. In normal tissues the proton coupled folate transporter is responsible for uptake of folic acid.(207) In tumor tissues, due to increased proliferation there occurs an upregulation of folate receptors. Ovarian, breast, lung, kidney and brain cancers are reported to have high folic acid receptors.(146) In addition, folate conjugates are easily produced and generally have minor impact on receptor affinity.(175) Previous studies have attempted to utilize chemically attached folate conjugates for adenoviral retargeting. In order to explore *O*-GlcNAz mediated folate modification we synthesized an alkyne probe containing a folic acid residue tethered by a small linker (Scheme 2-2, Figure 2-8).



Scheme 2-2. Synthesis of Alk-PEG-Folate.

2.2.4.1. Synthesis of alkyne-PEG-folate

The folic acid based targeting ligand to be used for virus targeting towards tumorous tissues was synthesized according to established protocols, shown in scheme 2-2.(41) Briefly, pentynoic acid was activated with N-hydroxy succinic acid in presence of dicyclohexyl carbo diimide. The crude activated acid was treated with O-(N-Trt-3-aminopropyl)-O'-(3-aminopropyl)-diethyleneglycol (MW 462) to generate C-protected PEG-alkyne. After TFA assisted trityl- group removal, the product was reacted with NHS-activated folic acid in DMSO. The final product was HPLC purified and characterized by ¹H NMR and ESI mass spectroscopy.

2.2.4.2. Targeting of murine breast cancer cells

O-GlcNAz enabled adenovirus, encoding a GFP transgene in the E1 deleted region of the viral genome regulated by a CMV promoter, was conjugated to alkyne-folate via CuAAC. Mouse breast carcinoma cells (4T1), known to express moderate to high levels of folate receptors(166) and naturally refractive to human adenovirus, were cultured in folate deficient media for 2 weeks. 24 hours after replating, the cells were infected with folate decorated virus at an MOI of 50. One day after infection the GFP expression was visualized. The results demonstrate a high level of GFP expression within the 4T1 cells infected with the folate labeled virus (Figure 2-8).

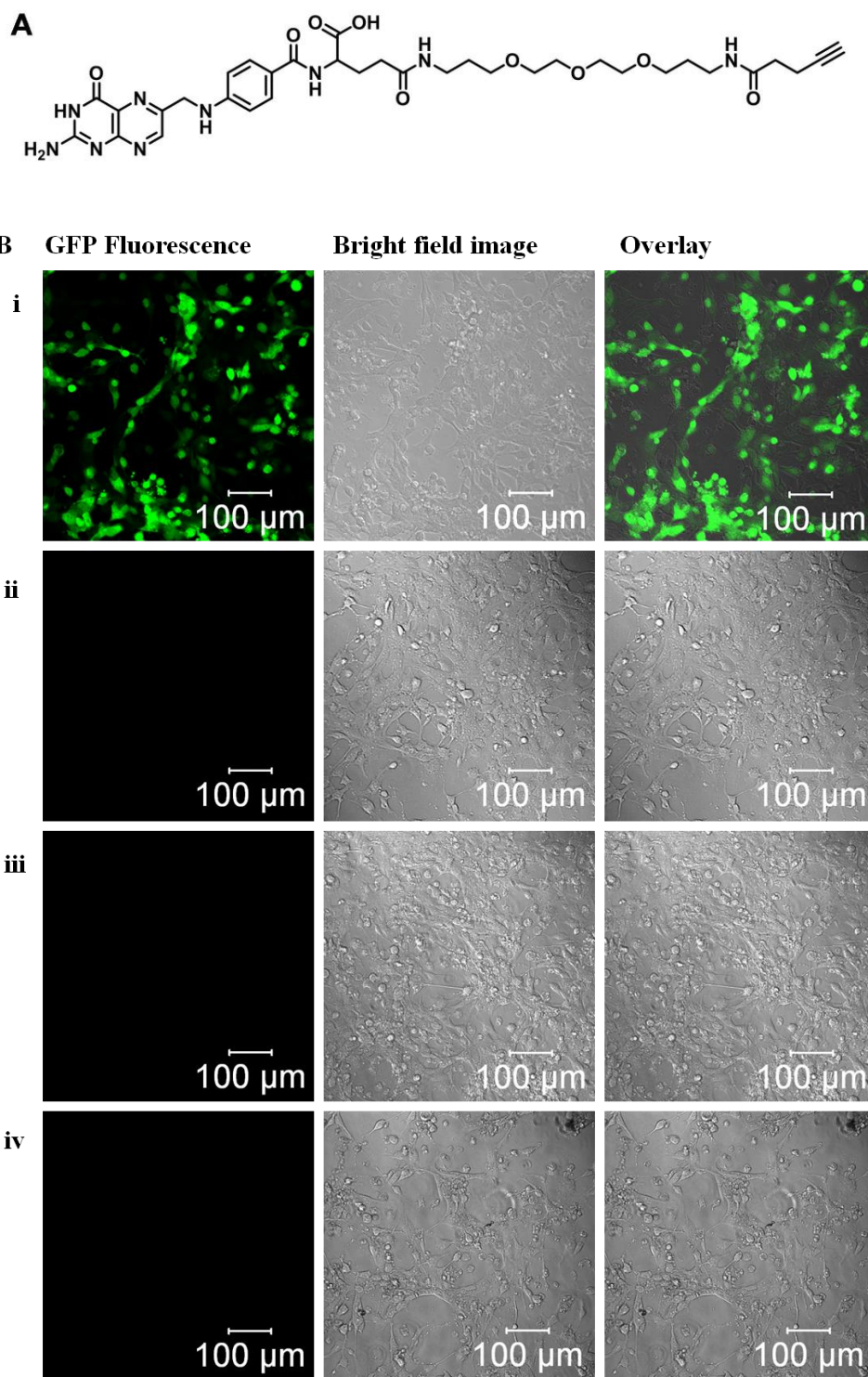


Figure 2-8. Effective gene transduction of murine breast cancer 4T1 cells with folate retargeted Ad5. A) Structure of alkyne-folate ligand. See Synthesis scheme 3 in supplemental information. B) GFP fluorescence microscopy images of alkyne-folate modified metabolically labeled Ad5 virus and

metabolically unlabeled Ad5 infected 4T1 cells. Microscopy was carried out on Glass Bottom dishes using a Zeiss LSM 510 fluorescence microscope. Cells were infected at an MOI of 50pfu/cell and images taken 24hours post infection. (lane i: 4T1 cells infected with folate modified Ac₄GalNAz labeled Ad5; lane ii: 4T1 cells infected with metabolically unlabeled Ad5 (no Ac₄GalNAz); lane iii: 4T1 cells infected with folate unmodified Ac₄GalNAz labeled Ad5 (no alkyne-folate); lane iv: 4T1 cells infected with folate modified Ac₄GalNAz labeled Ad5 pre-treated with 1 mg/L folic acid).

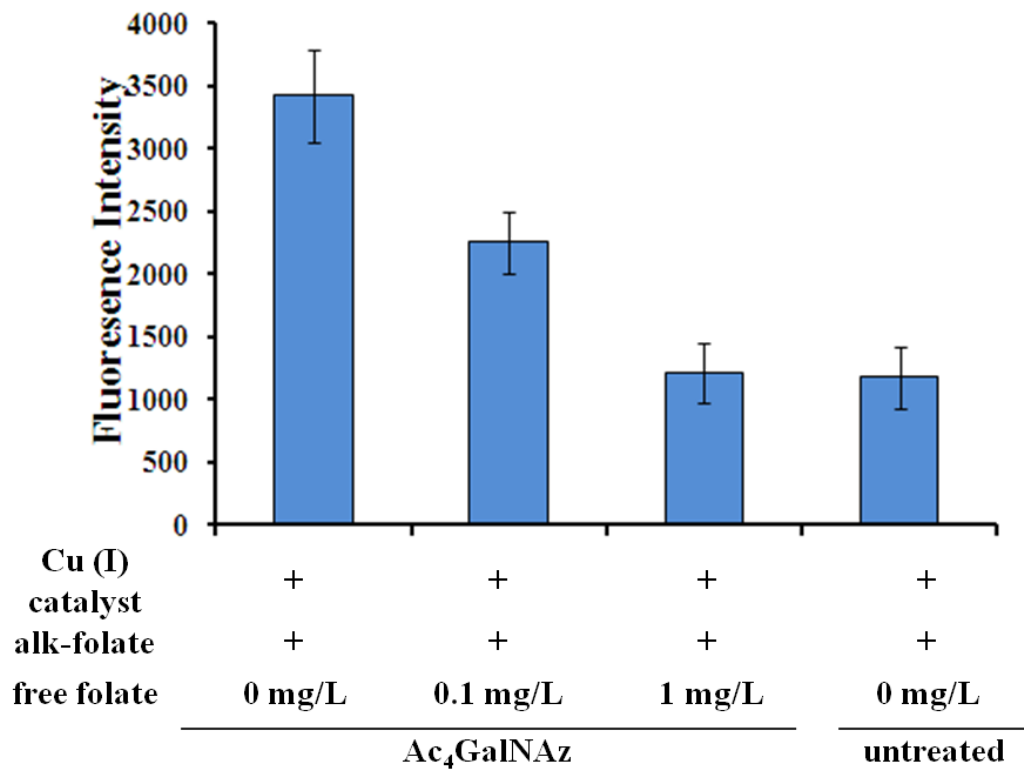


Figure 2-9. Quantification of gene transduction of murine breast cancer 4T1 cells with folate retargeted Ad5. Gene delivery efficiencies (GFP) of alkyne-folate modified Ad5 in the presence or absence of exogenous free folate measured using a Synergy 2 fluorescence plate reader (murine breast cancer cell line (4T1); MOI = 50; 24 hr post-infection; ex: 485 ± 10 nm; em: 528 ± 10 nm). The results are shown as the mean ± standard deviation of the percent relative transduction of at least three independent observations. *, P < 0.05.

Human Ad5 produced without azido sugar, but treated with the folate reagent under CuAAC conditions, failed to produce significant transgene expression. In addition, free folate completely abrogated infection of folate modified hAd5, indicating folate receptor mediated gene delivery.

Quantification of infection was assessed using a Synergy 2 fluorescence plate reader (excitation 485 ± 10 nm; emission 528 ± 10 nm) which showed a 3-4 fold increase of GFP expression in cells infected with metabolically and chemically modified virions versus unmodified virus. Infection assayed in the presence of increasing free folate concentration demonstrated dose dependent transfection inhibition of 4T1 cells (Figure 2-9).

2.3. Discussion

We showed here that adenovirus type 5 particles could be labeled at a specific site on its capsid with an unnatural azidosugar. Using an azido galactosamine derivative, GalNAz, the azide chemical handle was incorporated in place of an *O*-GlcNAc residue occurring on the Ad5 fiber protein. Subsequently the virion can be modified at this specific site by a small molecule or a peptide. Using this two step labeling method, the Ad5 particles can also be retargeted towards tumor tissues.

Two different azido sugar analogs were used in the present study. We synthesized per acetylated forms of both the precursor analogs for efficient cell permeability and added them within virus growth media to incorporate capsid proteins with these analogs. Our analysis showed that, as with previously observed nucleoporin proteins, azidoacetyl galactosamine acts as a more effective surrogate for *O*-GlcNAc residues than azidoacetyl glucosamine. Confirmation of azido sugar incorporation was done via the use of a hexosaminidase assay. It is interesting to note that the *O*-GlcNAc residue is buried inside the virus fiber trimer structure in the fully mature virions, and this structure is inaccessible to enzymatic cleavage. Yet chemical modification occurs effectively at this site – showing chemical accessibility herein. Quantification of chemically modified *O*-GlcNAz labeled virions showed presence of 20 to 22 modifiable sites on each particle. Since one complete virus contains 36 fiber copies, approximately 60% of all available sites seem to be labeled. Earlier analysis showed that about 50 to 60% of fully assembled fibers are *O*-GlcNAc modified. Based on such observations our data suggests not only complete *O*-GlcNAc substitution of virions with the azide surrogates, but even complete chemical modification.

Targeting the viruses using a folic acid ligand shows efficient infection and hence transgene expression within cancer cells. Given the completely unoptimized nature of the alkyne-PEG-folate ligand, presence of the azido sugar on the fiber protein at a site proximal to the natural targeting motif of the virion probably results in ease of receptor access via the attached ligand.

2.4. Summary

In conclusion, we have metabolically labeled human Ad5 viruses with an unnatural sugar derivative, azidoacetyl glucosamine. Fully formed virions isolated from producer cells showed efficient chemical labeling with an alkyne-peptide and a small molecule dye. We could also quantitate the amount of dye per virion labeled using fluorescence based quantification techniques; this gives us an estimate of the total available sites for chemical attachment per virion. Incorporation of this unnatural residue did not in any way hamper virus production or infectivity. We were also able to efficiently target our virions towards murine breast cancer cells using a folic acid targeting ligand. This two step modification can be used to label fully active viruses with not only small molecules, but peptide and proteins as well. This method can theoretically be used to metabolically label other virions containing different glycoproteins. Hence this method provides a novel technique to site specifically modify fully active virus capsid and use them for tissue targeting/ oncolytic therapy.

Chapter 3.

Metabolic incorporation of an unnatural amino acid onto adenovirus capsid

3.1. Introduction

3.2. Results

3.3. Discussion

3.4. Summary

Note. Most of the material in this chapter has been published. (Banerjee, P. S.; Ostapchuk, P.; Hearing, P.; Carrico, I. S. *J. Virol.* **2011**, *85*, 7546). This chapter contains direct excerpts from the manuscript that was written by me with suggestions and revisions by Prof. Carrico.

3.1. Introduction

Adenoviruses (Ad) are widely employed vehicles for gene replacement, cancer gene delivery and vaccine development. As a result of the broad distribution of the coxsackie-adenovirus receptor (CAR), and significant interactions with alternative receptors, most gene delivery applications benefit from more restrictive vector targeting. As a result, significant effort is being invested in both transductional and transcriptional targeting of these vectors.(6, 7, 83)

In the present study a new adenoviral vector platform that retains a number of prerequisites for clinical gene delivery, vaccine applications and diagnostic techniques has been developed. This potentially combines the specificity and covalent attachment of the genetic modifications with the flexibilities of the chemical and adapter systems. This process utilizes residue specific incorporation of a non-natural amino acid azidohomoalanine, a methionine surrogate, onto the viral capsid proteins. Unnatural amino acids have been introduced into simple capsid protein assemblies derived from bacteriophage, plant viruses or hepatitis B.(25, 65, 184) Advantageously, such non-covalent homopolymeric structures are easy to produce from *e.coli* and, as a result, straightforward to engineer.(191) These chemically addressable nanoparticles are excellent candidates for imaging and drug delivery applications; however their simple architecture prohibits infection and gene delivery into mammalian cells. (21)

Metabolic incorporation of amino acids onto mammalian viruses, fully capable of infection and gene expression requires their production from mammalian producer cells.

Labeling of cellular proteins with unnatural amino acids via residue specific incorporation was initially shown by Schumann *et al.* Using a Bio-orthogonal Non-canonical Amino acid Tagging (BONCAT) technique they showed incorporation of Azidohomoalanine (Aha), a methionine surrogate onto newly synthesized proteins within neuronal cells. Subsequently Tirrell *et al.* have spatiotemporally labeled mammalian cells with two different methionine analogs, Aha and HPG and visualized protein expression by dual dye labeling.

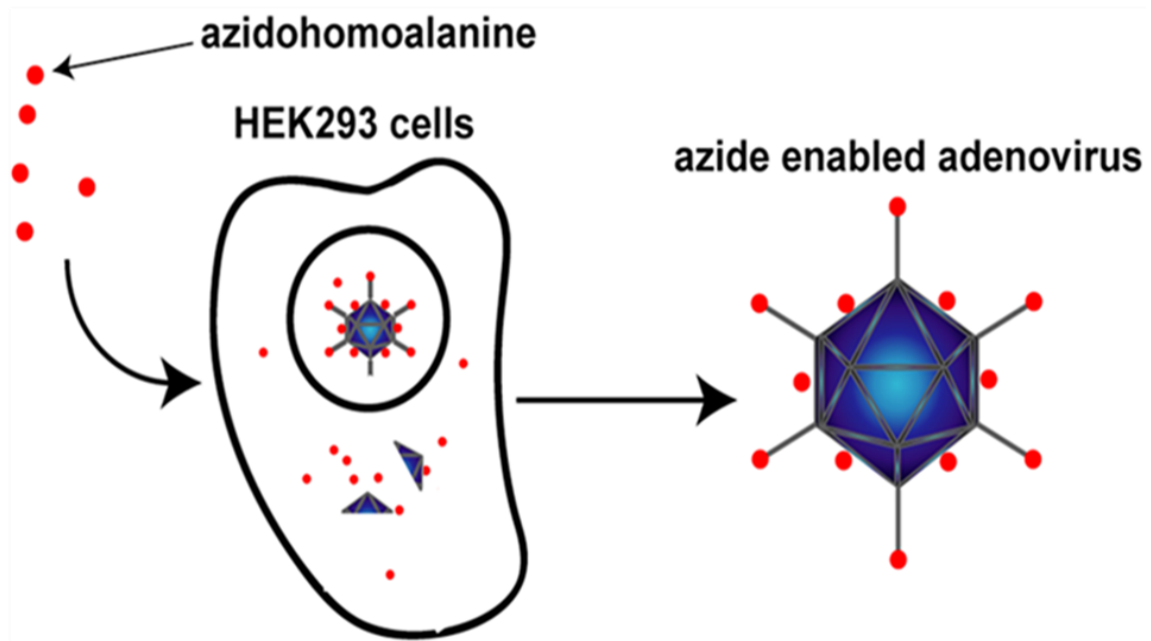


Figure 3-1. Schematic representation of metabolic incorporation of Azidohomoalanine onto adenovirus capsid.

Our approach to labeling adenoviral capsid proteins via this method was based on pulse labeling of the virus producer HEK cells for a six hour window during viral growth

phase. This was done to maximize labeling of structural proteins without substantial effects on other cellular or viral protein synthesis. The six hour time window beginning from 18 hours post infection to 24 hours post infection was utilized for this purpose. A brief look at the Ad5 protein expression profile showed this time to be maximal for structural protein expression (Figure 3-2). A methionine deficient growth media supplemented with the unnatural amino acid was utilized for labeling purposes. Based on previous reports of cellular protein labeling by Aha, within our initial experiments we utilized 4 mM concentrations of Aha for metabolic labeling. This method can be used to substitute a number of capsid methionine residues with Aha – this contains the azide functional group which couples with its bio-orthogonal pair alkyne through electrochemical cyclization to form a triazole adduct.

Use of metabolic labeling approach using mammalian producer cells restricts high levels of azide incorporation due to a pre-existing methionine pool within these cells. Moreover, constant protein degradation, that already contains methionine, presumably increases the endogenous concentrations of the natural amino acid. Studies have shown that charging of the methionyl t-RNA with Aha is the rate limiting step for residue specific unnatural amino acid incorporation.

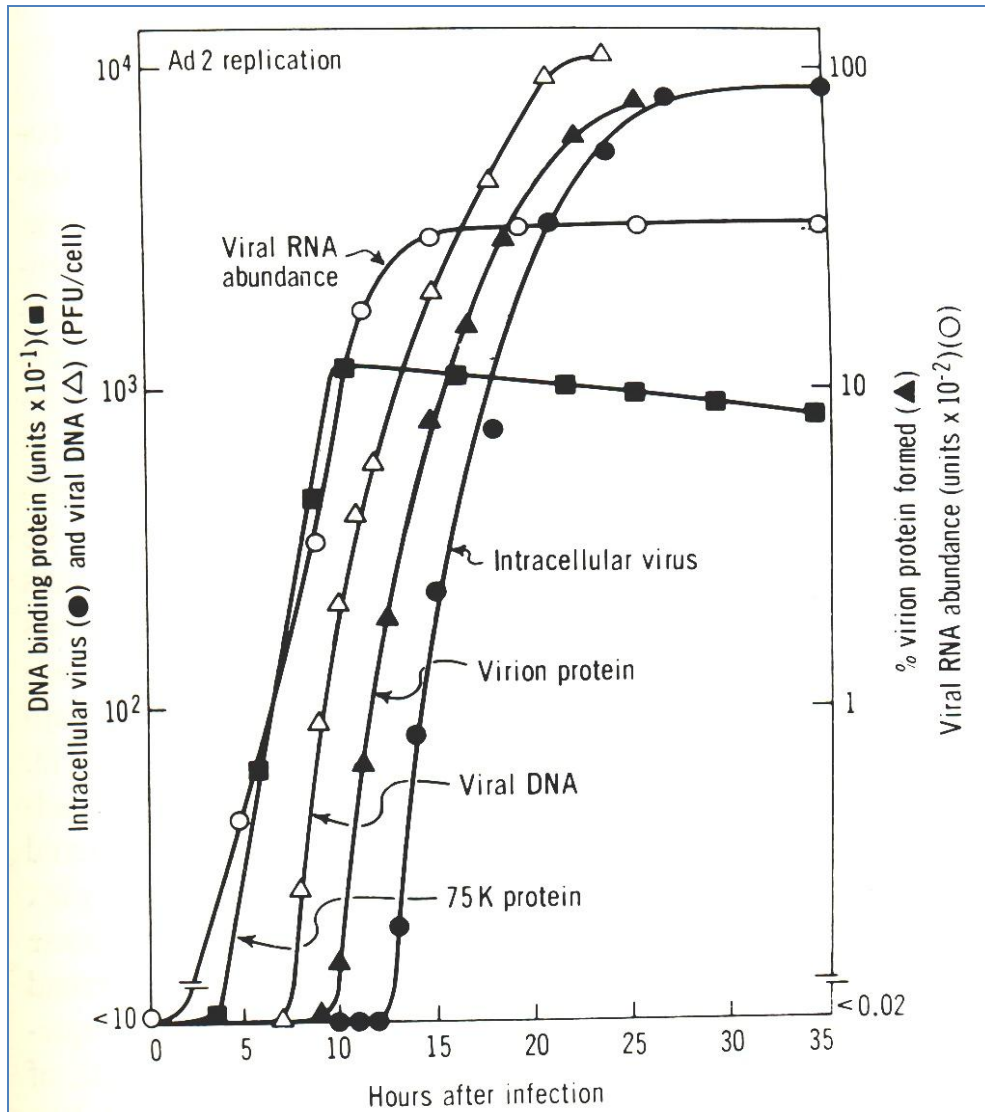


Figure 3-2. Production of adenoviral type 5 proteins hours after infection

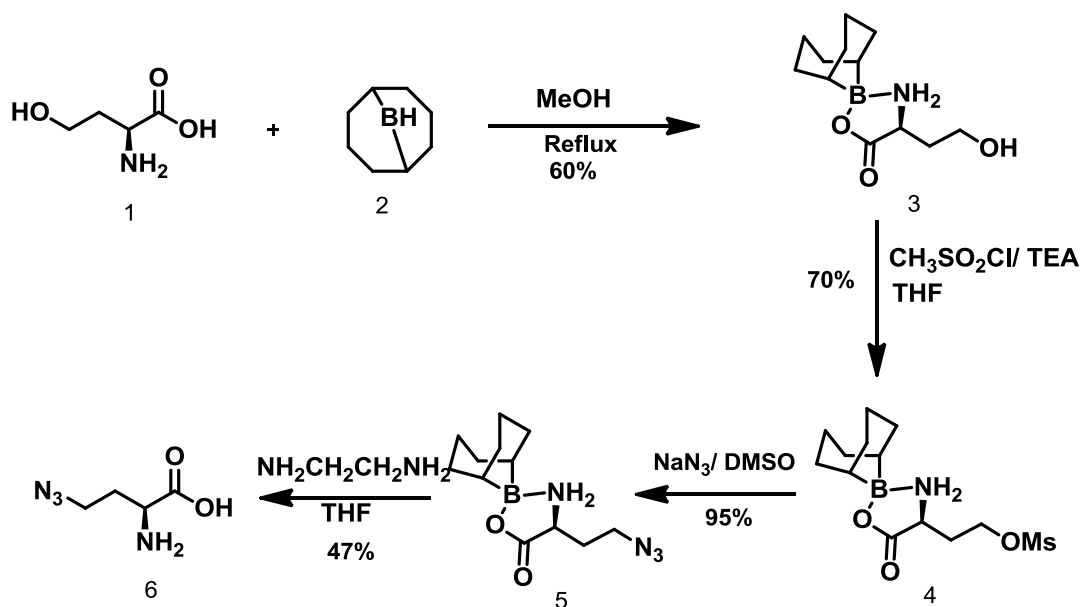
Met is a 490 fold better substrate for the cognate t-RNA synthetase compared to Aha.(86, 95) In spite of such preferences for the native substrate, metabolic labeling would not only be a simple technique to enable adenoviruses with Aha, but more importantly virions produced would probably retain near native structure and infectivity. This is important, since the incorporation of Aha should not impede virus growth or its

subsequent infectivity. We have shown subsequently that the azide enabled adenoviruses can be modified with peptides, fluorophores and cell targeting ligands. Analysis by mass spectrometry and fluorescent scanning confirms substantial incorporation of the azide within viral proteins. Chemically labeled virions can also be retargeted towards breast cancer tissues via folic acid conjugates.

3.2. Results

3.2.1. Synthesis of Azidohomoalanine (Aha)

Azidohomoalanine was synthesized from L-homoserine in four steps. The synthetic scheme is shown in scheme 3-1. L-homoserine was first protected on the amine and the carboxy terminus using a borabicyclononane, 9BBN group. The serine alcohol was then activated with methane sulphonyl chloride and subsequently converted to the azide via substitution with sodium azide. Final de-protection with ethylene diamine afforded the amino acid as a white powder. The synthesized compounds were purified by flash chromatography and characterized by ^1H NMR spectroscopy and ESI mass spectroscopy.



Scheme 2-1. Synthesis of L-azidohomoalanine from L-homoserine.

3.2.2. Production and characterization of Aha labeled adenovirus particles.

Metabolic incorporation of Aha was accomplished by production of adenovirus particles in the presence of methionine-free medium containing the free, unnatural amino acid. Specifically, we infected HEK 293 cells with Ad5 particles at an MOI of 5. Eighteen hours post infection, growth media was removed from the cells and the cells washed with Tris buffer. Methionine-free media, supplemented with 4 mM Aha (–Met/+Aha), was added to each plate of infected cells and the infection allowed to proceed for six hours. At this time the –Met/+Aha media was removed and substituted with complete media until the cells were harvested for virus. At 48 hours post-infection the cells were harvested, lysed and the virus was purified by CsCl equilibrium gradient

centrifugation. In order to generate the appropriate controls, particle production was also carried out with 4 mM methionine and a mixture of 4:1 Aha: Met labeling media.

Incorporation of the non-natural amino acid in the Ad5 capsid was assessed by mass spectrometry analysis. Virus particles were ethanol precipitated, subjected to urea denaturation, followed by dilution and trypsin digestion. LC-MS analysis revealed a number of predicted peptides demonstrated a -5 m/z shift, which is consistent with Met replacement by Aha. In all cases, these peptides were found to co-elute with peptides that corresponded to the natural Met containing sequence. Mixtures of Aha/Met containing peptides indicate that Aha replacement of Met is incomplete, which was expected given our partial metabolic labeling conditions. All of the putative Aha containing peptides were subjected to MS/MS analysis. In all cases, the -5 m/z shift was found to occur at positions corresponding to Met codons confirming the incorporation of Aha. It was tempting to quantitate Aha incorporation via direct comparison of Aha and Met containing peptides. However, this analysis demonstrated very different results indicating either that the incorporation is influenced by sequence, folding constraints or that ionization is impacted by Aha incorporation in a non-linear manner. The latter conclusion is supported by chemical labeling, which largely reflects the product of protein copy number and methionine occupancy. As a result, we have no direct evidence indicating site bias in Aha incorporation.

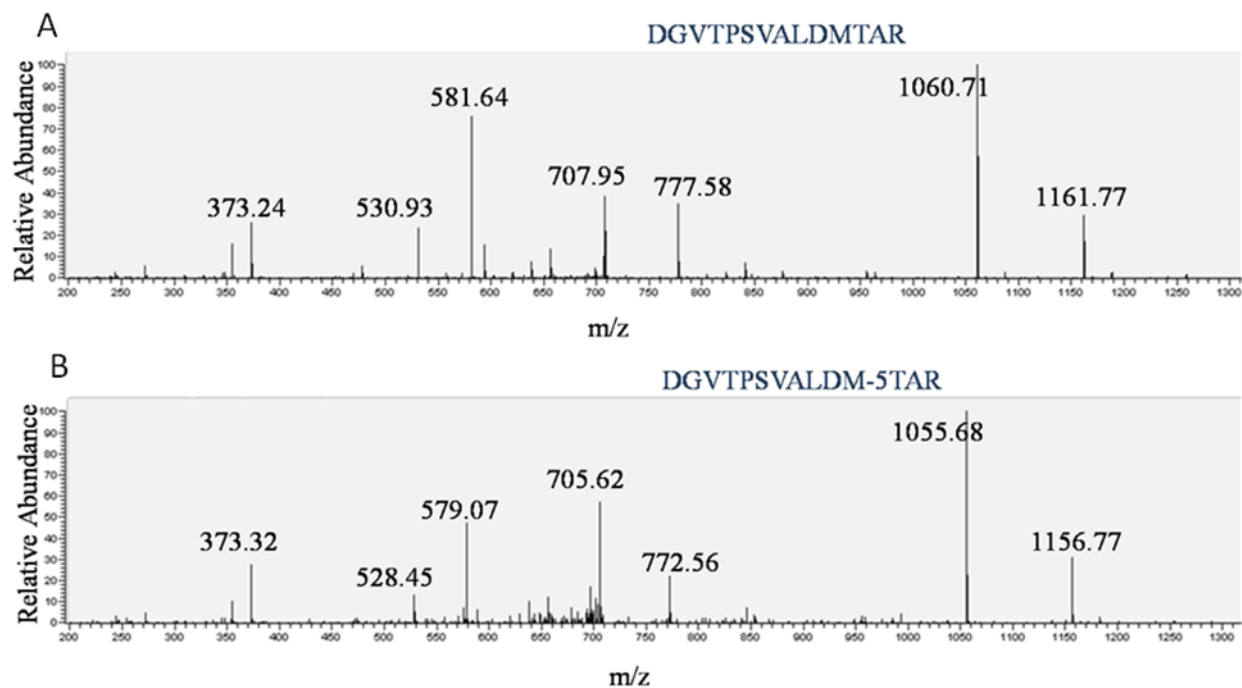


Figure 3-3. Mass spectrometry characterization of Aha labeled adenovirus particles.(11) Representative spectra for a number of peptides visualized after azide labeled modification. Mass spectra of peptide DGVTPSVALDMTAR obtained from adenoviral hexon protein. Figure shows ms/ms spectra of the unmodified (A) and modified (B) peptide obtained after LC/MS analysis respectively. Note the mass difference of 5amu similar to that between methionine and azidohomoalanine. Parent peak for unlabeled peptide occurs at 1432.72 while that for labeled peptide at 1427.72. Peaks observed at 1161.77, 1060.71 and 777.58 are singly charged while those at 530.93, 581.64 and 707.95 are doubly charged.

peptide sequence	charge	parent peak	parent mass	labeled parent mass	labeled parent peak	Adenoviral protein
R.WSLDYMDNVNPFNHHR.N	3	682.31	2044.92	2039.92	680.64	Hexon
R.AAAAAAAAAAISAMTQGR.R	2	716.37	1431.74	1426.74	713.87	Protein VII
R.DGVTPSVALDMTAR.N	2	716.86	1432.72	1427.72	714.36	IIIa
R.YVQQSVSLNLMR.D	2	719.38	1437.76	1432.76	716.88	IIIa
R.SMLLGNGRYVPFHIQVPQK. F	3	728.73	2184.19	2179.19	727.06	Hexon
R.LSEPLVTSNGMLALK.M	2	786.93	1572.86	1567.86	784.43	Fiber
K.ISDNPNTYDYMNK.R	2	787.84	1574.69	1569.69	785.34	Hexon
R.ESGDLAPTVQLMVPK.R	2	792.92	1584.84	1579.84	790.42	Protein V
R.MYSFFRNFQPMR.Q	2	855.90	1710.80	1705.80	853.40	Hexon
K.IGHGLEFDSNKAMVPK.L	2	871.95	1742.90	1737.90	869.45	Fiber
R.AQQQGNLGSMAVALNAFLST QPANVPR.G	3	904.80	2712.40	2707.40	903.13	IIIa
K.VVLYSEDVDIETPDTHISYM PTIK.E	3	922.46	2765.37	2760.37	920.79	Hexon
R.LMVTETPQSEVYQSGPDYF FQTSR.Q	3	937.44	2810.31	2805.31	935.77	IIIa
K.GLMFDATAIAINAGDGLF GSPNAPNTNPLKTK.I	3	1115.90	3345.69	3340.69	1114.23	Fiber

Table 3-1. List of the peptides identified after Inspec search following LC/MS treatment of trypsin digestion of Aha labeled adenovirus particles.

A number of viral peptides were observed to incorporate the M-5 modification (Aha being 5 mass units less than Met) as shown in Figure 3-3, details of peptides incorporating Aha is listed in Table 3-1. Sequencing of the flagged M-5 peptides revealed the mass change occurred at methionine codons. Furthermore, analogous peptide determination of the amount of incorporation was challenging with the LC/MS approach due to inherent differences in peptide migration under mass spectrometry conditions. Thus we decided to focus on the percent of chemically modifiable residues, which would present a more appropriate picture of the attachment sites available due to Aha incorporation.

3.2.3. Chemical modification of Aha labeled virus

For specific chemical labeling of azides, three different reaction techniques have been developed. Copper assisted “click” reaction, the Staudinger ligation reaction and the strain promoted electrocyclization. For our experiments we have used both the copper assisted “click” reaction and the Staudinger ligation reaction. For this the purified Ad5 viral particles were subjected to copper assisted azide alkyne cycloaddition reaction (64) with an alk- TAMRA ligand. Reaction was carried out in a deoxygenated glove bag overnight in the presence of 1 mM copper (I) bromide and 3 mM SBP

(bathophenanthroline disulphonic acid disodium salt) ligand. Fluorescent gel scanning was performed on the whole virus particle run on a SDS-PAGE gel. Gel scanning showed strong labeling on a number of the adenoviral capsid proteins (Figure 3A) for samples labeled with 4 mM Aha. No signal was observed with metabolically unlabeled virus or “click” reactions carried out in the absence of copper.

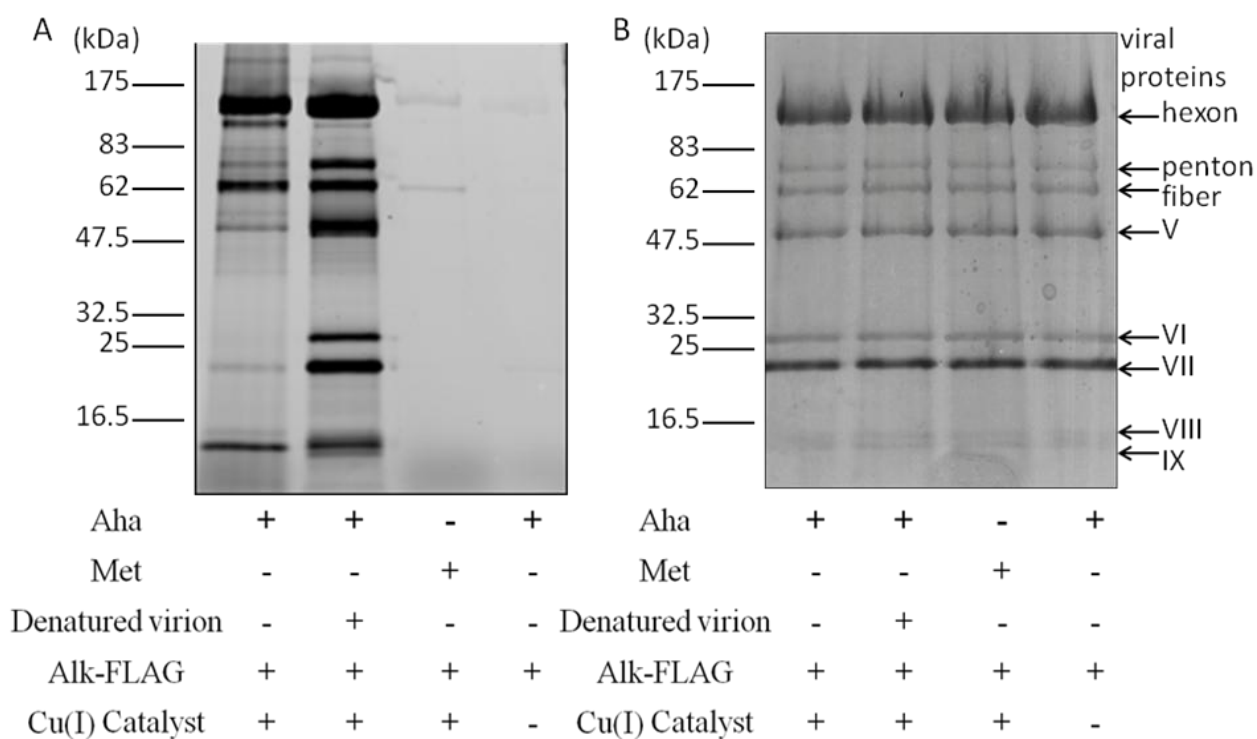


Figure 3-4. Chemical labeling of Aha incorporated into adenovirus particles. A) Gel scanning analysis of adenovirus particles metabolically labeled with azidohomoalanine and chemically modified with an alk-TAMRA via CuAAC chemistry (for lanes 1-3 chemical labeling is performed on intact virus particles; lane 4 shows “click” labeling on denatured virus. Since the SDS gel shown in B cannot discriminate between protein IIIa or fiber, both or either are possibly getting labeled by Aha and “click”). B) SDS-PAGE gel of CBB stained adenovirus proteins with individual proteins indicated. Viral particles are metabolically labeled with Aha and chemically modified with alk-TAMRA as in (A).

Virus particles denatured before chemical labeling showed greater dye labeling on a number of viral proteins with couple of the core proteins also showing chemical modification. TAMRA labeling suggests modification occurs in hexon, penton, fiber and pIIIa on the intact virus. Protein IX can also be seen to be labeled with the alkyne-TAMRA supporting the observation that the N-terminal is solvent exposed. Together these data suggest that adenoviral capsid proteins bear Aha at methionine sites and are exclusively labeled at solvent accessible methionine sites.

3.2.4. Assessment of viral fitness

In order to discern the impact of Aha incorporation on viral fitness, virus particle production and standard plaque forming assays were performed. There was no discernable effect of Aha incorporation in the viral particle production as estimated by standard UV absorption assay (Figure 3-5). In addition, plaque forming ability of metabolically labeled virion was equivalent to unlabeled virus (Figure 3-5).

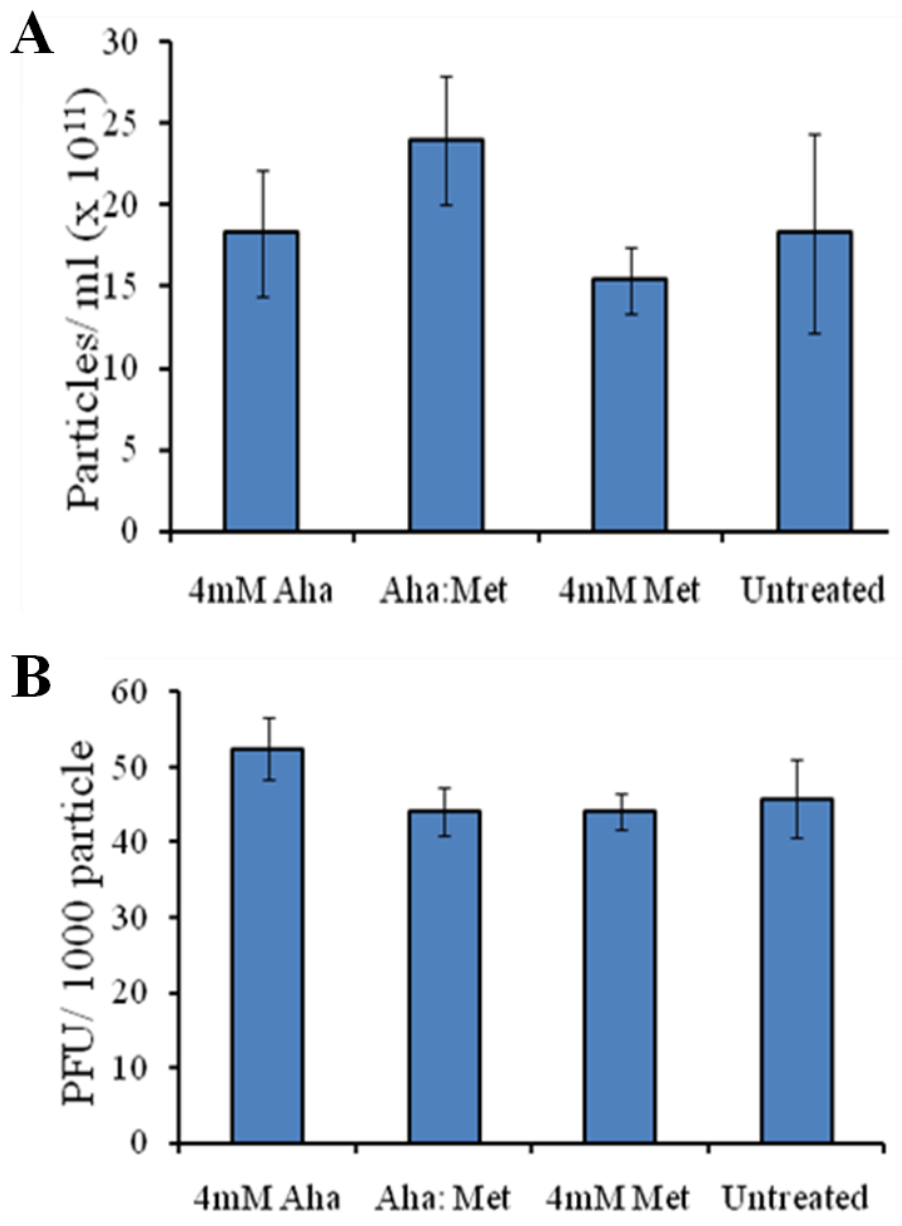


Figure 3-5. Effects of unnatural amino acid incorporation on adenoviral particle production and infectivity

A) Particle count of virus produced in the presence of azidohomoalanine, methionine, a mixture of Aha and Met and without metabolic label. Labeling carried out by pulsing with Aha or Met supplemented media between 18 to 24 hours post-infection using 4 mM concentrations of surrogate amino acid. Particle counts are measured by absorbance at 260 nm. B) Infectivity of azide enabled viral particle by plaque forming assay. 293 cells infected with 10^3 azide-Ad5 particles. Infected cells were overlaid with bacto-agar containing Neutral Red and plaques counted 7 days after initial infection.

To estimate if viral protein expression was somehow hampered during the period of Aha exposure, Ad5 infected cells labeled for 6 hours (18 to 24 hours post infection) with 4 mM Aha were lysed 24 hours after infection and analyzed for penton production by western blot with an anti-penton antibody.

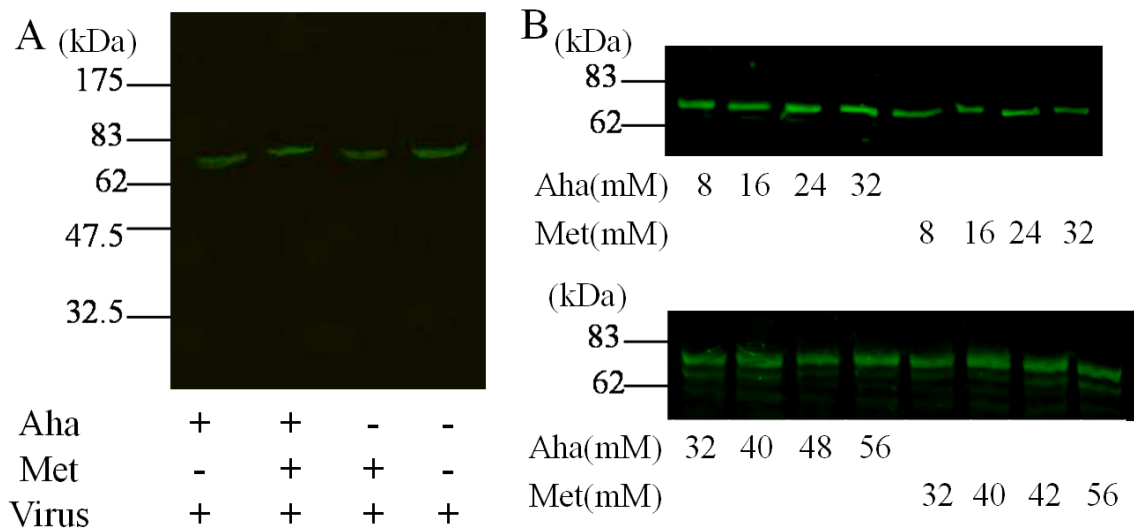


Figure 3-6. Determination of adenoviral penton protein production during metabolic labeling of Aha. A) Infected cells grown in the presence of Aha, Met, Aha+Met or unlabeled from 18 to 24 hours post infection were lysed 24 hours post infection and protein production probed using an anti-penton antibody. B) Determination of adenoviral protein production during labeling with increasing Aha concentration as compared to increasing Met concentration. Infected cells grown in the presence of different concentrations of Aha or Met, 18 to 24 hours post infection were lysed 24 hours post infection and protein production probed using anti-penton antibody. An IR680 dye was used as secondary. The blots were visualized using an Odyssey LICOR, excitation at 680 and emission at $700 \pm 15\text{nm}$.

Development of the blot with an IR fluorescent dye showed no loss in penton expression during labeled infection as compared to particles produced in complete media or in methionine-free media with exogenous methionine supplied (Figure 3-6). Taken together, normal protein expression through the metabolic labeling period, standard particle production and fully infective viruses indicate that Aha has little impact on either structural protein folding or particle virus assembly. While this is surprising at a superficial level, a closer examination of the surface charge and steric occupancy of Met and Aha demonstrate that they are very similar.(86)

Thermo stability of virus labeled with Aha was assessed by measuring intrinsic tryptophan fluorescence of the virion as a function of temperature.(158-160) Results showed (Figure 3-7) that structural transition of the metabolically labeled virions followed similarly to that of unlabeled particles with virus disassembly occurring between 45°C to 50°C.

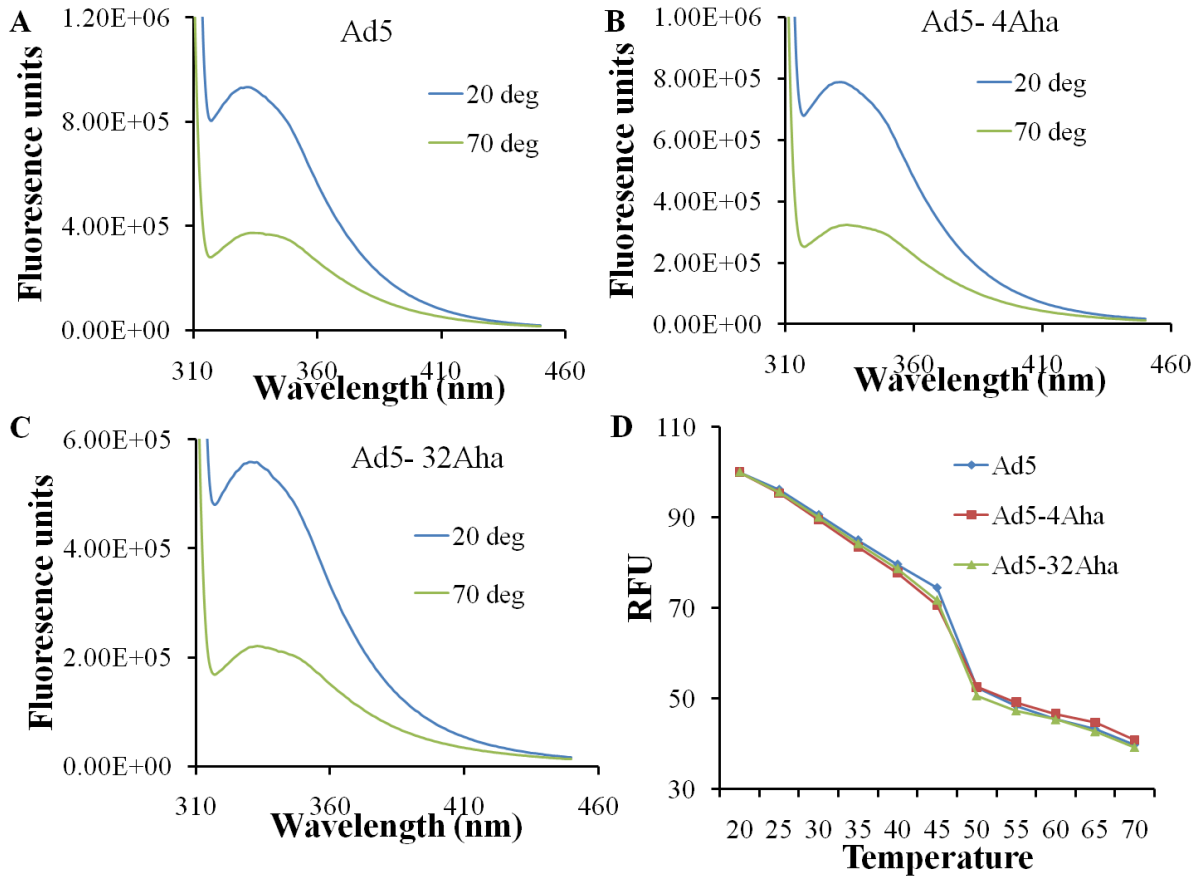


Figure 3-7. Shelf life and thermo-stability of Aha labeled adenovirus. Virions metabolically labeled with 4 mM (B) and 32 mM (C) Aha and metabolically unlabeled (A) with Aha were checked for intrinsic tryptophan fluorescence as a function of temperature. Results showed no appreciable change in virion stability as a result of unnatural amino acid incorporation. Relative fluorescence maxima plotted against temperature showed all samples undergoing structural changes between 45 to 50 °C.

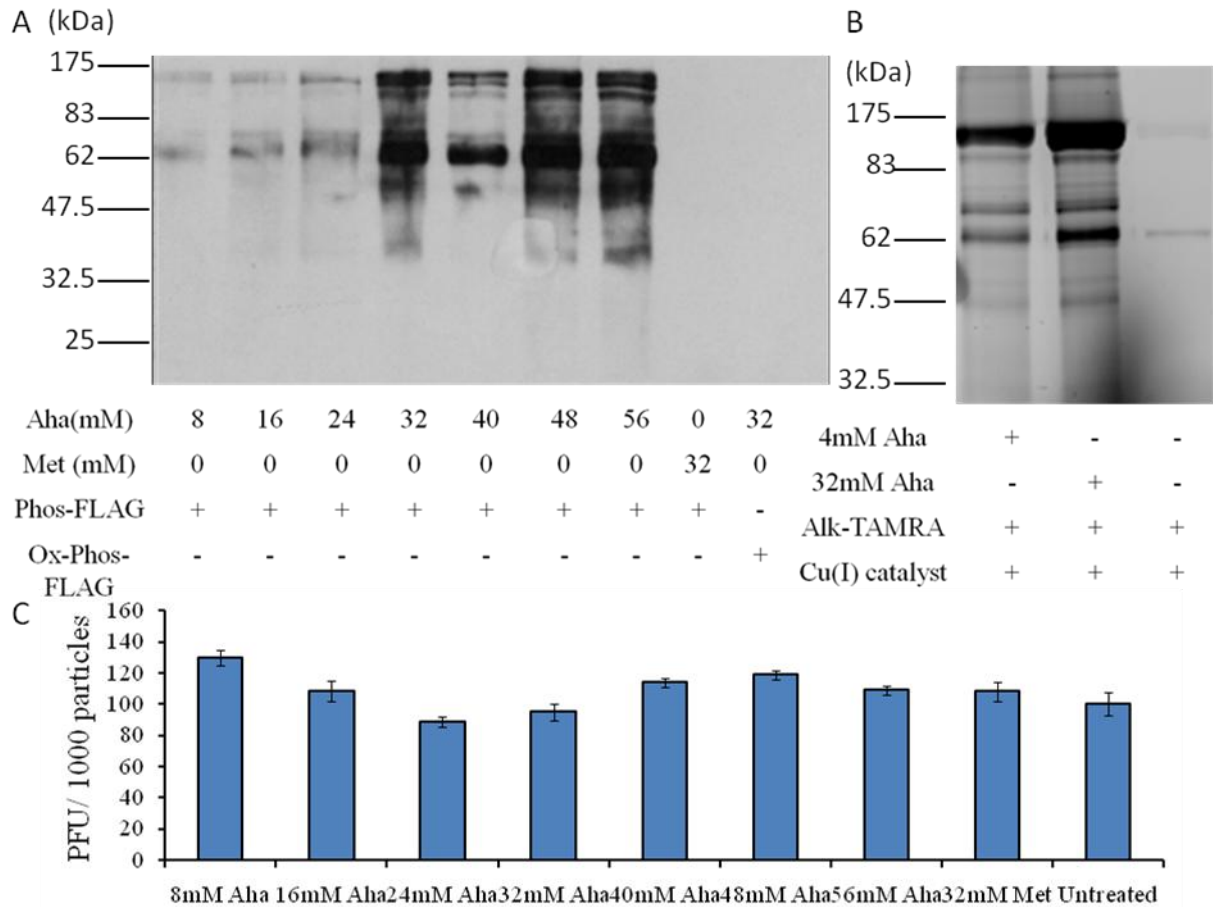


Figure 3-8. Increasing concentrations of Aha shows higher levels of azide incorporation without substantial loss of viral fitness. A) Western blot of virus particle produced with increasing Aha concentration from 8 mM to 56 mM. The particles were modified with a phosphine-FLAG reacted for 2 hours and probed with an anti-FLAG antibody. B) Fluorescent gel scan of virus particles labeled with alkyne-TAMRA (a rhodium dye) produced at 2 different concentrations of Aha, 4 mM and 32 mM. Standard concentrations of TAMRA were used to determine the number of dye molecules coupled to each viral particle. Based on the protein marker the Hexon, Penton and Fiber appear to be labeled with Aha. Total number of dyes per particle was calculated by estimating number of label for each of these three proteins. C) Infectivity of increasing Aha incorporated adenoviral particles was assayed by plaque forming ability as compared to Met labeled controls.

As virus production seemed unaffected while labeling with 4 mM Aha, we wanted to assess whether an increase in the concentration of the non-natural amino acid in the growth media reflects an increase in azide dependent labeling and whether this results in any detrimental effects on virus growth and infectivity. Thus we repeated the labeled infection process with 8 mM, 16 mM, 24 mM, 32 mM, 48 mM and 52 mM Aha supplemented methionine-free media from 18 to 24 hours post-infection. Staudinger ligation reaction with FLAG peptide bearing phosphine probe and labeled cell lysate 24 hours after infection followed by anti-FLAG western analysis with anti-FLAG antibody demonstrated saturation of metabolic labeling at 32 mM (Figure 3-8). Assessment of protein production during this time showed no reduction in penton protein production as a result of increased Aha labeling (Figure 3-6). Plaque assays were also performed in parallel with increasing Aha labeled virus. The results show that there occurs no effect on the infectivity of these azide enabled particles even at 56 mM Aha. This suggests that Aha is not toxic to the cells and does not hamper normal cellular processes even at high concentration. Also virus particles labeled with high levels of Aha seem to behave normally with respect to particle stability and infectivity (Figure 3-8). For subsequent quantification of Aha incorporation and targeting of these tagged viruses towards cancerous cell types, both 4 mM as well as 32 mM Aha labeled virus samples were used.

Infectivity of dye labeled virions was also assessed to determine effects of chemical incorporation on virus fitness. Aha enabled AdLuc modified with TAMRA and used to infect 293 cells at an MOI of 1 and luciferase expression of infected cells were quantified 24 hours post infection. Viruses without being subjected to chemical modification were

also used for comparison. Results showed (Figure 3-9) a small loss in infectivity of chemically treated versus untreated virus.

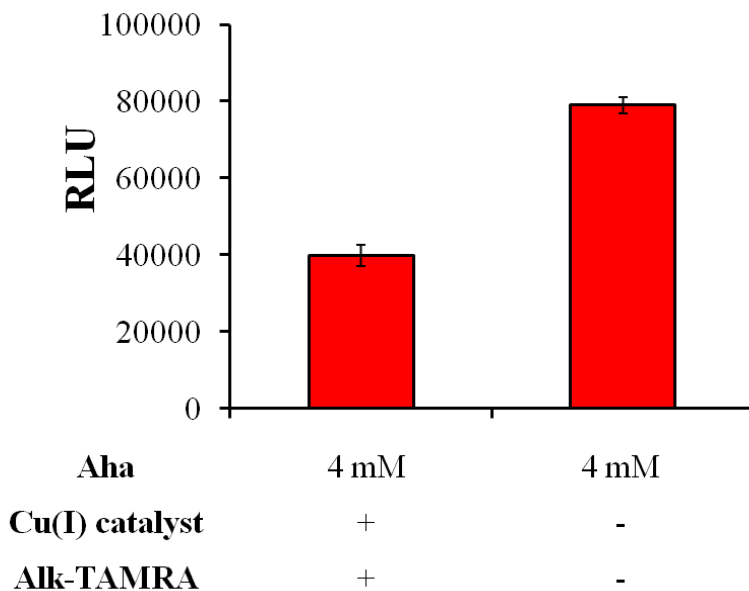
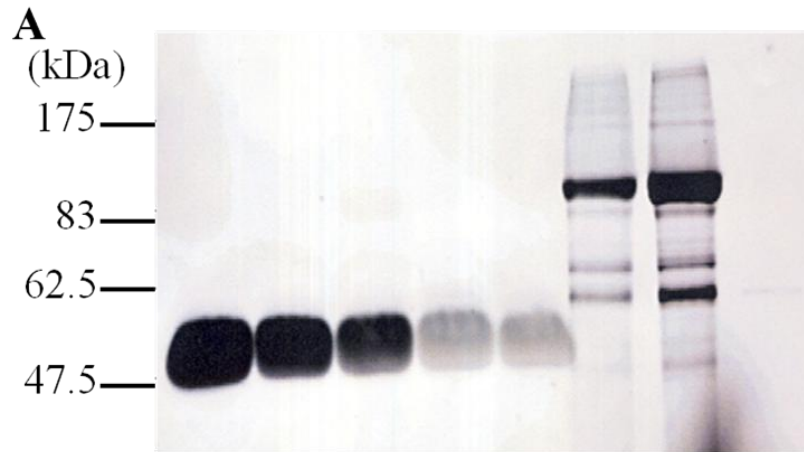


Figure 3-9. Effect of chemical labeling on adenovirus infectivity. Aha enabled AdLuc were chemoselectively labeled with alk-TAMRA via copper catalyzed “click” chemistry. These were used to infect 293 (human embryonic kidney) cells at an MOI of 1. Luciferase activity was measured 24 hours post infection.

3.2.5. Quantification of chemical labeling of Aha-enabled hAd5

The exposed surface of adenovirus capsid is thought to be composed of five structural proteins based on X-ray crystallographic and cryo-EM structural data.(52, 170, 171) Of these, hexon, the most abundant capsid protein is about one-third solvent exposed surface

area.(168, 193) The penton and fiber proteins also are largely solvent accessible.(135, 205) In contrast, protein IIIa and IX have only small exposed segments.(53, 120, 173) As chemical derivatization was performed on intact particles, modification of Aha by alkyne probes is expected to occur only when solvent exposed. In addition, the number of attached probes on the viral capsid should be proportional to the effective percent incorporation of azidohomoalanine within the viral proteins. The number of exposed methionine sites within the three main structural proteins, hexon, penton and fiber are 8, 5 and 3 respectively, estimated by analysis of X-ray structures for these proteins. As shown in Table 3-2 this analysis estimates ~6000 exposed methionine on the adenoviral capsid. To calculate the number of modifiable azides on the adenovirus capsid, the 4 mM and 32 mM Aha-labeled viral particles were modified with a fluorophore, an alkyne-tetramethyl rhodamine dye (alk-TAMRA) using copper assisted “click” chemistry. The modified virus was separated from excess catalyst and probe on a spin column and the subsequent particle count estimated with QuantIT picogreen assay (132). TAMRA labeled particles were run on 10% SDS PAGE and analyzed on a fluorescent gel scanner. Known concentrations of alk-TAMRA were also run as standard (Figure 3-10). The scanned gel was analyzed with Image Quant TL1D gel analyzer software and the average number of dye molecules on 3 major coat proteins with three independent reactions was calculated (Table 3-2). The average total number of modified sites on each 4 mM and 32 mM Aha labeled virus being 279.5 ± 8.6 and 512.0 ± 7.8 respectively. Thus covering about 5.5% and 10% of the estimated total exposed methionine sites for adenovirus type5 (Table 3-2).



Alk-TAMRA(nM)	200	150	100	50	40			
Aha labeled Ad5 (mM)						4	32	0

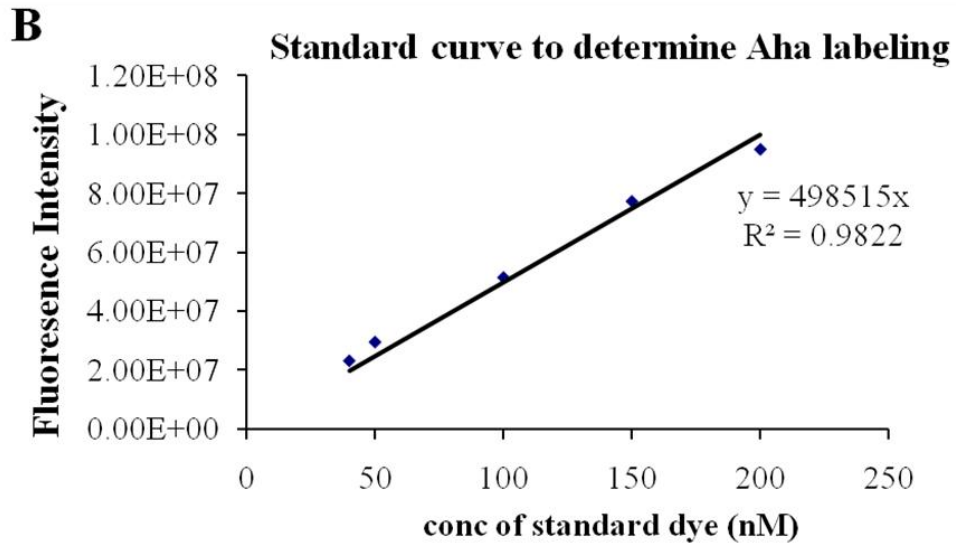


Figure 3-10. Determination of labeling of Aha enabled virus with alkyne-fluorophore by Cu catalyzed “click” chemistry. A) Fluorescent gel scanned image of Aha enabled virus reacted with alkyne-TAMRA (well 6 and 7) and unlabeled virus reacted with alkyne-TAMRA (well 8). The “click” reaction was run overnight in a deoxygenated glove bag. Well 1-5: Decreasing concentrations of standard dye (TAMRA) for

determining the concentration of label. B) Standard curve drawn between fluorescence intensity and concentration of dye loaded on gel. Slope of graph was used to determine concentration of labeled protein.

Adenoviral structural proteins*	Total no. of methionine residues per polypeptide	Estimated solvent exposed methionine (from crystal str.)	Copies of protein per VP	Estimated total no of solvent exposed MET per VP	Average number of chemically labeled dyes per VP	
					4 mM Aha	32 mM Aha
Hexon	20	8	720	5760	196.1 ± 4.6	358.3 ± 10.4
Penton	12	5	60	300	36.6 ± 1.8	57.3 ± 3.6
Fiber	10	3	36	108	47.1 ± 2.8	96.5 ± 0.7

*these 3 protein X-ray crystal structures were used to estimate the average number of exposed methionines per VP

Table 3-2. Estimated number of solvent exposed methionine residues on adenoviral capsid proteins based on X-ray and Cryo-EM structural information (PDB ID 1P30, 1X9P, 1X9T AND 1QHV) and the observed number of Aha residues incorporated in each of the discussed proteins.

3.2.6. Targeting of Aha enabled virions

To evaluate the potential of using sites of azide introduction for targeting element attachment, we modified Aha-enabled hAd5 with alk-folate. Folate conjugates have been extensively used over the past decade to target cytotoxic and imaging agents to a number of different types of cancer (111). Advantageously, the folate receptor (FR) has high affinity for folate conjugates, mediates endocytosis, is restricted to the apical surface of polarized epithelium (except in the kidneys), and is over expressed in variety of tumors (166). Breast carcinoma cells 4T1, of murine origin, reported to have over expressed folate receptors were used for our study. Use of folic acid in retargeting of adenoviruses has also been attempted by the attachment of PEGylated folate to lysine residues on adenoviral coat proteins (140).

We followed a similar targeting approach by synthesizing an alk-PEG-folate ligand containing a 462 MW PEG as linker (Figure 3-11). A GFP or Luciferase transgene bearing Ad5 was produced in the presence of 4 mM and 32 mM of Aha as has been described earlier, metabolically unlabeled and methionine labeled particles were used as control. The targeting molecule (alk-PEG-folate) was “clicked” onto azide enabled adenoviral particles with GFP or Luciferase as reporter and the virus purified on a Centriscip spin column and quantified with QuantIT picogreen

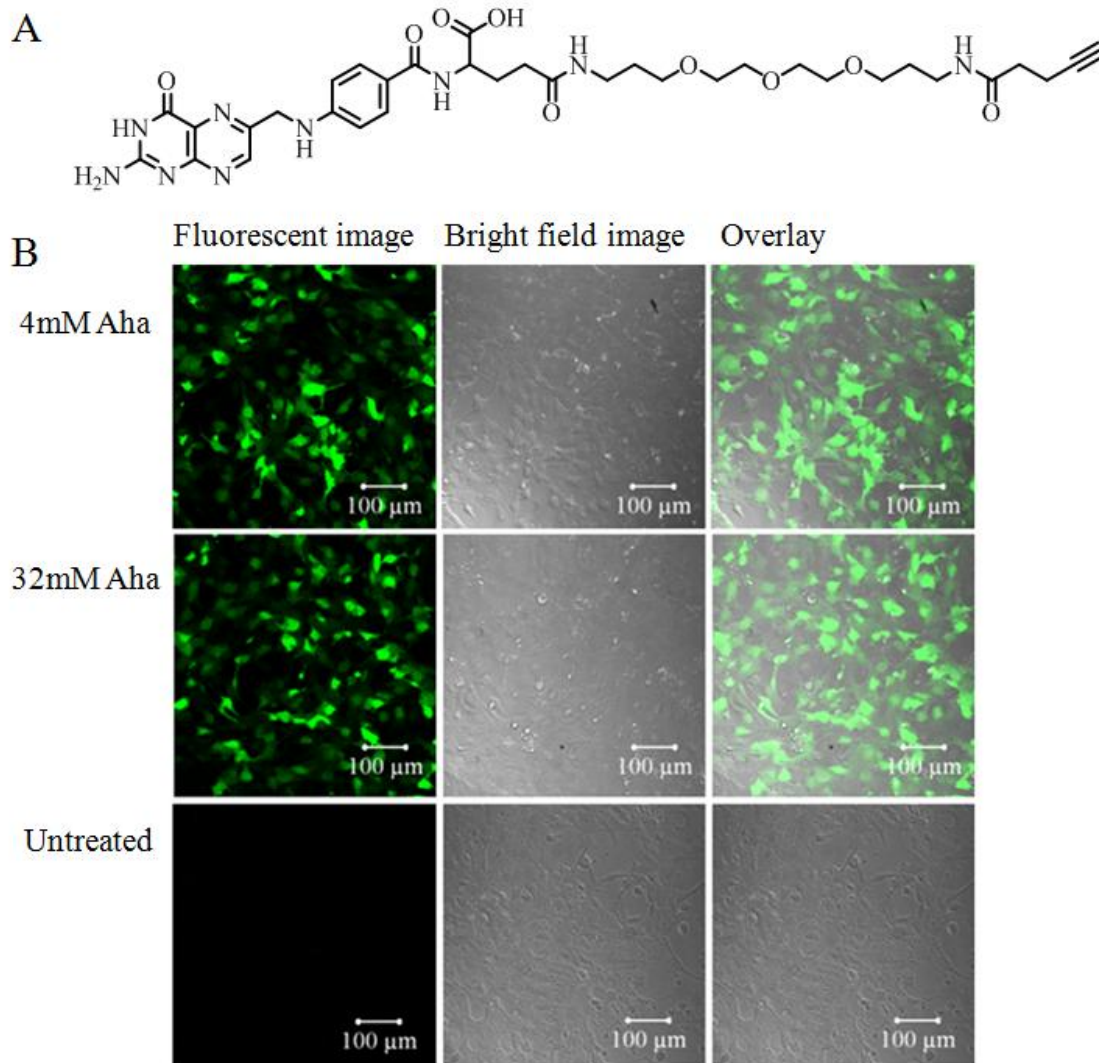


Figure 3-11. Viral particles metabolically labeled and chemically modified used to target a murine breast cancer cell line, 4T1. A) Structure of alkyne-PEG-Folate used to modify azide enabled adenovirus capsid encoding a GFP transgene. B) Fluorescence microscopy of 4T1 cells infected with 4 mM and 32mM Aha labeled virus and metabolically unlabeled virus that have subsequently been modified with alkyne-peg-folate using "click" chemistry. Cells were infected at an MOI of 50, and images captured 24 hours post infection. Microscopy was carried out on a glass bottom dish mounted on a Zeiss LSM 510 microscope. Fluorescent images were taken with a GFP filter.

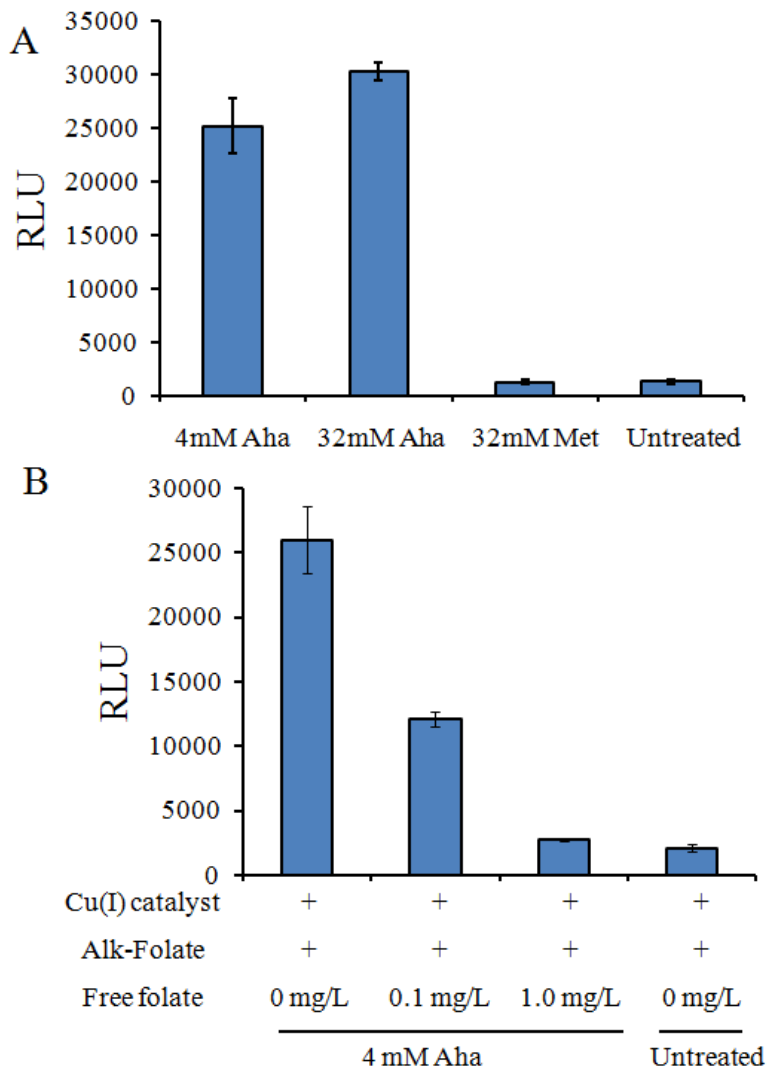


Figure 3-12. Quantification of gene delivery of virus particles targeted towards a murine breast cancer cell line, 4T1 with and without competing free ligand. A) Luciferase expression of 4T1 cells 24 hours post infection with azide labeled (4 mM and 32 mM), methionine labeled and metabolically unlabeled virus particles (Ad-Luciferase) all treated with alkyne-peg-folate. Luciferase activity was measured using a Perkin Elmer chemiluminescence plate reader (ex: 485 ± 10 nm; em: 528 ± 10 nm). B) Luciferase activity measurement as in part A using virus particles labeled with 32 mM Aha but this time infection carried out in presence of external folic acid 0 mg/L, 0.1 mg/L and 1 mg/L.

. Confocal microscopy of 4T1 cells infected with folate labeled and metabolically unlabeled virus was also performed using a Zeiss LSM 510. For this 1.1×10^5 4T1 cells were seeded in glass bottom dishes and infected with the modified and unmodified virus particles. 24 hours post-infection the cells were imaged and data analyzed in Zeiss LSM 510 software. The results (Figure 3-11) show a high level of GFP expression in these breast cancerous cell types with the folate targeted virus as compared to the unmodified particles. For quantification of transgene expression, 4T1 cells were grown on minus folate media for 2 weeks after which time they were seeded in 24 well plates at a concentration of 1×10^6 cells per well. They were infected with labeled adenovirus the next day at an MOI of 50 and Luciferase expression was used to monitor transductional retargeting ability 24 hours post-infection using a Perkin Elmer Victor X5 luminescence plate reader (Figure 3-12). The data showed an 18 to 20 fold increase in transgene expression with the modified adenoviral particles compared to the unmodified samples. Competition experiments with free folic acid showed loss of Luciferase activity at higher folate concentrations. Overall the targeting results with the fluorescent microscopy and luciferase quantification experiments suggest effective retargeting of the viral particles towards folate receptor over expressing murine breast cancer cell types.

3.2.7. Dye labeled Ad5 for cell imaging

To determine whether the dye labeled virions could be used to image cell infection, TAMRA labeled adenovirus particle were used to infect mammalian embryonic kidney cells, HEK 293. These cells are naturally Ad infective and hence were used as models to determine imaging of infection. 293 cells were seeded on glass bottom dishes at concentrations of 1×10^4 cells and infected with dye labeled Ad5 at two different MOI of 5 and 10. Twenty minutes post infection, the cells were washed with TD buffer and covered with complete media. The cells were then imaged on a Zeiss 2 photon con-focal microscope and data analyzed in Zeiss LSM 510 software. The results showed that a number of dye labeled virions could be visualized on the cell surfaces. This showed that dye labeling could be used as a potential too for bio-distribution studies of Aha enabled viral particles.

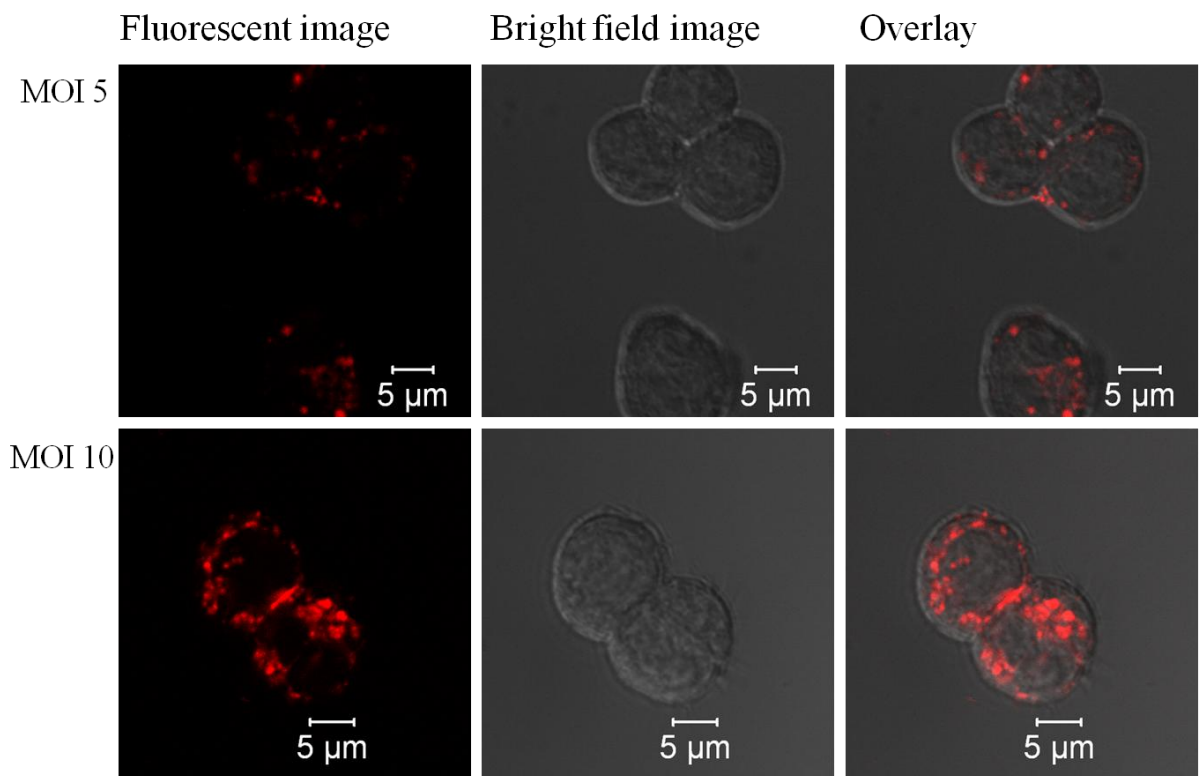


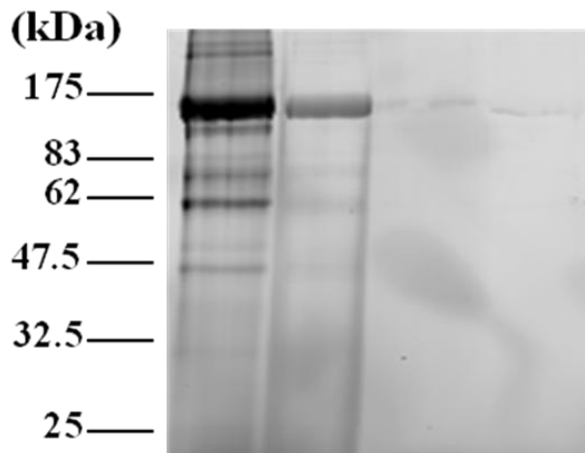
Figure 3-13. Con-focal imaging of 293 (human embryonic kidney) cells infected with TAMRA labeled Ad5 particles. Cells on glass bottom dishes were infected with 2 different MOI's and 30 minutes post infection the cells were imaged using a Zeiss LSM 2 photon confocal microscope through a rhodamine filter.

3.3. Discussion

Despite being heavily developed for gene therapy, the use of adenovirus vectors has been hampered by the inability to easily tune virus-host interactions. Here, we report a strategy that introduces unnatural amino acids into adenovirus particles in order to serve

as chemoselective attachment points. We have shown that production of metabolically labeled virion is exceedingly straightforward, requiring only addition of the unnatural amino acid to virus production medium. Viral particles bearing these unnatural azido amino acids have no impact on either particle production or infectivity. Importantly, the installed azides afford access to several highly selective chemistries, which were used to attach small molecules and peptides. Given the utility of unnatural amino acid incorporation, the commercial availability of both Aha and azide-selective reagents and the ease with which Aha-enabled hAd5 can be produced, we anticipate that the described method could easily be adopted by researchers working with adenovirus vectors.

Incorporation of Aha is accomplished via production of hAd5 under completely standard conditions with one exception; producer cells are shifted from normal to methionine-free/+Aha media between 18 – 24 hours post-infection. Despite previous reports demonstrating an absence of toxicity when Aha is used to label mammalian cellular proteins, we chose to metabolically label hAd5 during a relatively brief, 6 hour, window to avoid potential complications stemming from Aha incorporation into cellular proteins. Chemical modification of the resultant particles and quantitation reveals >500 dye molecules/virion, when viruses are produced with 32 mM Aha. Notably, Aha produced no apparent effects on viral or cellular physiology even at concentrations above saturation. Although initially counterintuitive, Aha is more similar to Met in both sterics and electrostatics than it would appear from 2-dimensional drawings(86). Although expanding the Aha labeling window is likely to lead to higher unnatural amino acid incorporation, 500 modifications/ particle is more than sufficient for most envisioned applications.



Aha	+	+	+	-
Met	-	-	-	+
Alk-FLAG	+	+	+	+
Cu(I) catalyst	+	+	-	+
Aha labeling - hrs post infection	18-24	10-16	18-24	18-24

Figure 3-14. Azide incorporation pattern of Aha enabled virus with different labeling times. Purified viral particles have subsequently been modified with alkyne-TAMRA by Cu catalyzed “click” chemistry. Virus produced by Aha labeling between 10 to 16 hours post infection (lane 1) show shifts in Aha incorporation and staggered labeling percentage when compared to Ad5 particles produced by labeling between 18 to 24 hours post infection (lanes 1, 3 and 4).

Chemical treatment, via either the Staudinger or Cu (I) catalyzed “click” ligations, yielded modified, infective viral particles. Selectivity, in this context, can be broken down into each process, metabolic labeling during viral production and chemical modification of the purified virion. Both CuAAC and Staudinger ligation demonstrate excellent selectivity (Figure 3-4, 3-7). No modification is evident when Aha is not

present, the copper is excluded or an inactivated (oxidized) Staudinger probe is used. This selectivity is independent of the nature of attached probe (peptide epitope or fluorophore). Incorporation of Aha is presumed to take place at each methionine codon independent of local sequence or structure. In support of this supposition, CuAAC mediated fluorescent labeling of full viral particles tracks with the number of methionine positions expected to be solvent exposed (Figure 3-10, Table 3-2). Mass spectral analysis of metabolically labeled hAd5 tryptic peptides demonstrates differences in the ratio of Met to Aha labeled peptides dependent upon the peptide analyzed. However, differences in ionization potential make this analysis difficult to quantitate and limit the value of these data.

Interestingly, shifting the Aha labeling closer to infection (10-16 hours post infection) shifts the labeling pattern (Figure 3-14). Presumably, this is due to the staggered production of adenoviral structural proteins. Exploitation of such pulse-chase labeling could allow biasing of Aha labeling towards one structural protein or another. However, due to the largely overlapping nature of Ad structural protein production any potential biasing would be limited. Alternatively, replacing methionine codons with those of structurally similar amino acids allow the restriction and control of Aha mediated chemistry. Ideally this will allow the production of programmable viral particles, where chemoselective handles can be placed site specifically by design. Precedence for this approach can be found with the removal of surface exposed asparagines, which hydrolyze upon storage, changing surface charge and physiological behavior of adenoviral vectors.(18) A general lack of conservation for these exposed methionine codons indicates that this strategy will likely be successful.

“Click” reagents are easier to access as many are commercially available and terminal alkynes are relatively simple to synthesize. However, simple desalting via size exclusion chromatography, while effective at removing the alkyne reagent, is insufficient to remove the copper catalyst. In these cases, a significant drop in infectivity was observed for virions chemically treated with alkyne reagent when compared to chemically untreated virions (2-3 folds). Cu (I) can be efficiently removed via treatment with a high affinity chelator (bicinchoninic acid (BCA) followed by size exclusion chromatography. Alternatively, the Staudinger ligation or newly developed strain promoted “click” chemistry may be utilized. At present, reagents for both of these chemistries are more difficult to access than the terminal alkynes required for CuAAC. However, with the growing popularity of the copper-free strain promoted “click” chemistry, commercial reagents may soon be available.

The copper assisted “click” reaction on the viral capsid retains the potential to tune number of chemically accessible sites based on the concentration of the reactant alkyne. Thus, reaction with increasing concentrations of alkyne dye results in linearly increased dye labeling per virion (Figure 3-15). The chemical labeling soon saturates at high micromolar probe concentrations. The chemistry can thus allow for multiple ligand decoration per virion using a single amino acid incorporation technique. This might also allow for controlled chemotherapeutic loading in the event of generating drug delivery systems based on adenoviral surface modification.

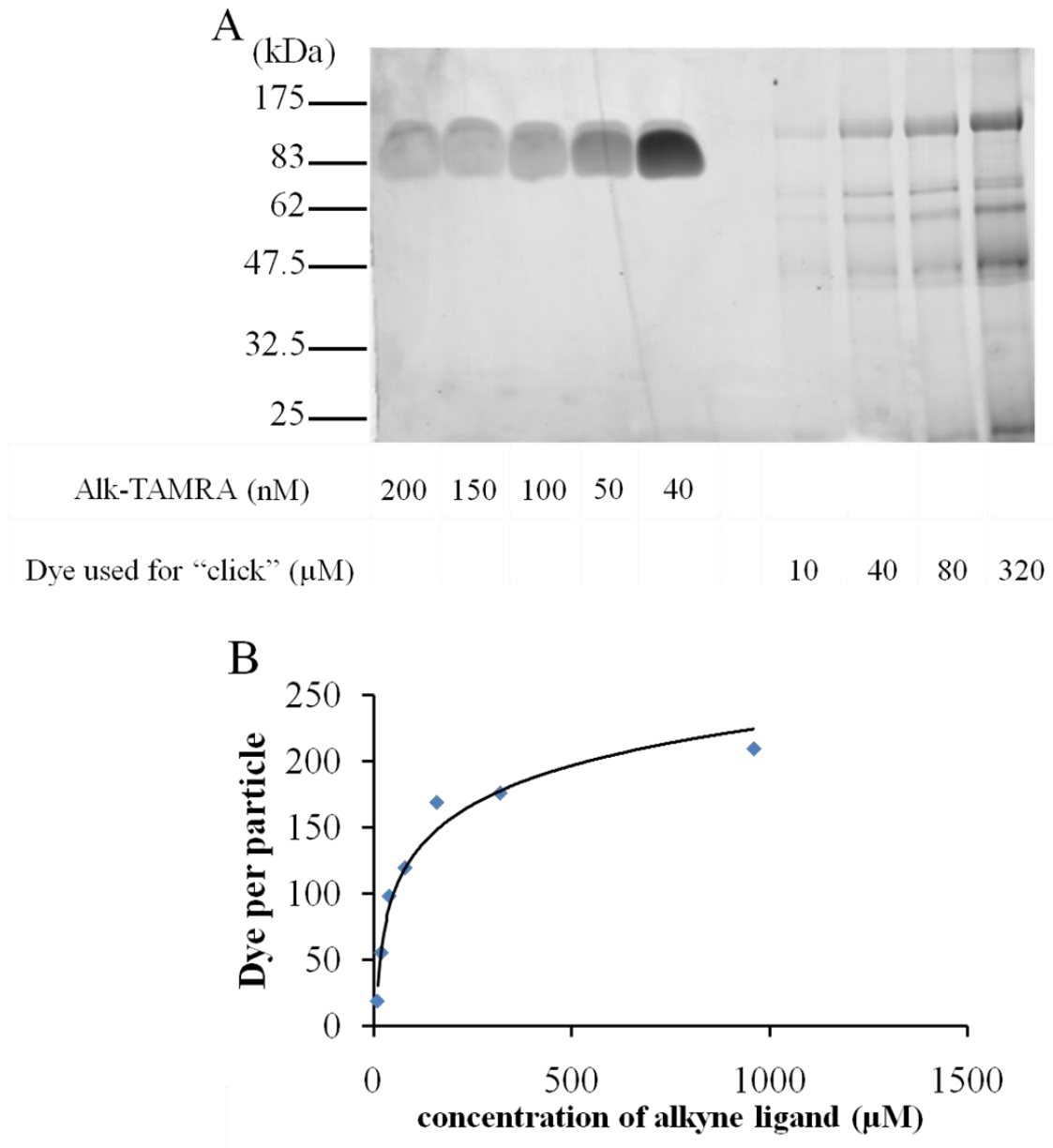


Figure 3-15. Concentration dependent “click” labeling of Aha enabled virus with alkyne-fluorophore by. A) Fluorescent gel scanned image of Aha enabled virus reacted with different concentrations of alkyne-TAMRA (lanes 7 to 10) and free dye (lanes 1 to 5). The “click” reaction was run overnight in a deoxygenated glove bag. B) Saturation curve shows relative dye labeling per virion against concentration of alkyne-dye used for each reaction.

We have demonstrated the targeting potential of Aha-enabled hAd5 via the straightforward attachment of well-utilized cancer specific ligand, folate. Although neither the physical nature nor linker length was optimized, folate decorated particles demonstrated a marked increase in infection of murine breast cancer cells (4T1), which are naturally refractive to infection. Although competition experiments indicate the folate receptor as the primary target for folate modified hAd5, we do not know whether secondary interactions (i.e. integrin) are required or whether direct internalization, via the FR, is the dominant entry method. No difference in folate-mediated infectivity was found with particles produced in the presence of 4 mM or 32 mM Aha, indicating that 250 ligands per particle is saturating with respect to infectivity. Given the relatively small nature of the conjugate, it is possible that only a subset of these modification sites, potentially Aha sites on the fiber knob, are necessary to mediate infection.

Given both its completely unoptimized nature, the significant increase in infection seen as the result of conjugation, and the generality of the chemistry, we believe this platform has broad potential. Azide specific chemistries, as a whole, are extremely selective. This is evident in their application to modify metabolically labeled unnatural post-translational modifications such as oligosaccharides and lipids, which are often in very low concentrations relative to the proteome. As a result of the demonstrated specificity and tolerance towards essentially any other functionality, Aha-enabled adenoviral particles should be amenable to modification with an extremely wide variety of targeting ligands. Further, given the standard nature of these chemistries,

characterization after modification may not be necessary, which would enable higher throughput screening of potential targeting ligands.

3.4. Summary

In conclusion, we have developed a novel strategy for the chemical modification of adenoviruses. It relies on a two-step strategy that takes advantage of the natural fidelity of protein synthesis and the most selective bio-orthogonal reactions described to date. As a result, this method demonstrates an unprecedented level of chemo selectivity. The high level of control limits impact on viral fitness and significantly expands the breadth of targeting and imaging moieties that can be approached. Despite these advantages, modification is remarkably straightforward, with minor modifications to standard Ad production protocols and requiring only widely available chemical reagents. In the future we anticipate the ability to control the placement of surface exposed azides via replacement of unwanted Met codons. In addition, given the standard nature of these chemistries, characterization after modification may not be necessary, which would enable higher throughput screening of potential targeting ligands. Further, this method is not limited to adenoviruses, but is expected to be robust when used in conjunction with most, if not all, viruses. We believe that this flexibility, in combination with the ease of implementation, make this method a significant addition to the currently available methods for capsid remodeling.

Chapter 4

Introduction of labeling specificity within unnatural amino acid enabled adenovirus

4.1. Introduction

4.2. Results

4.3. Summary

4.1. Introduction

Chapter 3 describes the metabolic labeling of adenoviral particles with an unnatural amino acid, Azidohomoalanine – a methionine surrogate. Given that labeling of the virion capsid proteins was attempted during a six hour labeling window determined by highest virus structural protein expression, our results demonstrated effective labeling of a number of adenovirus proteins with Aha. We were also able to demonstrate subsequent chemical modification of surface exposed residues via the use of copper assisted cycloaddition reactions. Our analysis showed approximately 5 to 10 % surface “click” modification of virus coat depending on the concentrations of the unnatural amino acid used during metabolic labeling. We were able to develop this technique further for vector targeting, yet the nature of metabolic incorporation determined this system with much reduced control compared to the unnatural sugar incorporation method developed previously. One of the key goals of this novel viral vector development strategy was to engineer systems with high specificities and control over site and amount of chemical modification. Towards such aim, our shifting of the metabolic labeling window, demonstrated that higher degrees of specificities could be built in even when dealing with global protein modification of a complex mammalian virion.

Chemical modification of metabolically labeled fully assembled Ad5 particles showed decoration of four different structural proteins. Specific site modification via unnatural amino acid incorporation could be engineered within the adenovirus particles by selectively mutating solvent exposed methionine residues on some of the viral

proteins. Towards such goals, mutational analysis of the solvent accessible sites within Ad fiber was attempted.

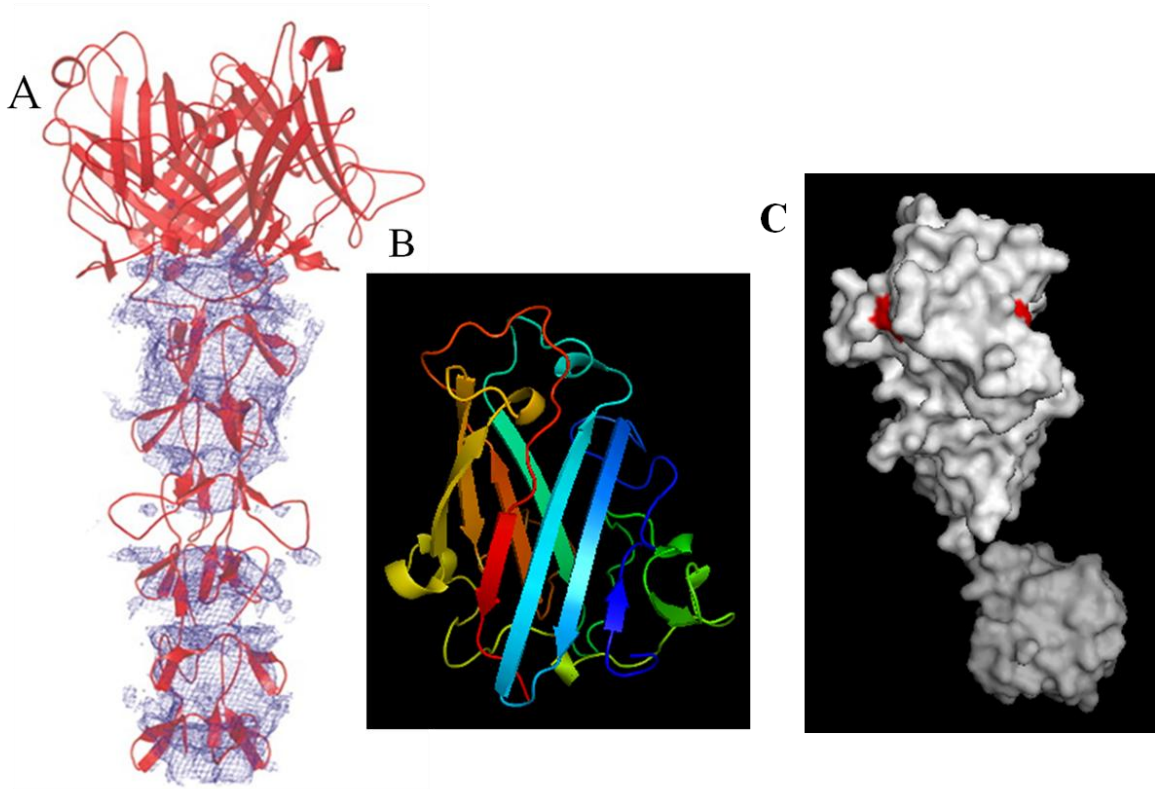


Figure 4-1. Crystal structure of the adenovirus type 5 and type 2 fiber. A) Crystal structure of complete Ad2 fiber obtained from protein data bank showing trimerized fiber knob and shaft domains. B) Structure of Ad5 fiber knob (PDB ID 1KNB). C) Solvent exposed surface of Ad2 fiber (PDB ID 1V1I) with exposed methionines (site 328) shown in red.

Structural analysis of the adenovirus fiber is necessary to determine solvent exposed methionine sites that could be targeted for mutations. Since complete structural information the adenovirus type 5 fiber is unavailable, a partial reconstruction of the Ad5

fiber knob and fiber shaft from Ad2 gives us a rough picture of the trimerization and solvent accessibility of the entire fiber protein (Figure 4-1). To determine which methionine sites would be suitably solvent exposed, analysis of the soluble knob domain of the Ad5 structure and that of Ad2 structure were undertaken. Sequence homology of Ad5 and Ad2 fiber revealed 69% sequence identity (See appendix for details). Using the crystal structure of the available Ad5 fiber knob (PDB ID 1KNB; structural information available from amino acids 396 to 581) it was estimated that none of the 2 methionine sites at 498 or 532 are solvent exposed. For further analysis of the knob structures between residues 319 and 396, knob of Ad2 fiber (PDB ID 1V1I) was utilized. Here the methionine residue at 373 remains conserved in both Ad5 and Ad2, but is unexposed; while site 328 for Ad5 is not conserved in Ad2. But the asparagine residue at 328 is solvent exposed for Ad2. Moreover methionine at 328 was observed in the mass spectral analysis (Table 3-1, chapter 3). Thus 328 was chosen for mutational analysis. Of the remaining methionine sites, no structural information is available, yet methionine at position 251 is conserved through a number of Adenovirus fiber proteins and is suitably positioned for Aha incorporation. Hence we also decided to mutate 251 for analyzing Aha incorporation. The remaining 5 methionine sites between positions 1 and 129 were expected to be buried within the penton base structure. Thus we decided to generate two methionine fiber mutants and a double mutant to understand specific incorporation of Aha with Ad5 capsid.

The adenovirus contains a 36 kb linear double stranded genome that is packaged within the icosahedra core. It consists of early phase genes that regulate infection and gene expression while the late phase proteins consist of structural elements of the

adenovirus. The viral fiber protein is expressed by the late E3 phase genes. The entire Ad5 genome is available within a 38 kB plasmid vector designated as pTG3602.(29) This allows for the use of traditional microbiological cloning techniques for generation of mutated viral structural proteins. But the sheer size of the entire plasmid makes any simple direct cloning methods unsuitable. Hence a homologous recombination approach to generate Ad5 fiber mutants was undertaken. Two plasmid vectors are necessary for employing recombination based mutant protein generation. One is a backbone plasmid containing the entire Ad5 genome – in this case the pAd5 backbone. For high efficiency recombination a singly cut DNA works better. Therefore the large backbone needs to be linearized at the fiber site to facilitate efficient recombination. Generation of fiber mutants involve cloning of the fiber gene from the adenoviral genome into a smaller shuttle plasmid vector – pFiber shuttle. Suitable flanking regions on the shuttle vector are necessary for faithful overlap. The fiber within the shuttle vector could be modified by conventional molecular biology protocols and the flanking sequences used for homologous recombination with the linearized Ad5 backbone (Figure 4-2). Post recombination the plasmid would be linearized to generate the mutant adenoviral DNA and transfected into 293 cells for Ad5 production. An *e.coli* strain, BJ5183, that is known to support efficient homologous recombination and has been previously utilized for mutant fiber generation would be suitable for this purpose.(71)

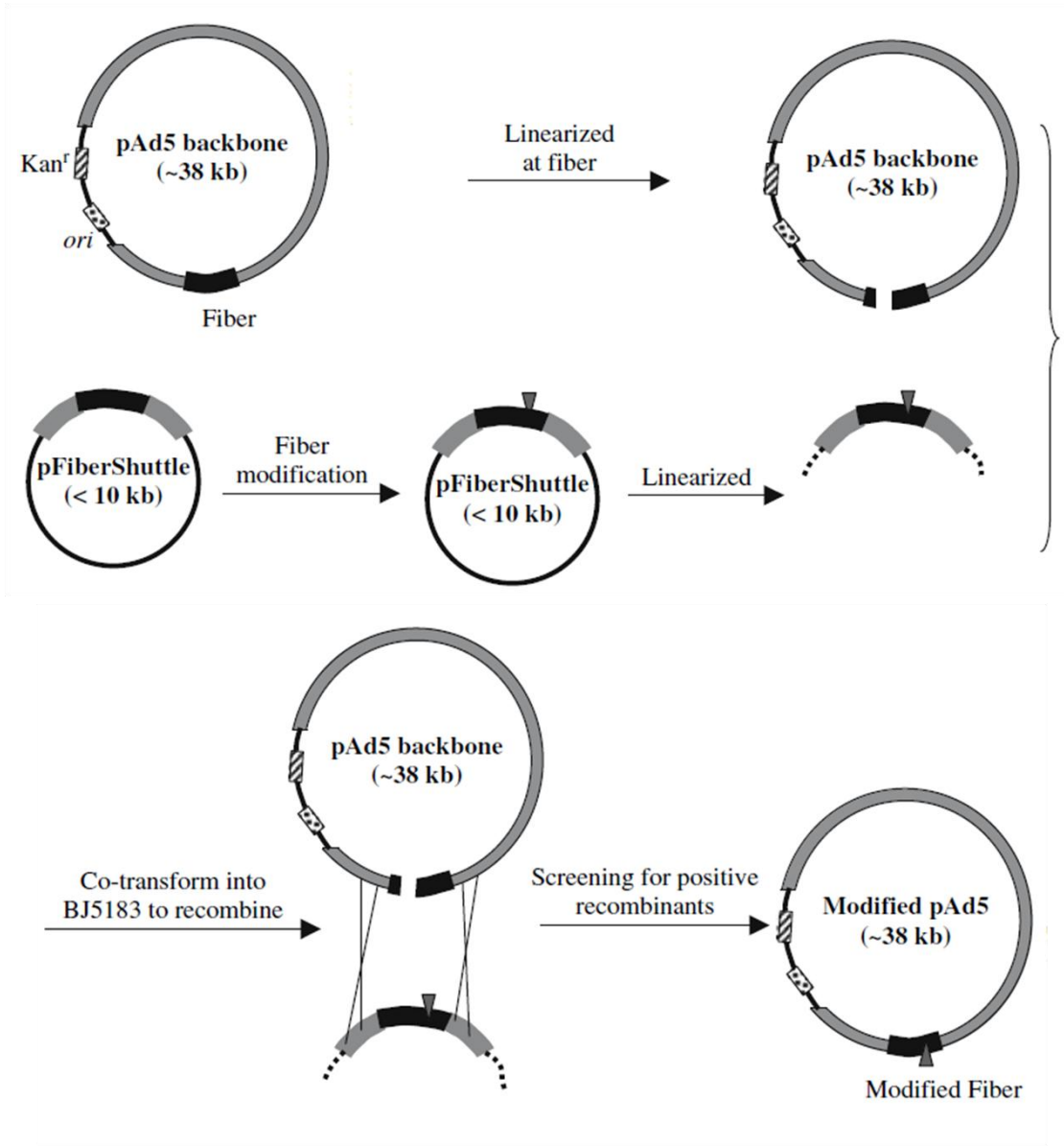


Figure 4-2. Cloning approach taken to generate virus fiber mutants.

4.2. Results

The plasmid pTG3602 containing the Ad5 genome is too large for direct modification using regular molecular biology protocols. To generate methionine mutants of Ad5, the fiber protein was first cloned into a shuttle vector. The Ad5 fiber sequence occurs between 31042 and 32787 base pairs. This segment in the backbone vector occurs between an EcoRI site lying at 30043 and a KpnI digestion site at 33588 base pairs – thus leaving suitable 1 kb overlapping regions on either end of the fiber sequence. The vector pTG3602 was digested with restriction enzyme EcoRI which created an 8 kb fragment containing the fiber sequence. Following gel purification, this fragment was re-digested with KpnI to generate the 3.5 kb fragment, containing the fiber gene flanked by 1 kb overhangs. The vector map and the restriction sites are shown in Figure 4-3. The fiber gene was then inserted into a 5 kb pBAD vector to generate the 8.5 kb pBADfib5 shuttle plasmid (Figure 4-3). Mutation of fiber sites 251 and 328 were carried out via quick change site directed mutagenesis kit to generate the mutants' pBADfib5M251L and pBADfib5M328L – the products were confirmed by sequencing.

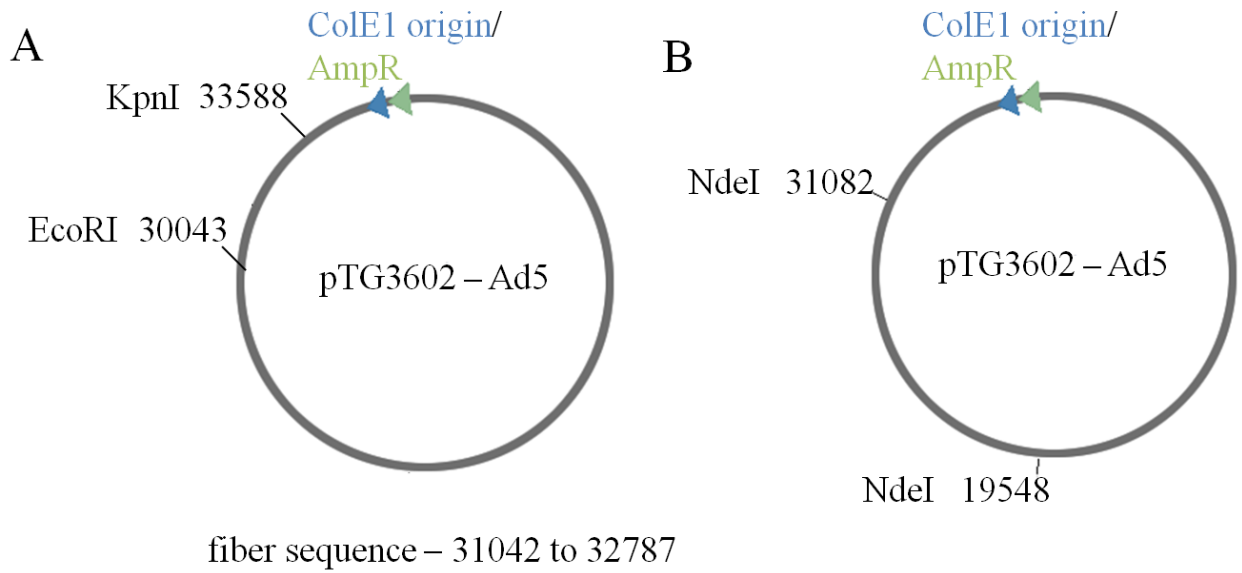


Figure 4-3. Vector map of pTG3602 showing restriction sites for fiber cloning and generation of linearized Ad5 backbone.

To generate the linearized backbone, cut precisely on the fiber sequence, we decided to insert a *SwaI* cut site at the N-terminus sequence of the fiber. Following partial *NdeI* digest, that possibly afforded 2 linearized pTG fragments; we ligated a small 15 base pair sequence that contained a *SwaI* restriction site. Subsequent cloning seemed to confirm insertion of this cleavage site, but sequencing results remained inconclusive. To correctly confirm backbone vector generation we are presently attempting to get better sequencing data on this vector.

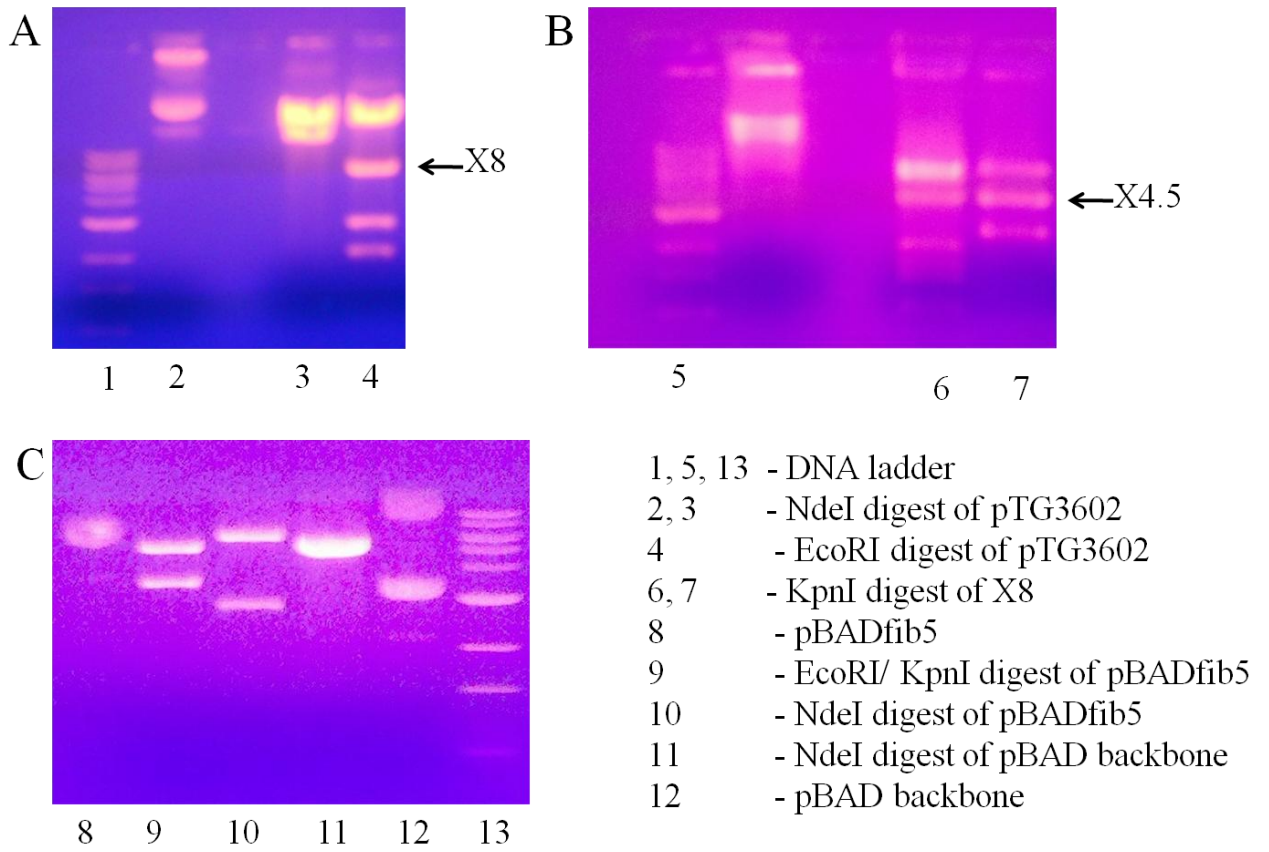


Figure 4-4. DNA agarose gel showing production of fiber shuttle plasmid pBADfib5. A) Digested pTG3602 with EcoRI generates a DNA fragment of approximately 8 kB (X8) that contains the fiber gene. B) Subsequent restriction of X8 with KpnI generates the fiber gene with 1 kB overhangs (X4.5). C) Final ligation with a pBAD plasmid backbone generates the correct plasmid that can be utilized for quick change site directed mutagenesis.

4 3. Summary

In conclusion we attempted to engineer in a greater degree of specificity within unnatural amino acid labeled virions. Since residue specific incorporation of amino acids within fully formed adenovirus particles results in labeling of four different structural proteins, generation of methionine mutants of one of those proteins was expected to limit incorporation. We have attempted to utilize a homologous recombination technique to generate mutant fiber Ad5. As a result, we have so far developed a fiber shuttle plasmid with surface exposed methionine residues mutated to leucine. We have also generated a backbone genome suitable for homologous recombination with our mutant fiber gene. In this regard developing the linearized pTG vector was the most challenging, as it involves cloning within a large 38 kB plasmid. Such large DNA sequences are easily sheared and can contain higher degrees of secondary structure that may reduce efficiency of steps drastically. Other methods like three plasmid ligation etc. to generate similar mutant clones are more technically difficult to access. Finally, virus production and subsequent amino acid labeling is expected to generate particles with no unnatural amino acid in its fiber region.

Chapter 5.

Dual surface modification of adenovirus particles

5.1. Introduction

5.2. Results

5.3. Discussion

5.4. Summary

Note: Most of the material in this chapter has been published (Banerjee, P. S.; Zuniga, E. S.; Ojima, I.; Carrico, I. S. *Bioorganic & Medicinal Chemistry Letters* **2011**, *In Press*, *Corrected Proof*). The chapter contains direct excerpts from the manuscript that was written by me with suggestions and revisions by Prof. Carrico.

5.1. Introduction

Despite substantial progress in understanding the molecular underpinnings of cancer, current chemotherapeutic options are limited and often unsuccessful. One promising alternative strategy is the use of conditionally replicative oncolytic vectors. Such viruses are designed to preferentially replicate in cancerous cells, such as those lacking common tumor suppressors (e.g. p53), leading to partially selective tumor toxicity. In addition, many carry a toxic transgene designed to amplify the inherent cytotoxic nature, which results from viral protein expression and immune stimulation – thus generating a so called “armed” adenovirus.(162, 209) One of the leading transgenes used to study combination effects of oncolytic adenovirus is TRAIL (TNF- α related apoptosis inducing ligand).(181) TRAIL belongs to the family of TNF cytokines that induce apoptosis by binding to death receptors. Upon binding these receptors initiate the formation of death-inducing signaling complexes (DISC), which ultimately activate caspase-8 for transduction of the apoptotic signal via the extrinsic apoptotic pathway.(2, 55) TRAIL can also sometimes activate the intrinsic apoptosis pathway, crosstalk mediated by the action of Bid.(87, 103) This transgene has been used extensively for targeting cancerous tissues via replicative Ad(54) – an important feature of its activity is upon exogenous administration to normal cells it exhibits minimal cytotoxicity.(42)

Despite this multifaceted cytotoxicity, the major limitation for oncolytic viruses in clinical trials has been efficacy.(152) Moreover lateral spread of virus infection through the tumor has been rendered ineffective in a number of cases. In an effort to increase

potency, oncolytic viruses have been used in combination with traditional chemotherapeutics.(75, 150, 192) In particular, conditionally replicative adenoviruses (Ads) have demonstrated significant synergism when used in combination with a number of different chemotherapeutics including doxorubicin, paclitaxel/docetaxel, cisplatin and histone deacetylase inhibitors.(143, 145, 185, 208) In the case of taxoid/oncolytic Ad combination therapy, an increase in viral replication is seen in addition to synergistic cytotoxicity. (31, 70, 106, 156, 212, 215) While the mechanistic origin of synergism is not completely well understood, it is clearly a general and significant phenomenon.(79, 105)

Paclitaxel treatment of cancer cells results in the up regulation of TNF related apoptosis inducing ligand (TRAIL) receptors.(134) This result in increased TRAIL binding through the over expressed death receptors – subsequently resulting in apoptosis activated through the extrinsic pathway. Taxoids have been reported to induce cell death via intrinsic cytochrome 450 release followed by apoptosis. Hence these two components seem to act through processes termed as targeted apoptosis.(24) Notably, one of the most promising oncolytic Ads in clinical trials bears the cytotoxic TRAIL transgene, which induces apoptosis in the infected cell and mediates substantial bystander cytotoxicity.(63) As a result, taxoid/AdTRAIL would be expected to have an additional source of synergism. SB-T-1214 is a next generation taxoid that exhibits significantly improved cytotoxicity, against a number of drug resistant cancer cell lines.(30, 97, 142) In addition, this taxoid exhibited substantial inhibition of cancer stem cell related genes (Oct4, Sox2, Nanog, and c-Myc) when screened against 3 unrelated invasive colon cancer cell lines.(19) These results indicate that SB-T-1214 has significant potential, particularly

with respect to cancer stem cells and cancers that are resistant to traditional chemotherapeutics.

While combination therapy demonstrates significant promise, it holds that efficiently targeted Ad particles bearing a therapeutic payload would provide an additional boost in efficacy. This would be a result of spatially and temporally concerted delivery of cytotoxicity, and may have the added benefit of reducing systemic toxicity. In order to achieve this goal, selective chemical modification routes for adenovirus are required, particularly those that allow the generation of multifunctional particles. Previously we reported the incorporation and modification of a non-canonical sugar residue, *O*-GlcNAz on serine 109 of the fiber protein, as a means of chemoselectively tailoring Ad particles.⁽¹⁰⁾ The specificity of this strategy, derived from the fidelity of the biosynthetic machinery and the highly selective chemistries developed for azide modification, allowed folate modification without compromising virus infectivity. Folate decorated Ad exhibited substantial (~20 fold) increase transgene delivery to breast cancer cells.⁽¹⁰⁾

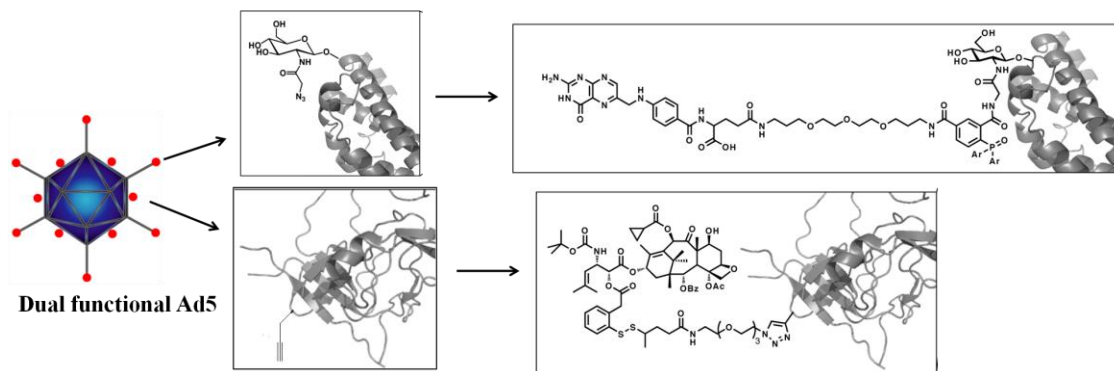


Figure 5-1. A cartoon illustrating adenovirus particles chemically modified with both a folate moiety, via Staudinger conjugation with an introduced *O*-GlcNAz, and SB-T-1214, via “click” modification of metabolically introduced homopropargylglycine.

We have also shown Ad5 capsid labeling via the use of an unnatural amino acid. Here, we extend this approach towards multimodal adenovirus particles(179) (Figure 5-1) via the simultaneous metabolic labeling with *O*-GlcNAz and an alkyne bearing non-canonical amino acid, homopropargylglycine (HPG) – another methionine surrogate. Introduction of these surrogates into Ad particles was envisioned to allow sequential Staudinger ligation of *O*-GlcNAz followed by copper assisted “click” modification of homopropargylglycine (HPG). Thus generating virions with dual-functionalization capabilities for development of targeted virions armed with covalently linked cytotoxic chemotherapeutic.

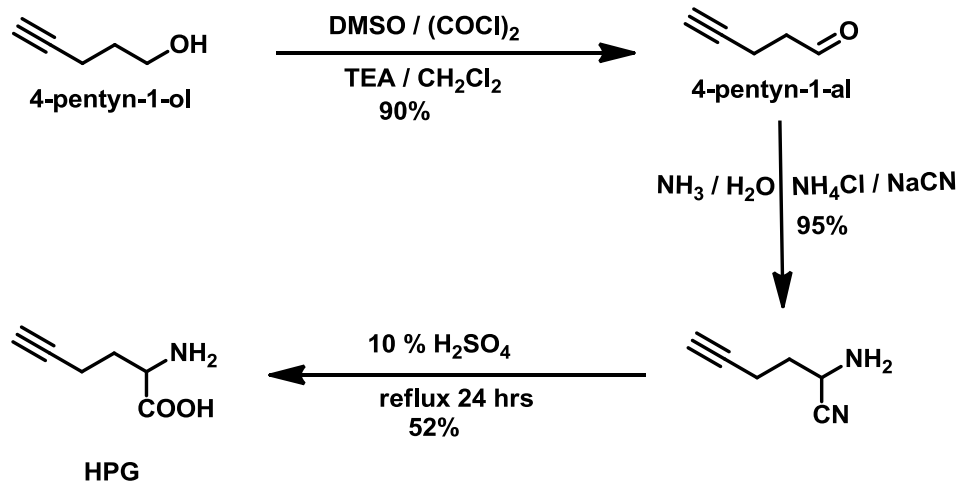
For analysis of the combination effects of conditionally replicative adenovirus and chemotherapeutics, we utilized our dual-modified CRAd virions for chemical attachment with a newly developed taxoid SBT-1214. Cytotoxic effects of such an assembly were

furthered by using a CRAd that expressed TRAIL within its E1A region(181) (generously obtained from Prof. Andre Lieber, University of Washington, Seattle).

5.2. Results

5.2.1. Synthesis of homopropargylglycine (HPG)

Homopropargylglycine was synthesized in a racemic mixture according to Dong *et al.* (Scheme 5-1). 4-pentyn-1-ol was converted to the corresponding aldehyde via Swern oxidation. The aldehyde was converted to the 2-aminohex-5-yne nitrile via action of sodium cyanide and ammonium chloride. Finally the nitrile was hydrolyzed in the presence of sulphuric acid to give a D- and L- mixture of HPG. The product was purified via flash chromatography and characterized via ¹H NMR spectroscopy and ESI mass spectroscopy.



Scheme 5-1. Synthesis of homopropargylglycine

5.2.2. Production and characterization of Ad5 particle with Ac₄GalNAz and HPG

Adenovirus type 5 particles were produced in the presence of a metabolic precursor of GlcNAz, per acetylated *N*-azidoacetylgalactosamine (Ac₄GalNAz), and HPG.(20, 82) Azido-sugar incorporation was accomplished by supplementing media with 50 μM Ac₄GalNAz for the entire duration of virus production (48 hours). Introduction of the alkyne-amino acid was mediated by exposure of producer cells to 4 mM HPG during a six-hour window (18-24 hours post infection), in a pulse chase format with methionine containing media. 48 hours post infection, the cells were harvested, lysed and viruses were purified via a standard two-step ultracentrifugation procedure in CsCl gradients.(190)

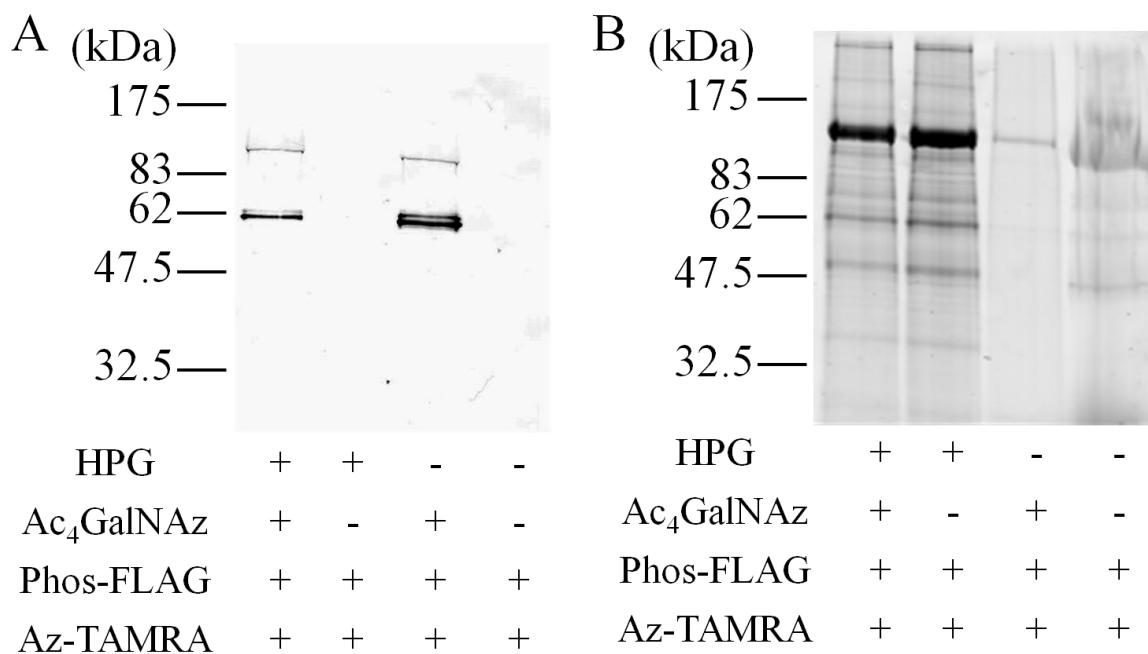


Figure 5-2. Chemoselective modification of GalNAz and HPG labeled adenovirus with Phosphine-FLAG and az-TAMRA. A) Anti-FLAG western blot of peptide and dye labeled Ad5, demonstrating incorporation of azido sugar onto adenoviral fiber. B) Same samples from A, analyzed for fluorescence as a reporter of HPG incorporation onto virus capsid.

Purified *O*-GlcNAc and HPG bearing virion were treated with 300 μ M of Staudinger probe bearing a FLAG epitope (PhosFLAG) (3 hours, RT).(113) Reaction mixtures were subsequently exposed to tetramethylrhodamine 5-carboxamido-(6-azido-hexanyl) (az-TAMRA) dye (500 μ M) using copper assisted “click” reaction conditions under de-oxygenating conditions in the presence of bathophenanthroline disodium salt (3 mM) and CuBr (1 mM) (RT, 12 hours).(64) Particles were purified by size exclusion (Sephadex G-25) and interrogated by western blot and fluorescent gel imaging.

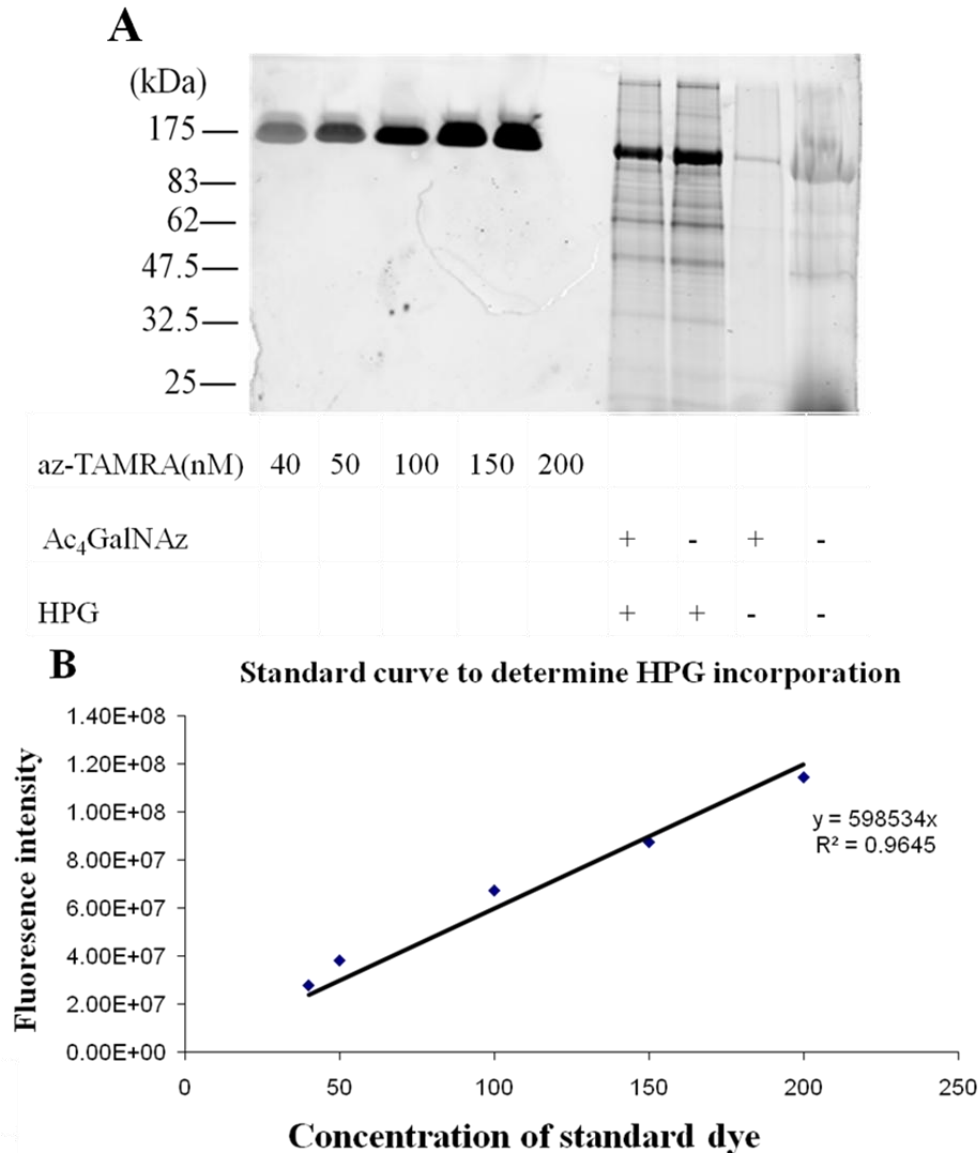


Figure 5-3. Determination of labeling of HPG enabled virus with azide-fluorophore by Cu catalyzed “click” chemistry. A) Fluorescent gel scanned image of HPG + GalNAz, HPG, GalNAz and unlabeled virus treated with azide-TAMRA. The “click” reaction was run overnight in a deoxygenated glove bag. Well 1-5: Increasing concentrations of standard dye (TAMRA) for determining the concentration of label. The gel was run at 200V for 1 hour at 4°C and scanned within 10 minutes of the end of run. B) Standard curve drawn between fluorescence intensity and concentration of dye loaded on gel. Slope of graph was used to determine concentration of labeled protein.

Western analysis demonstrated that virus particles produced in the presence of both Ac₄GalNAz and HPG and only Ac₄GalNAz are labeled on a single coat protein occurring at 62 kD by PhosFLAG (Figure 5-2). No PhosFLAG labeling is seen on particles produced in the absence of Ac₄GalNAz, consistent with previous studies demonstrating the specific labeling of the fiber protein via *O*-GlcNAz. Fluorescent gel imaging of az-TAMRA labeled HPG-Ad and HPG/*O*-GlcNAz-Ad demonstrated labeling of a number of different proteins, consistent with the presence of solvent exposed methionine sites (Figure 5-2).(157)

Previous characterization of *O*-GlcNAz labeled Ad particles demonstrated 22 ± 1.5 chemically addressable azides per particle.(10) In order to quantitate HPG incorporation, TAMRA labeled virion were quantified via fluorescent gel imaging against a free az-TAMRA standard addition curve (Figure 5-3), demonstrating an attachment of 193 ± 12 dyes per virion (Table 5-1).

Vector production and infectivity are often compromised during genetic engineering of Ad particles, which has slowed the pace of vector development and effectively limited the production of multifunctional particles. While previous results indicate that *O*-GlcNAz incorporation does not impact either particle production or infectivity, the incorporation of HPG into the protein backbone at significantly higher incorporation levels was a concern. Surprisingly, no significant loss in either particle production or infectivity was observable for either of the singly modified Ad particles or particle bearing both *O*-GlcNAz and HPG (Figure 5-4).

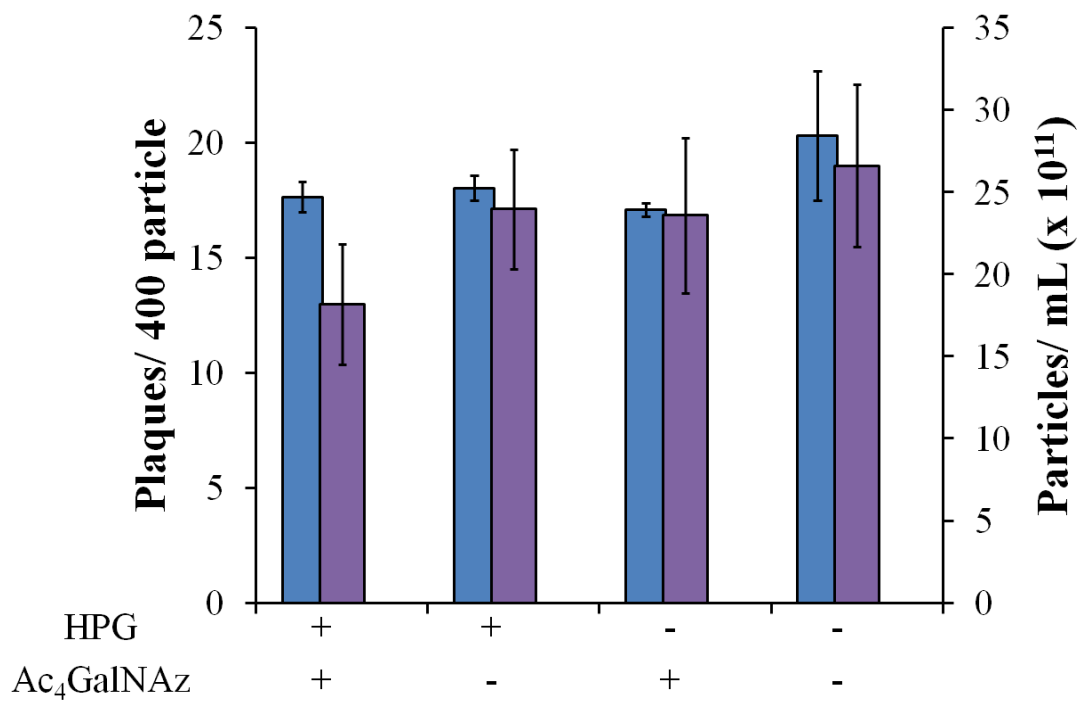


Figure 5-4. Viral fitness analysis for Ad metabolically labeled with GalNAz and HPG. Adenoviral particle count was assessed after purification (purple bars) as assayed by UV detection showing efficient particle generation in presence of different non-natural substrates. Virus plaque assay (blue bars) showing infectivity of modified virus particles.

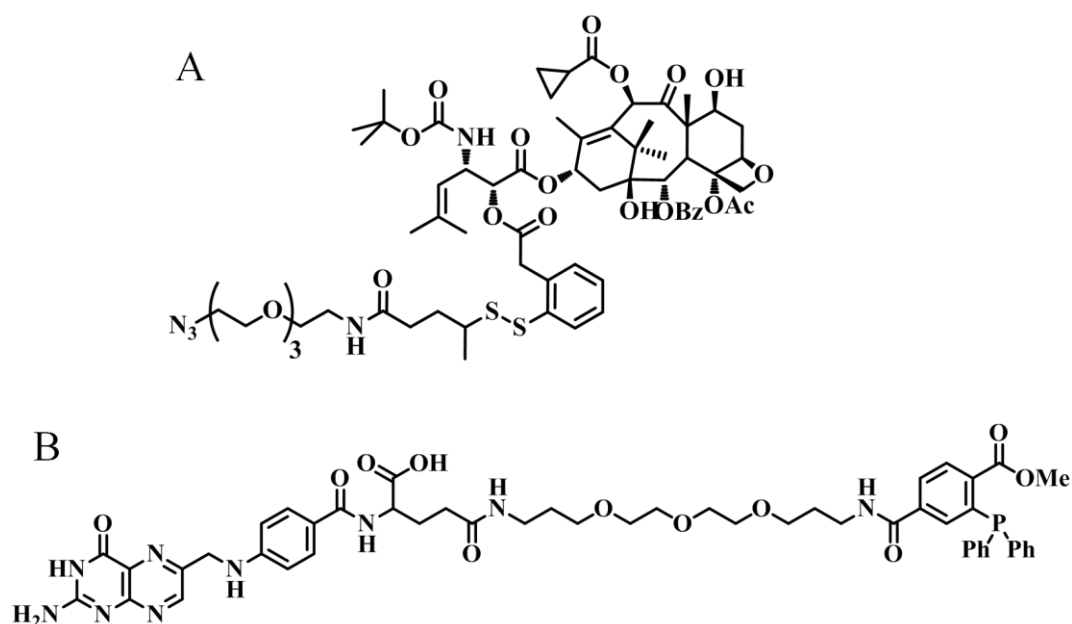
Adenoviral structural proteins*	Estimated total no of solvent exposed Met per VP	Average number of chemically labeled dyes per VP with 4 mM HPG
Hexon	5760	132.3 ± 6.6
Penton	300	36.6 ± 3.8
Fiber	108	23.1 ± 1.6

Table 5-1. Estimated number of solvent exposed methionine residues and the observed number of HPG residues incorporated in each of the discussed proteins.

5.2.3. Toxicity and targeting of chemically armed dual modified adenovirus

In order to generate a chemotherapeutically “armed” Ad particle, an azido derivative of SB-T-1214 (az-SB-T-1214) was synthesized that included a reductively self-immolative linker, designed to release the taxoid after Ad particle endocytosis (Scheme 4-1). This linker has demonstrated efficient endosomal release of SBT-1214 in cell culture studies.(30, 141) Modification of AdTRAIL with az-SB-T-1214 was accomplished in an identical manner to az-TAMRA modification of Ad described above.

Chemically modified virion (SB-T-1214AdTRAIL) were purified by size exclusion and used to infect ovarian cancer cells, ID8, at multiplicities of infection (MOIs) that were expected to be subtoxic for AdTRAIL alone. Levels of free SB-T-1214 equivalent to that loaded on virion, as well as unmodified AdTRAIL were used for comparison.



Scheme 5-2. Structures of az-SBT1214 and phosphine-folate used to chemoselectively modify *O*-GlcNAz and HPG labeled Ad-Luc.

Importantly, the only difference between the processing of AdTRAIL and SB-T-1214AdTRAIL was the addition of HPG during production of the latter. Specifically, AdTRAIL was exposed to identical “click” conditions as SB-T-1214AdTRAIL, however due to the absence of HPG was presumably unmodified. Five days post infection, cytotoxicity was assessed via MTT assay (Roche, KitI).

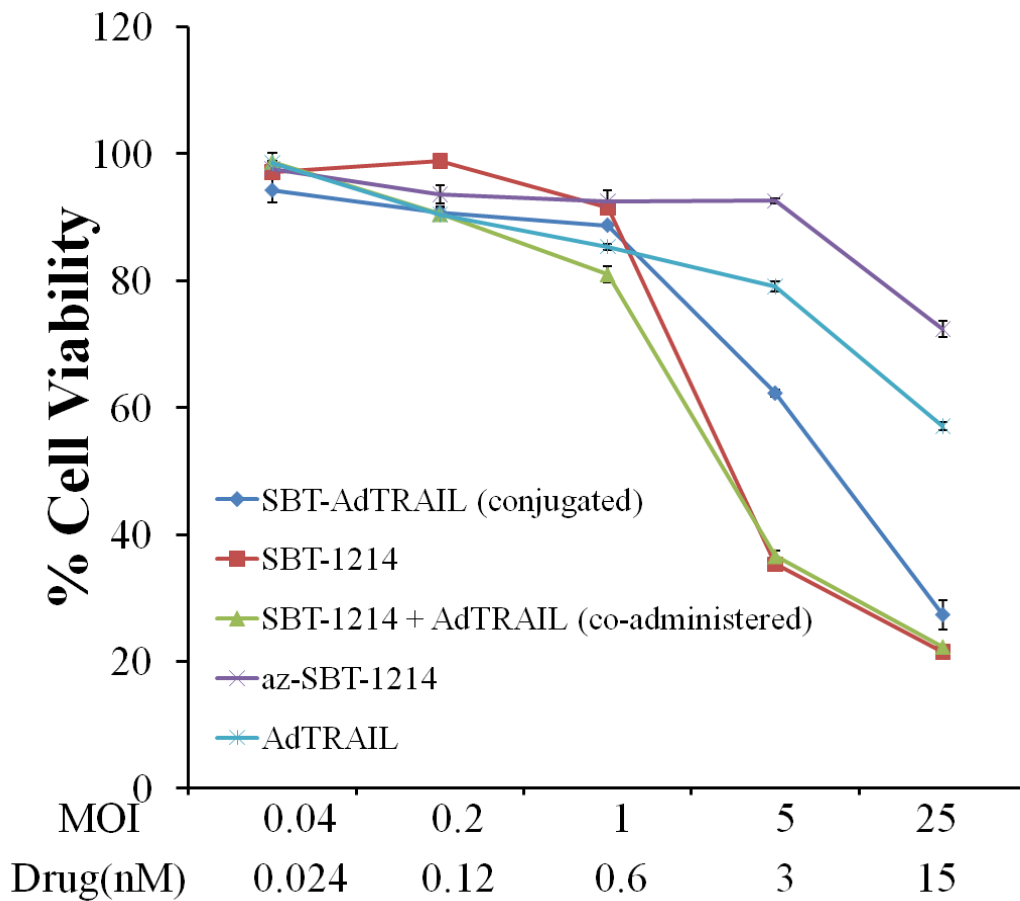


Figure 5-5. MTT assay to determine cytotoxicity of HPG and GalNAz incorporated TRAIL-Ad5 – chemically labeled with SBT-1214.(12) Comparison of cytotoxicity profiles of metabolically unlabeled TRAIL-Ad5 (AdTRAIL), free drug (SBT-1214), free azide-drug conjugate (az-SBT-1214), and co-administered AdTRAIL and SBT-1214 (SBT-1214 + AdTRAIL) with drug labeled TRAIL expressing adenovirus (SBT-AdTRAIL) on murine ovarian carcinoma cells (ID8). Cells seeded on 96 well plates were infected with shown concentrations of virus and/ or drug. After 5 days, MTT assay was performed to determine cell death.

TRAIL expressing viruses that were covalently linked with az-SB-T-1214 demonstrated an increase in cytotoxicity compared to free azSB-T-1214 and AdTRAIL alone (Figure 5-5), consistent with the proposed synergistic effect. Unmodified SB-T-1214, both alone and co-administered with AdTRAIL demonstrated higher levels of cell cytotoxicity. Presumably, this effect is due to a difference in the kinetics of cellular penetration of the free drug versus covalently linked SB-T-1214 and AdTRAIL.

As many cancers demonstrate significantly higher levels of folate receptor (FR), folate conjugates demonstrate selectivity for this receptor and folate conjugates are efficiently internalized, folate has been widely used for cancer targeting.(110, 207) Although we have previously demonstrated the gene delivery of folate-Ad particles, those modified with both az-SB-T-1214 and folate may demonstrate altered uptake profiles. In order to explore these effects, dually modified Ad bearing a luciferase transgene (AdLuc) were screened against a murine breast cancer cell line, 4T1.(81) Cells grown under folate free media for 2 weeks were seeded on 96 well plates at concentrations of 1×10^4 cells/well. Infection was accomplished at a MOI of 50 and cells were examined for luciferase activity 24 hours post infection (Luc-Bright-Glow). Folate targeted SB-T-1214AdTRAIL demonstrated (Figure 4-6) a ~30 fold increase in transgene expression on breast cancer cell type (4T1) compared to virion lacking *O*-GlcNAz. In addition, treatment of cells with free folate prior to infection led to a dose dependent loss in virus infection (Figure 5-6).

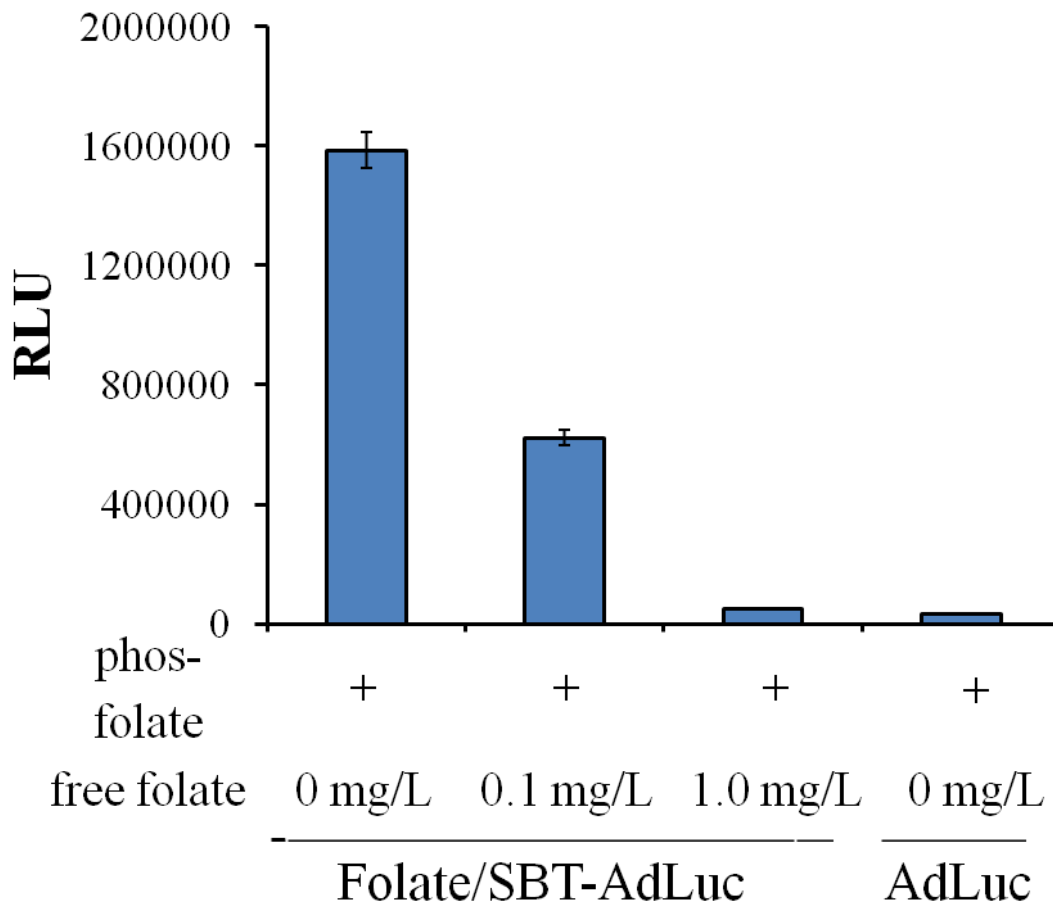


Figure 5-6. Targeting analysis of SB-T-1214 and folate modified AdLuc. Luciferase analysis of 4T1 (murine breast cancer) cells 24 hours post infection with modified virions both in the presence and absence of external folic acid showing dose dependent gene expression.

5.3. Discussion

A growing body of literature suggests the effective development of conditionally replicative adenoviruses for cancer cytotoxicity.(144) Yet abundant clinical data points to

inefficiencies of such virotherapy modalities within treated patients. Thus efficacy appears to be a large issue for development of functional therapeutics. Combination effects of virotherapy and chemotherapies have already demonstrated positive clinical effects. Here we have attempted to utilize targeted virotherapy with chemotherapeutics by covalent attachment of multifunctional Ad and Taxoid molecule.

Production of such multi-functional virions was attempted via metabolic unnatural substrate incorporation technique – using an azido sugar and an alkynyl amino acid surrogate. Our results demonstrated effective labeling of the virions with both the substrates without substantial effects on viral fitness. Incorporation of the unnatural sugar derivative is assumed to be similar to the earlier reported vector based on the fact that the labeling precursors were same. For the amino acid though, the incorporation seems to be lower than was previously reported with azidohomoalanine. This presumably reflects the ability of HPG to be charged with the methionyl t-RNA. Aha has been shown to be a 2 fold better substrate for the cognate t-RNA synthetase within bacterial systems. Such effects within mammalian systems can be assumed to be the cause of lower metabolic incorporation in the present scenario.

Sequential chemistry on the dual labeled vectors is important for introducing effective modifications. Use 300 μM of a phosphine ligand helps to saturate the available azides on the viral capsid; with any excess being oxidized within the reaction time. Using a higher concentration of alkyne-probe for click labeling with the HPG residues not only allows for saturation of remaining phosphine derivatives, it also prevents particle aggregation via inter-virion click reactions.

Cell viability studies using ovarian cancer cells demonstrated the cytotoxic nature of AdTRAIL covalently modified with SBT drug. When compared to only AdTRAIL, this combination does seem to demonstrate added toxicity. This effect was slightly higher when virus infection was assayed with non-covalently linked drug. Faster uptake of free drug may result in higher toxicity effects due to increased viral burst. We are currently analyzing infective virion release from infected cells to determine whether greater virus spread accounts for this enhanced toxicity of unlinked virion, drug formulation.

4.4. Summary

In summary we report the development of a novel multi-functional adenoviral platform via non-canonical substrate incorporation and chemoselective modification. We utilized the platform to develop a combination vector targeted towards the folate receptor and armed with a next generation taxoid. The described system allowed the efficient modification with both functionalities without impact on viral fitness. Further, initial studies indicate significant synergistic cell toxicity. Ongoing studies will evaluate the construct in the context of different cancers, both in cell culture and within *in vivo* xenograft model systems. In principle the described dual modification methodology can be utilized to append targeting, imaging, diagnostic and chemotherapeutic modules to replication selective Ad, potentially accelerating vector development and allowing the evaluation of alternative combination therapies.

Chapter 6

6.1. Future Directions

Capsid surface modification of adenoviruses and other clinically relevant virions provide an important technique for development of oncolytic therapies, gene based therapeutics and vaccine development strategies. The unnatural substrate based metabolic incorporation technique described herein provides an easy and versatile technique for the same with potential towards utilization of a vast array of targeting/ imaging/ chemotherapeutic ligands. A number of directions can be utilized for the further development of this system.

An initial approach by varying the length of PEG linker within the targeting ligand systems could potentiate not just higher levels of modified virus targeting, it could also provide interesting insights into de-targeting of the virions from off target cells. Attachment of some “self” proteins, e.g. albumin, on to the virus capsid via the chemoselective labeling method could be undertaken to determine if such techniques could increase in vivo stability of adenoviral based virions. Further analysis of the imaging capabilities of the chemically labeled virions could be utilized to interrogate the fate of specific proteins after cellular internalization. Such experiments could provide insights into the biology of viral escape from endosomes and its interactions with the nuclear pore complexes.

Towards the development of a single capsid protein modification of the adenovirus with the unnatural amino acid labeling technique, greater insight into the sites of chemical labeling is necessary. Towards such goals initial mass spectroscopy based experiments proved unsuccessful. A more wholesome approach could be developed by initially denaturing the virion and subsequently carrying out chemical labeling with a small ionizable ligand. This would drastically increase the number of available sites for chemical labeling and provide greater probability of MALDI based site identification. In this regard collection of the “empty” virion band (which is generally discarded) after CsCl ultracentrifugation might be useful.

One of the more interesting approaches for generating bias within the amino acid incorporation methodology would be to analyze in greater detail the possibility of pulse labeling at different time windows between 10 to 20 hours post infection. In this regard using high concentration of targeting non-natural substrate labeled for a very short time (1 to 2 hours) could be useful.

Finally to develop a completely de-targeted Ad which retains the possibility of chemoselective modification, genetic incorporation of peptide tags on the fiber HI loop can provide a merging of the genetic based and metabolic incorporation based virus labeling techniques. Possible utilization of the aldehyde tag on the HI loop may provide an additional modification site for development of a truly multi-functional viral platform.

Chapter 7

Experimental methods

7.1. Synthetic methods

7.2. Adenovirus production using unnatural substrates

7.3. Chemical modification and characterization of substrate labeled virions

7.4. Targeting, imaging, cytotoxicity

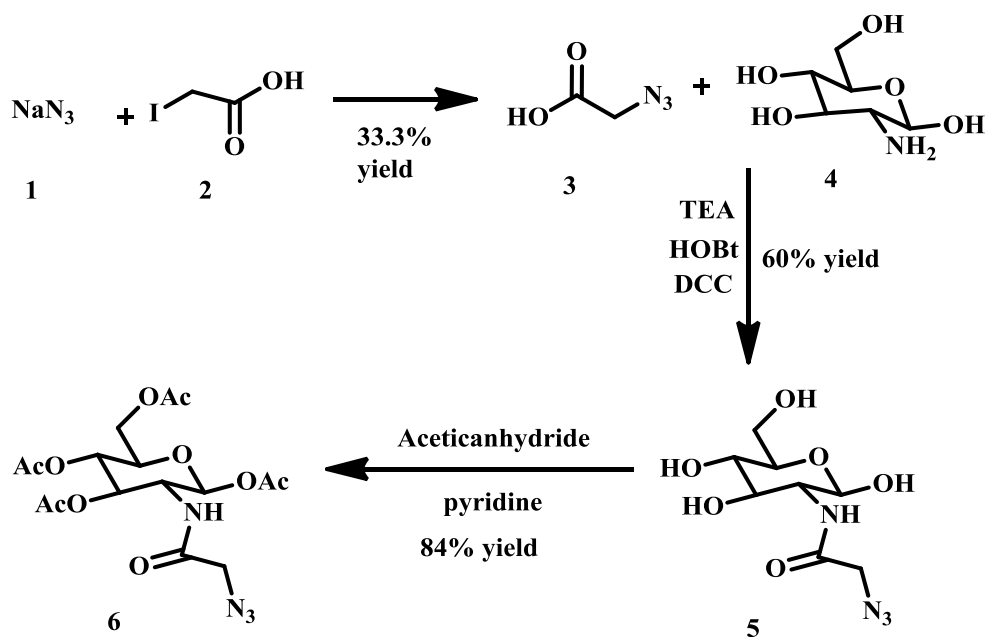
7.5. Cloning

Materials and Methods

Reagents and equipment. All chemical reagents were obtained from commercial sources and used without further purification unless otherwise noted. NMR spectra were recorded on a Varian 300 NMR spectrometer. Mass spectra for the small molecules were obtained using an Agilent 1100 LC/MSD VL instrument. Matrix-assisted laser desorption/ionization (MALDI) mass spectra were obtained using a Bruker Autoflex II MALDI/TOF/TOF. Thin Layer Chromatography (TLC) was performed on Merck DC-alufolien with Kieselgel 60F-254 and column chromatography was carried out on silica gel 60 (Merck; 230-400 mesh ASTM). The α -FLAG M2 conjugate was obtained from Sigma (St. Louis, MO). Centri Sep spin columns were obtained from Princeton Separations (Adelphia, NJ). MTT reagent obtained from Cell Proliferation KitI (Roche, Eugene, OR). RP-HPLC was performed using a L201243 Shimadzu on a C18 Jupiter column (250 x 10mm; Phenomenex). Mouse breast cancer cell line, 4T1 was obtained from ATCC (Manassas, VA). Fetal calf serum was purchased from HyClone. IR fluorescence was obtained using an Odyssey LI-COR instrument at the Department of Molecular Genetics, Stony Brook University. UV-Visible absorbance was recorded on a Beckmann Coulter DU 730. Electrophoresis gels were scanned on a Typhoon 9400 fluorescent gel scanner and GFP expression read on a Synergy 2 fluorescent plate reader. Absorbance and chemiluminescence was measured using a PerkinElmer Victor X plate reader. Fluorescence microscopy was carried out under a Zeiss LSM 510 META NLO 2-photon laser scanning confocal microscope system

7.1. Synthetic methods.

1,3,4,6-tetra-O-acetyl-N-azidiacetyl- α,β -D-glucosamine and 1,3,4,6-tetra-O-acetyl-N-azidoacetyl- α,β -D-galactosamine. The per acetylated sugars were synthesized exactly as described by Bertozzi(101) *et al.* The synthesis of per acetylated N-Azidoacetylglucosamine is described below; per acetylated N-Azidoacetylglucosamine has been synthesized similarly.



Scheme 6-1. Synthesis of per acetyl azidoglucosamine

Synthesis of N-Azidoacetylglucosamine: Azidoacetic acid was synthesized as described by Luchansky²⁹ *et al.* D-Glucosamine hydrochloride (1.5g, 7mmol) was added to a solution of azidoacetic acid (0.98g, 9.7mmol) in methanol (50ml). Triethylamine (2.5ml,

17mmol) was added and the reaction mixture stirred for 5 minutes at room temperature. The solution was cooled to 0⁰ C and N-hydroxybenzotriazole (0.86g, 7mmol) was added followed by 1-[3-(dimethylamino) propyl]-3-ethylcarbodiimide hydrochloride (2.68g, 14mmol). Reaction was allowed to warm to room temperature overnight when TLC with ceric ammonium nitrate showed the reaction to be complete. The solution was concentrated and the crude GlcNAz was purified by silica gel chromatography eluting with 10% methanol in dichloromethane. The product was obtained as a white solid in 60% yield. R_f: 0.32

Synthesis of 1,3,4,6-tetra-O-acetyl-N-azidoacetyl- α , β -D-glucosamine (per acetylated

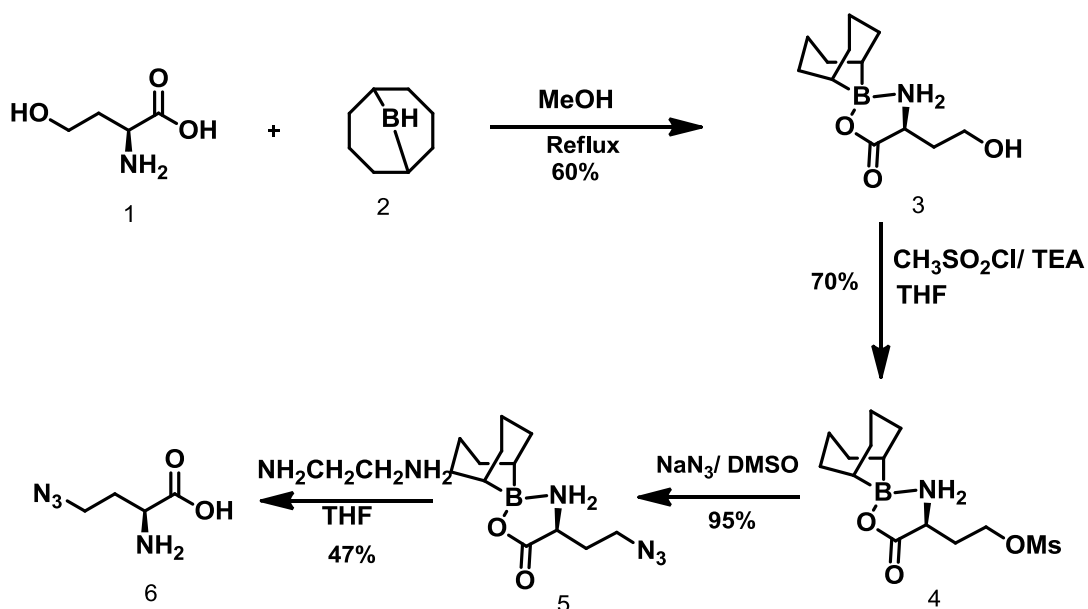
GlcNAz): Acetic anhydride (10.0ml, 110mmol) was added to a solution of GlcNAz (1g, 3.8mmol) in pyridine (40ml) and the reaction mixture stirred overnight at room temperature. The solution was then concentrated and resuspended in dichloromethane. Then washed with 1M HCl, saturated NaHCO₃ and saturated NaCl. The organic layer was dried, filtered and concentrated. The crude per acetylated GlcNAz was purified by silica gel chromatography eluting with 50% ethylacetate-hexane. The product was obtained as white crystals in 80% yield. R_f:0.45. ¹H NMR (300MHz, CDCl₃): δ 2.0 (12H, s), 2.1 (9H, s), 2.2 (3H, s), 3.9 (5H, s), 4.0 (2H, m), 4.2 (3H, m), 4.4 (2H, ddd), 5.2 (5H, m), 6.2 (1H, d), 6.4 (2H, d) ppm. ESI MS calculated for C₁₆H₂₃N₄O₁₀ (MH⁺) 403, found at 403.2.

Synthesis of 1,3,4,6-tetra-O-acetyl-N-azidoacetyl- α,β -D-galactosamine (per acetylated GalNAz): ^1H NMR (300MHz, CDCl_3): δ 2.0 (12H, s), 2.1 (9H, s), 2.2 (3H, s), 3.9 (5H, s), 4.0 (2H, m), 4.2 (3H, m), 4.4 (2H, ddd), 5.2 (5H, m), 6.2 (1H, d), 6.4 (2H, d) ppm. ^{13}C NMR (400 Mz, CDCl_3): δ 20.564, 20.617, 20.814, 47.017, 52.443, 61.193, 66.551, 67.590, 68.622, 90.864, 90.910, 166.925, 168.814, 170.014, 170.287, 170.909. ESI MS calculated for $\text{C}_{16}\text{H}_{23}\text{N}_4\text{O}_{10}$ (MH^+) 403, found at 403.2.

Alkyne- and Phosphine-FLAG. Synthesized as described by Bertozzi(114) *et al.*

Briefly, all peptides were synthesized by standard Fmoc SPPS protocol using diisopropyl carbodiimide and HOBt to form activated esters. Alkyne functionalized peptides were produced by on-bead *N*-terminal functionalization with propynoic acid. Phosphine FLAG was obtained by on-bead *N*-terminal derivitization with 2-(Diphenylphosphino)terephthalic acid 1-methyl 4-pentafluorophenyl diester (Sigma-Aldrich 679011). During all deblocking steps 0.1 M HOBt was added to the 20% piperidine solution to alleviate aspartamide formation.

Synthesis of Azidohomoalanine (Aha). Azidohomoalanine was synthesized in four steps as described:



Scheme 6-2. Synthesis of azidohomoalanine

Compound 3. L-Homoserine (1.45 g, 12.7 mmol) was added to a solution of 9-Borabicyclo(3.3.1)nonane or 9-BBN (1.51 g, 12.4 mmol) in methanol (25 mL). The reaction mixture was refluxed for 3 hours under argon, at which time TLC analysis showed the reaction to be complete. The reaction mixture was concentrated and the crude product was purified by silica gel chromatography using a gradient elution (50% ethyl acetate-hexane to 100% ethyl acetate). 9-BBN protected L-homoserine was obtained as a white solid in 51% yield and purity was assessed as a single spot in TLC (R_f : 0.32) and $^1\text{H NMR}$. $^1\text{H NMR}$ (300 MHz, CD_3OD): δ 1.38-1.50 (2H, m), 1.60-1.98 (13H, m), 2.25 (1H, m), 3.75-3.85 (3H, m) ppm. ESI-MS calculated for $\text{C}_{12}\text{H}_{22}\text{BO}_3\text{N}$ (MH^+) 239.81 found at 239.1.

Compound 4. Methylsulfonyl chloride (0.87 mL, 7.5 mmol) was added to a solution of compound **3** (1.5g, 6.3 mmol) in tetrahydrofuran (20 mL) followed by triethylamine (1.2 mL, 12 mmol) at 0 °C. The reaction mixture was warmed to room temperature and stirred overnight. Subsequent TLC analysis showed the reaction to be complete. The resulting mixture was concentrated and purified by silica gel chromatography with gradient elution (50% ethyl acetate-hexane to 100% ethyl acetate). The product was obtained as a white solid in 70% yield. Purity was ascertained by TLC (R_f : 0.55) and ^1H NMR. ^1H NMR (300 MHz, CD_3OD): δ 1.38-1.50 (2H, m), 1.60-1.98 (12H, m), 2.15 (1H, m), 2.45 (1H, m), 3.12 (3H, s), 3.86 (1H, t), 4.40-4.58 (2H, m) ppm. ESI-MS calculated for $\text{C}_{13}\text{H}_{24}\text{BSO}_4$ (MH^+) 319.81, found 319.1.

Compound 5. Sodium azide (0.5 g, 7 mmol) was added to a solution of compound **4** (1.5 g, 5 mmol) in dimethylsulfoxide (10 mL). The mixture was stirred at 60 °C for 3 hours. The mixture formed a thick solid that was extracted into ethyl acetate and washed with water. The product was light yellow oil obtained in 95% yield. ^1H NMR (300 MHz, CD_3OD): δ 1.38-1.50 (2H, m), 1.60-1.98 (13H, m), 2.20 (1H, m), 3.55-3.70 (2H, m), 3.75 (1H, t) ppm. ESI-MS calculated for $\text{C}_{12}\text{H}_{22}\text{BO}_2\text{N}_4$ (MH^+) 264.1, found 264.1.

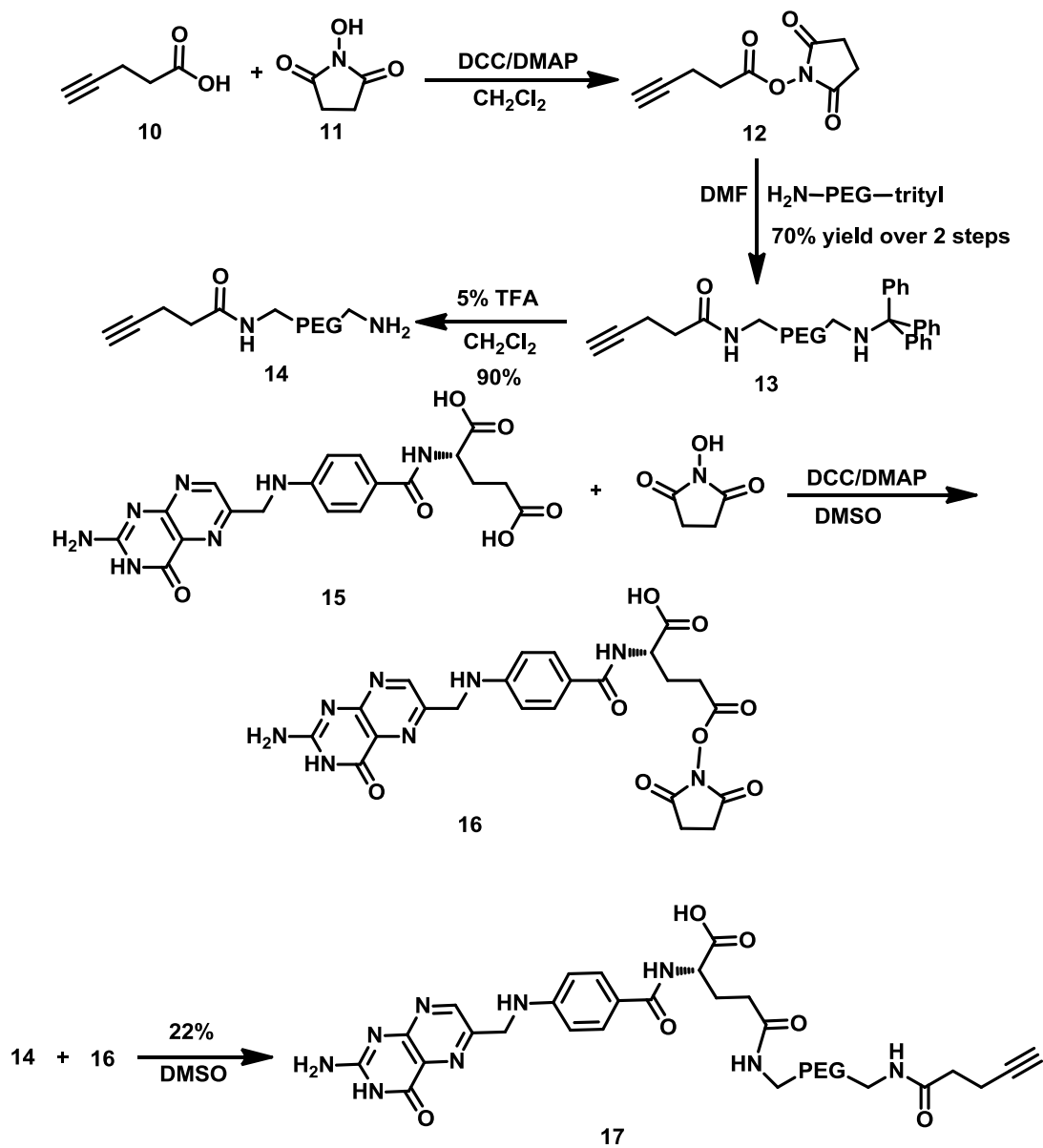
Azidohomoalanine (compound 6). Ethylene diamine (1 mL, 21 mmol) was added to a solution of compound **5** (1.5 g, 5.6 mmol) in tetrahydrofuran (10 mL) and refluxed for 2 hours. The mixture was concentrated and triturated with ethyl acetate. This was filtered through a glass column over sand and cotton. The solid residue was dissolved in

methanol and purified by silica gel chromatography eluting with 50:30:20 ethyl acetate: methanol: water. The pure amino acid was obtained as white solid in 47% yield. ^1H and 2D NMR confirmed its purity. R_f : 0.47. ^1H NMR (300Mz, D_2O): δ 1.92-2.12 (2H, m), 3.42-3.50 (2H, m), 3.72 (1H, t) ppm. ^{13}C NMR (400 Mz, D_2O): δ 30.937, 47.920, 53.316, 176.285. ESI-MS calculated for $\text{C}_4\text{H}_8\text{O}_2\text{N}_4$ (MH^+) 145.1, found 145.1.

Synthesis of alk-PEG-folate. Pentynoic acid (200 mg, 2.0 mmol) was activated by N,N' -dicyclohexylcarbodiimide (824 mg, 4.0 mmol) and N -hydroxysuccinimide (460 mg, 4.0 mmol) in methylene chloride at RT for 3 hours and filtered with a syringe filter (pore size 0.2 μm). O -(N -trityl-3-aminopropyl)- O' -(3-aminopropyl)-diethyleneglycol (MW 462) was added to the solution at a molar ratio of 5:1 (alkyne: PEG) and stirred vigorously overnight. The resulting solution was acidified with trifluoroacetic acid (final concentration 1%) to remove C- protecting trityl group. The reaction was then neutralized with triethyl amine and concentrated in *vacuo*. Folic acid was activated with NHS in presence of DCC in dry DMSO at RT for 3 hours. After filtration to remove the urea produced, Folate NHS ester was added to the alkyne-PEG under an atmosphere of argon in DMSO and allowed to react for 12 hours. Since purification of the folate NHS is not possible by normal flash chromatography, the crude product was used for coupling with the alkyne-PEG-amine. The alkyne-PEG-folate was precipitated by addition of diethyl ether. Trituration with DMSO/ether was repeated 3 times. Crude product was purified on a Jupiter C-12 column with a gradient of 5% to 25% acetonitrile containing 0.1% TFA. Product eluted at 35 minutes. ^1H NMR (300 Mz, DMSO): δ 0.97 (1H, t), 1.01 (1H, m), 1.10 (4H, s), 1.69 (4H, m), 2.52 (12H, m), 2.71 (1H, s), 2.87 (1H, s), 3.40 (2H, m), 3.50-

3.51 (2H, m), 4.47 (2H, s), 6.36 (2H, d), 7.61 (2H, d), 8.63 (1H, s) ppm. ESI-MS

calculated for $C_{34}H_{45}O_9N_9$ (MH^+) 724.3, found 724.3.



Scheme 6-3. Synthesis of alkyne-PEG-folate

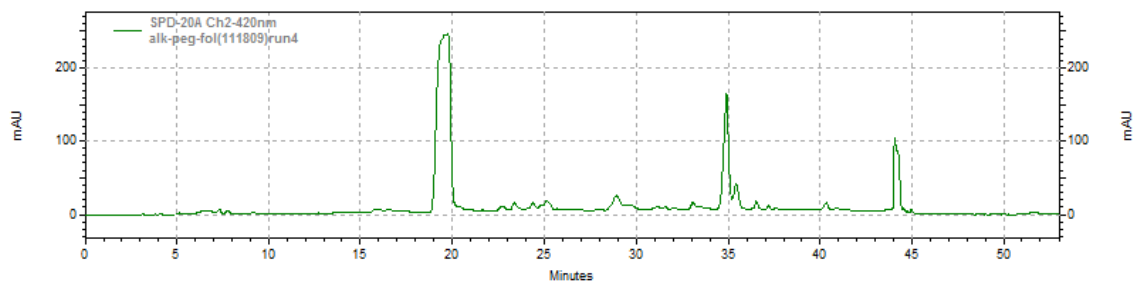
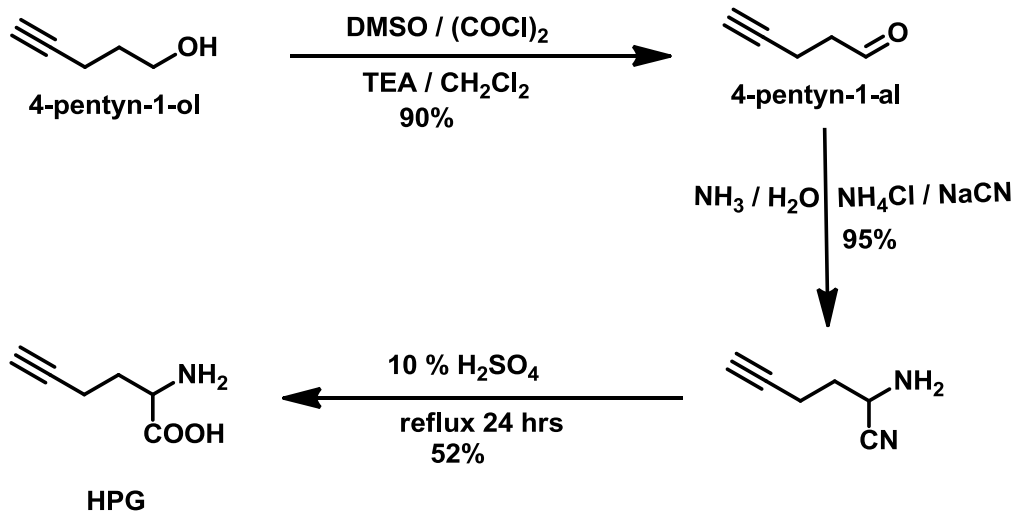


Figure 7-1. HPLC purification of alkyne-PEG-folate. Monitoring absorbance at 420 nm, on a C18 column running gradient of 5 to 25% acetonitrile containing 0.1% TFA. Product eluted after 35 minutes.

Synthesis of alkyne and phosphine FLAG. Synthesized as described by Bertozzi *et al.* (114). Briefly, all peptides were synthesized by standard Fmoc solid phase peptide synthesis protocol. In this case activated esters were formed using *N,N'*-diisopropylcarbodiimide and 1-Hydroxybenzotriazole. Alkyne functionalized peptides were produced by on-bead *N*-terminal functionalization with propynoic acid. Phosphine FLAG was obtained by on-bead *N*-terminal derivitization with 2-(Diphenylphosphino)terephthalic acid 1-methyl 4-pentafluorophenyl diester (Sigma-Aldrich 679011). During all de-blocking steps 0.1 M HOBt was added to the 20% piperidine solution to alleviate aspartamide formation.

Synthesis of Homopropargylglycine (HPG). Homopropargylglycine was synthesized as reported by Dong *et al.*(47) This is described below:



Scheme 6-4. Synthesis of Homopropargylglycine

Synthesis of 4-Pentynal. To a solution of oxalyl chloride (9.12 mL, 104.6 mmol) dissolved in dichloromethane (200 mL) at $-78\text{ }^\circ\text{C}$ was added dimethyl sulfoxide (14.8 mL, 209.2 mmol) dissolved in dichloromethane (40 mL) over 20 min. The reaction solution was kept under a positive pressure of argon until workup. After the solution was stirred for an additional 30 min 4-pentynol (8.0 g, 95.1 mmol) dissolved in dichloromethane (80 mL) was added over 10 min. The reaction mixture was stirred at $-78\text{ }^\circ\text{C}$ for an additional 60 min. Triethylamine (66.2 mL, 475.5 mmol) was added at $-78\text{ }^\circ\text{C}$ and the reaction mixture was stirred for 60 min and then allowed to warm to $10\text{ }^\circ\text{C}$ over an additional hour. Water (200 mL) was added, and the two layers were separated. The aqueous layer was acidified with 1 % aqueous hydrochloric acid (saturated with NaCl) and then back-extracted with additional dichloromethane (3 x 100 mL). The combined organic layers were washed with 1% hydrochloric acid (saturated with NaCl, 6 x 100 mL) followed by 5% aqueous sodium bicarbonate solution (2 x 50 mL). The aqueous

extracts were back-extracted with dichloromethane (2 x 100 mL) and the combined organic extracts were washed with brine (2 x 50 mL) and dried (MgSO₄). The solvent was removed by rotary evaporation to obtain 7.18 g (95%) of 4-pentynal as a yellow oil. ¹H NMR (CDCl₃): δ 1.99 (t, 1 H), 2.32-2.79 (m, 4 H), 9.82 (s, 1 H).

Synthesis of 2-aminohex-5-ynenitrile. NaCN (1.28 g, 26 mmol) and NH₄Cl (1.41 g, 26 mmol) were dissolved in 25% ammonia solution. After stirring for an hour at room temperature, 4-pentynal (1.25 g, 15 mmol) was added to this solution and stirred at 40 °C for 4 hours. The reaction was then quenched by 5% NaHCO₃ and the solution extracted with dichloromethane. The combined organic extracts were washed with bicarbonate and brine, dried over MgSO₄ and taken to dryness when the product was obtained (1.5 g, 95%) as yellow oil.

Synthesis of Homopropargylglycine. The aminonitrile was dissolved in dioxane and to this was added a 35% solution of hydrochloric acid. The mixture was stirred for 4 hours at 100 °C in an oil bath. The solution was cooled and washed with dichloromethane. The aqueous layer was neutralized with sodium bicarbonate. The resultant solution was lyophilized and the solid residue was dissolved in methanol and purified by silica gel chromatography eluting with 50:30:20 ethyl acetate: methanol: water. The pure amino acid was obtained as a white solid in 50 % yield. R_f: 0.43. ¹H NMR (300Mz, D₂O): δ 1.82-1.92 (2H, m), 2.0 (1H, t), 2.32-2.50 (2H, m), 3.82 (1H, t) ppm. ESI-MS calculated for C₆H₉O₂N (MH⁺) 128.3, found 128.3.

Synthesis of Phosphine-PEG-folate. Folic acid (50 mg, 0.114 mmol) was activated by *N,N'*-dicyclohexylcarbodiimide (82.4 mg, 0.4 mmol) and *N*-hydroxysuccinimide (46 mg, 0.4 mmol) in dry dimethylsulphoxide at RT for 3 hours and filtered with a syringe filter (pore size 0.2 μm). *O*-(*N*-trityl-3-aminopropyl)-*O'*-(3-aminopropyl)-diethyleneglycol (MW 462) was added to the solution at a molar ratio of 5:1 (folate-NHS: PEG) and stirred vigorously overnight. The resulting solution was acidified with trifluoroacetic acid (final concentration 1%) to remove C- protecting trityl group. The reaction was then neutralized with triethyl amine and concentrated. Folate-PEG dissolved in DMSO was purified over HPLC to remove unreacted folate and PEG samples. Purification was carried out using a Jupiter C-18 column with a gradient of 5% to 20% acetonitrile containing 0.1 % TFA. Product eluted after 25 minutes was concentrated in *vacuo*. A solution of the phosphine-PFP ester (10 mg, 0.02 mmol) and diisopropylethylamine (5 μL , 0.02 mmol) was made in anhydrous DMSO and added to the Folate-PEG (8.0 mg, 0.012mmol) under an atmosphere of argon. The mixture was rocked for 3 hours. The Phosphine-PEG-folate was precipitated by addition of diethyl ether. Crude product was purified on a Jupiter C-18 column with a gradient of 5% to 50% acetonitrile containing 0.1% TFA. Product eluted at 37 minutes. ^1H NMR (300 Mz, D_2O): δ 1.07 (2H, t), 1.10 (4H, t), 1.89 (4H, m), 1.92 (12H, m), 2.71 (1H, s), 3.40 (2H, m), 3.50-3.51 (2H, m), 3.92 (3H,s), 6.7 (2H, d), 7.5 (2H, d), 7.26 (4H, m), 7.78 (6H, m), 8.04 (1H, s), 8.47 (1H, d), 8.56 (1H, d), 9.0 (1H, s) ppm. ESIMS calculated for $\text{C}_{50}\text{H}_{56}\text{O}_{11}\text{N}_9\text{P}$ (MH^+) 990.0, found 990.3.

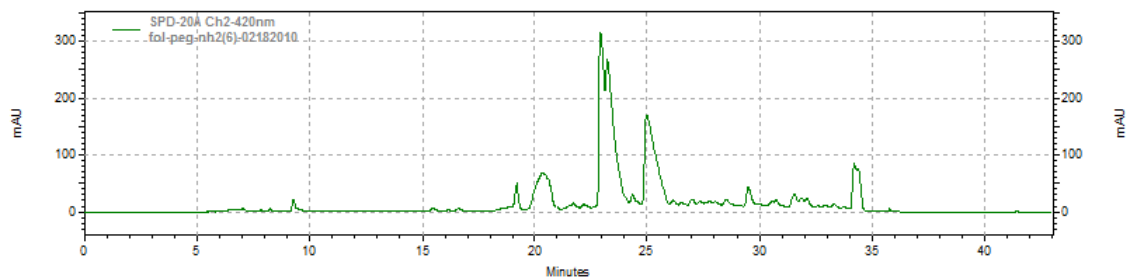


Figure7-2. HPLC purification of folate-PEG-NH₂. Monitoring absorbance at 420 nm, on a C18 column running gradient of 5 to 20% acetonitrile containing 0.1% TFA. Product eluted after 25 minutes.

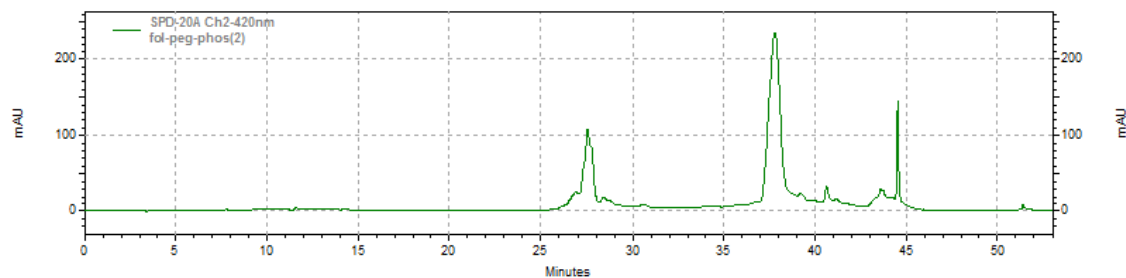


Figure7-3. HPLC purification of folate-PEG-phosphine. Monitoring absorbance at 420 nm, on a C18 column running gradient of 5 to 50% acetonitrile containing 0.1% TFA. Product eluted after 37 minutes.

Synthesis of 3-azidopropan-1-amine. 140 mg of *tert*-butyl (3-azidopropyl)carbamate was dissolved in DMSO and to it was added 850 mg of sodium azide. This mixture was warmed at 40 °C for 1 hour and the product extracted into dichloromethane and washed with water. To the extracted organic layer 4 mL of 5% TFA in dichloromethane was added and the solution stirred at room temperature for 1 hour. The resultant solution was concentrated and neutralized with 2N KOH. The solution was extracted with

dichloromethane and concentrated to obtain the product as yellow oil. ^1H NMR (300 Mz, CDCl_3): δ 1.72-1.82 (2H, m), 2.82-2.90 (2H, t), 3.42 (2H, t) ppm.

Synthesis of TAMRA-azide. TAMRA-NHS (1 mg) obtained from GBiosciences was dissolved in methanol and to it excess 3-azidopropane-1-amine was added. The mixture was stirred for 2 hours in the dark after which the product was loaded onto a small glass pipet silica column and washed with dichloromethane to remove excess azido-propane amine. The product was finally extracted into methanol and concentrated. ESIMS calculated for $\text{C}_{24}\text{H}_{19}\text{O}_5\text{N}_5\text{S}$ (MH^+) 512.2, found 513.2.

7.2. Adenovirus production using unnatural substrates

Cell culture. Dulbecco's modified Eagle's medium (DMEM), RPMI 1640, Penicillin/Streptomycin and 0.5% Trypsin-EDTA were purchased from GIBCO (Grand Island, NY). RPMI 1640 minus Folic acid was obtained from Sigma (St. Louis, MO). Fetal calf serum (FCS) and Bovine Calf Serum (BCS) was from HyClone (Logan, UT). 293 cells were maintained in DMEM supplemented with 10% BCS, 2 mM glutamine, 100 U/mL penicillin, 100 $\mu\text{g}/\text{mL}$ streptomycin. 4T1 cells were maintained in RPMI 1640 medium containing 10% FCS, 2 mM L-glutamine, 100 U/mL penicillin, and 100 $\mu\text{g}/\text{mL}$ streptomycin. For 4T1 cells grown without Folate, RPMI 1640 minus Folic acid was supplemented with 10% FCS, 0.3 mg/mL L-glutamine, 2 mg/mL sodium bicarbonate,

100 U/mL penicillin, 100 µg/mL streptomycin. ID8 cells were maintained in RPMI 1640 medium containing 10% FCS, 2 mM L-glutamine, 100 U/mL penicillin, and 100 µg/mL streptomycin. All cells were maintained in 100 x 20 mm Tissue Culture Dishes obtained from BD biosciences (Franklin Lakes, NJ) at 37°C and 5% CO₂.

Metabolic labeling of Adenovirus type 5 with 1,3,4,6-tetra-O-acetyl-N-

azidoacetylgalactosamine. HEK 293 cells were infected with wild type adenovirus particles with an MOI of 5pfu/cell. The complete media was supplemented with 50 µM per acetyl-N-azidoacetylgalactosamine or 50 µM per acetyl-N-azidoacetylglucosamine and the infected cells incubated at 37°C. The plates were harvested 42-46 hours post infection and virus particles purified over a gradient of 1.4 g/mL and 1.25 g/mL CsCl centrifuged at 32,000 rpm for 1 hour at 15°C. The virus band at the junction of the two CsCl bands was collected and further purified by an 18 hour centrifugation at 35,000 rpm over 1.33 g/mL of CsCl.

Metabolic labeling of adenovirus type 5 with Azidohomoalanine (Aha). HEK 293 cells were infected with wild type adenovirus particles with an MOI of 5 pfu/ cell. 18 hours post infection complete media was removed and the cells washed with TD buffer (25 mM Tris, 125 mM NaCl, 5 mM KCl and 1 mM Na₂HPO₄ at pH 7.5) at 37 °C for 20 minutes. Aha supplemented DMEM (-Met) media was then added to the infected cells and allowed to grow until 24 hours post infection. The labeling media was then removed and the cells were supplemented with complete media. The plates were harvested 46-48

hours post infection and virus particles purified over a gradient of 1.4 g/mL and 1.25 g/mL CsCl centrifuged using an SW41 rotor (Beckman) at 32,000 rpm for 1 hour at 15 °C. The virus band at the junction of the two CsCl bands was collected and further purified using an SW60 rotor (Beckman) by an 18 hour centrifugation at 35,000 rpm over 1.33 g/mL CsCl.

Metabolic labeling of adenovirus type 5 with Homopropargylglycine (HPG). HEK 293 cells were infected with wild type adenovirus particles with an MOI of 5 pfu/ cell. 18 hours post infection complete media was removed and the cells washed with TD buffer (25 mM Tris, 125 mM NaCl, 5 mM KCl and 1 mM Na₂HPO₄ at pH 7.5) at 37 °C for 20 minutes. HPG supplemented DMEM (-Met) media was then added to the infected cells and allowed to grow until 24 hours post infection. The labeling media was then removed and the cells were supplemented with complete media. The plates were harvested 46-48 hours post infection and virus particles purified over a gradient of 1.4 g/mL and 1.25 g/mL CsCl centrifuged using an SW41 rotor (Beckman) at 32,000 rpm for 1 hour at 15 °C. The virus band at the junction of the two CsCl bands was collected and further purified using an SW60 rotor (Beckman) by an 18 hour centrifugation at 35,000 rpm over 1.33 g/mL CsCl.

Metabolic labeling of adenovirus type 5 with Homopropargylglycine (HPG) and *N*-azidoacetylgalactosamine. HEK 293 cells were infected with wild type adenovirus particles with an MOI of 5pfu/cell. The complete media was supplemented with 50 µM

per acetyl-*N*-azidoacetylgalactosamine and the infected cells incubated at 37°C. 18 hours post infection growth media was removed and the cells washed with TD buffer (25 mM Tris, 125 mM NaCl, 5 mM KCl and 1 mM Na₂HPO₄ at pH 7.5) at 37 °C for 20 minutes. 4 mM HPG and 50 µM Ac₄GalNAz supplemented DMEM (-Met) media was then added to the infected cells and allowed to grow until 24 hours post infection. The labeling media was then removed and the cells were supplemented with complete media containing 50 µM Ac₄GalNAz. The plates were harvested 46-48 hours post infection and virus particles purified over a gradient of 1.4 g/mL and 1.25 g/mL CsCl centrifuged using an SW41 rotor (Beckman) at 32,000 rpm for 1 hour at 15 °C. The virus band at the junction of the two CsCl bands was collected and further purified using an SW60 rotor (Beckman) by an 18 hour centrifugation at 35,000 rpm over 1.33 g/mL CsCl.

7.3. Chemical modification and characterization of substrate labeled virions

Reaction of azide labeled virus with alkyne-FLAG. 50 µL of 1×10^{12} azide labeled virus particles/mL in a 100 mM tris buffer pH 8.0 was mixed with Bathophenanthroline disulphonic acid disodium salt at a final concentration of 3mM and alkyne-FLAG at a final concentration of 400µM were kept in a deoxygenated glove bag for 6 hours after which copper bromide was added to the mixture at a final concentration of 1mM and the reaction allowed to proceed for 12 hours(64) inside the glove bag. The samples were then taken out and the reaction quenched by 10 mM EDTA. The samples were then analyzed by western blotting technique to determine incorporation of FLAG on the viral proteins.

Reaction of azide labeled virus with alk-TAMRA. A solution of 50 μL of 1×10^{12} azide labeled virus particles/mL in 100 mM tris pH 8.0, with bathophenanthroline disulphonic acid disodium salt (3 mM) and alk-TAMRA (400 μM), 5-tetramethylrhodamine (GBiosciences, Maryland Heights, MO) was kept in an argon-filled glove bag for 6 hours to deoxygenate. After which copper bromide at a final concentration of 1 mM was added to the mixture and the reaction allowed to proceed for 12 hours (64) inside the glove bag. The samples were then removed from the glove bag and quenched by addition of 10 mM EDTA. All samples were then analyzed by fluorescent gel scanning to determine the extent of chemical labeling.

Reaction of azide labeled virus with phosphine-FLAG. 50 μL of 1×10^{12} azide labeled viral particles/mL in a 100 mM tris buffer at pH 8.0 was treated with phosphine-FLAG at a final concentration of 400 μM in room temperature for 2 hours and then analyzed by western blotting.

Western Blotting. To all samples coupled with alkyne- and phosphine-FLAG loading dye was added and phosphine-FLAG labeled samples boiled at 95°C for 10 minutes. The samples were run on a 10% polyacrylamide electrophoresis gel and transferred onto nitrocellulose at 40V over 2 hours in a western transfer buffer (25 mM tris, 192 mM glycine, 0.5% SDS and 10% methanol). Blots were blocked by 5% milk in PBST and treated with anti-FLAG M2 HRP conjugate at a ratio of 1:12000 in 5% milk in PBST. Blots were washed with milk and PBST and developed by chemiluminescence (Millipore

Immobilon Western kit). For IR fluorescence the blots were treated with an anti-penton antibody followed by an IR 680 dye as secondary and the blots visualized on the Odyssey LICOR, excitation at 680 nm and emission at 700 ± 15 nm.

GlcNAcase Assay. For treatment with GlcNAcase, adenoviral fiber was partially purified from complete virus particles. GlcNAz labeled adenoviral particles were dialyzed overnight in a tris-maleate (5mM tris, 5mM maleic acid, 1 mM EDTA) buffer at pH 6.5. The dialyzed solution was centrifuged at 14.2 rpm for 60 minutes after which the supernatant containing the Penton and Fiber proteins were separated from the remaining viral capsid which precipitates. The mixture of Fiber and Penton was treated with 5M guanidinium hydrochloride and subjected to acetone precipitation. The protein was resuspended in 50 mM tris, 12.5 mM $MgCl_2$ at pH 7.5 to a concentration of 0.5 mg/mL after which it was treated with 5 $\mu\text{g}/\mu\text{L}$ Hex-C at 1:10 (Fiber: Hex-C) overnight at 37°C(195). The reaction mixture was subjected to Staudinger reaction with phosphine-FLAG for 2 hours and analyzed by western blotting as described above.

Plaque Assay. Complete overlay solution was prepared by adding 5% sodium bicarbonate, 2.5 mL of 1 M HEPES, 10 % serum and 36 mL of 2.8% bacto-agar to 50 mL of 2X DME solution. This solution was equilibrated at 55 °C. HEK 293 cells cultivated in 6 mL culture plates were infected with 400 μL of labeled virus particles at concentrations of 10^3 , 10^4 and 10^5 particles/ml. After incubation of infected cells at 37 °C for an hour, the plates were overlaid with complete media containing 2.8% bacto-agar and 10% BCS.

After 3 days the cells were again overlaid with same agar overlay solution containing 2% BCS. After the 6th day when plaques became visible the cells were overlaid with agar overlay solution containing 0.1% neutral red. The plaques were counted within a day after the final overlay.

MS analysis. Matrix-assisted laser desorption/ionization (MALDI) mass spectra were obtained using a Bruker Autoflex II MALDI/TOF/TOF. LC-MS sequencing of the viral peptides were performed on a Thermo Fisher Scientific LTQ XL. Virus particles labeled metabolically with Aha were treated with 8 M urea to dissociate the particles and denature viral proteins. The solution was diluted with ammonium bicarbonate to 0.5 M urea. The resulting solution was treated with 0.1 µg/µL of trypsin at 1:50 (protein: protease) ratio and digestion was allowed to proceed overnight at 37 °C. The reaction was quenched with 1/10th volume of 100% formic acid and concentrated to 1/10th the reaction volume. The peptide mixture was subjected to LC/MS treatment using a C18 column. MS data was searched against the SPROT database with Inspect for the following modifications C+57 (iodoacetamide adduct of cysteine), M+16 (methionine oxidation), M-5 (methionine substituted by azidohomoalanine. Molecular weight of Aha being 144.1, it is 5 mass units less than methionine) and STY+80 (serine, threonine and tyrosine phosphorylation). For quantification of Aha incorporation, elution profiles of daughter ions that should be the same in both the modified and unmodified peptides were traced and areas calculated.

Fluorescent Gel Scanning Assay. Azide enabled viral particles (with 50 μM GalNAz) were labeled with an alkyne-TAMRA dye using Cu catalyzed “Click” chemistry as described above for FLAG labeling and reaction was quenched with 10 mM EDTA. The particles were purified using Centri-Sep spin columns and quantified with QuantIT Picogreen Dye labeling(132). 1×10^{12} viral particles/mL were run on a polyacrylamide electrophoresis gel using the alkyne-TAMRA dye as standard. Standard dye was loaded 10 minutes before the end of the run. Gels were scanned using a typhoon gel scanner in the fluorescence mode with excitation filter at 532 nm and emission filter at 580 ± 15 nm. The scans were subsequently analyzed with Image Quant TL 1D gel analyzer software. All gels were run at 4°C for 60 minutes and scanned within 10minutes of the end of run.

Concentration dependent dye labeling of adenoviral particles. Ad5 particles metabolically labeled with 4 mM Aha were treated with increasing concentrations of Alkyne-TAMRA (10 μM , 20 μM , 40 μM , 80 μM , 160 μM , 320 μM and 600 μM). After chemical modification the virions were purified and run on an SDS-PAGE gel using alkyne-TAMRA as standard. . Standard dye was loaded 10 minutes before the end of the run. Gels were scanned using a typhoon gel scanner in the fluorescence mode with excitation filter at 532 nm and emission filter at 580 ± 15 nm. The scans were subsequently analyzed with Image Quant TL 1D gel analyzer software. All gels were run at 4°C for 60 minutes and scanned within 10minutes of the end of run. Number of dye per virion was plotted against concentration of alkyne-dye used.

Intrinsic Ad5 fluorescence to determine virus thermo-stability. 5×10^{11} viral particles/ mL of both metabolically labeled with Aha and unlabeled were used to determine thermo stability.(160) Intrinsic fluorescence emission spectra were obtained in 5°C increments from 20 to 80°C employing a QuantaMasterTM spectrofluorometer (Photon Technology International, Inc.) equipped with a 4-position cell holder and temperature control device. A 5-min equilibration time was used at each temperature before data acquisition. The intrinsic fluorescence spectra was collected by exciting samples at 295 nm while the emission was monitored between 300 and 450 nm using excitation and emission slit widths of 4 nm . The wavelength of fluorescence maxima was plotted against temperature to determine thermo stability of Aha enabled and unlabeled Ad5.

Reaction of HPG and GalNAz labeled virus with phosphine-FLAG and azido-TAMRA. $50\ \mu\text{L}$ of 1×10^{12} metabolically labeled viral particles/mL in a 100 mM tris buffer at $\text{pH } 8.0$ was treated with phosphine-FLAG at a final concentration of $300\ \mu\text{M}$ in room temperature for 3 hours. After which time, to the solution bathophenanthroline disulphonic acid disodium salt (3 mM) and azido-TAMRA ($500\ \mu\text{M}$), 5-tetramethylrhodamine (GBiosciences, Maryland Heights, MO) was added and kept in a argon-filled glove bag for 6 hours to deoxygenate. Next copper bromide at a final concentration of 1 mM was added to the mixture and the reaction allowed to proceed for 12 hours (64) inside the glove bag. The samples were then removed from the glove bag and quenched by addition of 10 mM EDTA. The particles were purified using Centri-Sep spin columns and quantified with QuantIT Picogreen Dye labeling(132). The

samples were then analyzed by western blotting technique to determine incorporation of FLAG on the viral proteins, and by fluorescent gel scanning to determine incorporation of TAMRA.

Reaction of HPG and GalNAz labeled AdTRAIL with phosphine-Folate and SBT-1214-PEG-azide. AdTRAIL was obtained from Prof. Andre Lieber, University of Washington, Seattle. The virions were metabolically labeled with HPG and GalNAz as described above. 50 μ L of 1×10^{12} metabolically labeled viral particles/mL in a 100 mM tris buffer at pH 8.0 was treated with phosphine-Folate at a final concentration of 300 μ M in room temperature for 3 hours. After which time, bathophenanthroline disulphonic acid disodium salt (3 mM) and SBT-1214-PEG-azide (500 μ M), was added and the resultant mixture kept in an argon-filled glove bag for 6 hours to deoxygenate. Next copper bromide at a final concentration of 1 mM was added to the mixture and the reaction allowed to proceed for 12 hours (64) inside the glove bag. The samples were then removed from the glove bag and quenched by addition of 10 mM EDTA. The particles were purified using Centri-Sep spin columns and quantified with QuantIT Picogreen Dye labeling(132). Subsequently, MTT and Targeting assays were performed using these modified virions.

7.4. Targeting, imaging, cytotoxicity

Targeting Assay. GFP transgene bearing Ad5 were labeled with GalNAz as described. The viruses were labeled with folate bearing alkyne probe (alkyne-folate) using Cu catalyzed “click” chemistry in a deoxygenated glove under same conditions (as for FLAG labeling) and the reaction quenched with 10 mM EDTA. Viruses were purified on Centri Sep spin columns and quantified using QuantIT Picogreen assay (Molecular Probes, Eugene, OR) and stored in a 0.9 mM CaCl₂ and 0.5 mM MgCl₂ buffer in PBS containing 10% glycerol. Mouse breast cancer cell line 4T1 was cultivated in minus folate media for 2 weeks after which they were seeded in 24 well plates at a density of 1 x 10⁶ cells/well and cultivated for a day in minus folate media containing 2% FCS. After 24 hours the cells were infected with labeled virus at an MOI of 50. 24 hours post infection; GFP expression was evaluated using a Synergy 2 fluorescence plate reader (excitation 485 ± 10 nm; emission 528 ± 10 nm).

Fluorescence Microscopy: For visualization of GFP expression within targeted 4T1 cells, the murine breast carcinoma cells grown in minus folate media for 2 weeks were plated on Glass Bottom Dishes at a density of 1 x 10⁵ cells/well and cultivated for 24 hours in negative folate media. After which time they were infected with folate-labeled virus, unlabeled virus and folate-labeled virus but with cells pretreated with 1mg/L folate 30 minutes before infection at an MOI of 50. Again 24 hours post infection the cells were

visualized under a Zeiss LSM 510 META NLO 2-photon laser scanning confocal microscope system. Images were taken both with a GFP and the bright fields filter.

Targeting assay and fluorescent microscopy for Aha enabled Ad5. Ad5, encoding GFP or luciferase in the E1 region, were labeled with 4 mM and 32 mM Aha as described. Viruses were labeled with folate bearing alkyne probe (alk-PEG-folate) using Cu catalyzed “click” chemistry in a deoxygenated glove under same conditions (as for TAMRA labeling) and the reaction quenched with 10 mM EDTA. Viruses were purified on G-25 sephedex desalting spin columns (Centri Sep spin columns; Adelphia, NJ), quantified using QuantIT Picogreen assay (Molecular Probes, Eugene, OR), and stored in a 0.9 mM CaCl₂ and 0.5 mM MgCl₂ buffer in PBS containing 10% glycerol. Mouse breast cancer cell line 4T1 was cultivated in minus folate media for 2 weeks after which they were seeded in 24 well plates at a density of 1 x 10⁶ cells/well. 24 hours after replating the cells were infected with metabolically and chemically labeled virus at an MOI of 50. 24 hours post infection; Luciferase expression was evaluated using a Perkin Elmer Victor X5 luminescence plate reader. 4T1 cells cultivated in minus folate media for 2 weeks were seeded in glass bottom dishes at 1.1 x 10⁵ cells per dish. Cells were infected with folate labeled Ad5 or the negative control, no metabolic Aha incorporation, both bearing the GFP transgene as described for the targeting assay. Notably, all viruses were exposed to the chemical labeling conditions irrespective of the presence of Aha. 24 hours post infection the dishes were mounted and cells imaged by confocal microscopy in a Zeiss LSM 510 equipped with a 63x, 1.4 NA C-Apochromat water immersion objective. Images were processed using Zeiss LSM 510 software.

Imaging of HEK 293 cell infection with TAMRA labeled Ad5. Adenovirus particles produced in the presence of 4 mM and 32mM Aha were used for chemical modification via alkyne-TAMRA. The chemically labeled virions were purified from copper and free probe using CentriSep spin columns. The purified virions were quantified using picogreen assay. HEK 293 cells seeded in glass bottom dishes at concentrations of 1×10^4 cells/ mL were then infected with the TAMRA-Ad5 at MOI of 5 and 10. Twenty minutes post infection the infection buffer was removed and the cells overlaid with growth media. The cells were then imaged on a Laser scanning confocal microscope system using Zeiss LSM 510 equipped with a 63x, 1.4 NA C-Apochromat water immersion objective using a Rhodamine filter. Images were processed using Zeiss LSM 510 software.

MTT assay with dual modified Ad5. Adenovirus bearing TRAIL were metabolically labeled with HPG and GalNAz as described. Chemical labeling of these viruses with SBT-1214-PEG-azide was carried via the copper catalyzed “click” reaction in deoxygenating conditions (as for azido-TAMRA). The viruses were purified over centriSep spin columns and quantified using QuantIT Picogreen assay. Human ovarian cancer cells, ID8 were seeded in 96 well plates at concentrations of 1×10^5 cells/ mL. 24 hours after seeding, these cells were infected with different MOI of SBT-1214 labeled AdTRAIL. Control experiments were run by infecting cells with metabolically unlabeled AdTRAIL (these were chemically treated exactly as the azide, alkyne enabled virions).

Cells were also treated with increasing concentrations of SBT-1214-PEG-azide – to account for the increasing MOI of infection. The cells were incubated at 37°C incubator for 5 days. After this they were treated with MTT reagent obtained from Cell Proliferation KitI (Roche, Eugene,OR). After a 4 hour incubation at 37°C the cells were again treated with solubilization buffer and left overnight. Absorbance was measured at 580 nm using a PerkinElmer Victor X plate reader.

Targeting of dual labeled virus. Luciferase transgene bearing Ad5 were metabolically labeled with HPG and GalNAz as described. The viruses were chemically labeled with folate bearing phosphine-probe (phosphine-PEG-folate) and SBT-1214-PEG-azide using Staudinger ligation and Cu catalyzed “click” chemistry in a deoxygenated glove under same conditions (as for FLAG/ TAMRA labeling) and the reaction quenched with 10 mM EDTA. Viruses were purified on Centri Sep spin columns and quantified using QuantIT Picogreen assay (Molecular Probes, Eugene, OR) and stored in a 0.9 mM CaCl₂ and 0.5 mM MgCl₂ buffer in PBS containing 10% glycerol. Mouse breast cancer cell line 4T1 was cultivated in minus folate media for 2 weeks after which they were seeded in 96 well plates at a density of 1 x 10⁵ cells/well and cultivated for a day in minus folate media containing 2% FCS. After 24 hours the cells were infected with labeled virus at an MOI of 50. 24 hours post infection the cells were treated with 100 µL of reconstituted luciferase substrate from Bright Glo™ Luciferase assay Kit (Promega, Madison,WI) ; luciferase expression was evaluated using a PerkinElmer Victor X luminescence plate reader (emission 528 ± 10 nm).

7.5. Cloning

Generation of fiber shuttle plasmid. The adenoviral plasmid pTG3602 was digested with restriction enzyme EcoRI for 3 hours at 37 °C. The digest was run on an agarose gel and the 8 kB fragment was gel purified. This fragment was redigested with KpnI and the 4.5 kB fragment gel purified. The backbone plasmid pBAD was double digested with EcoRI and KpnI and gel purified. Ligation was carried between the fiber fragment and the backbone plasmid overnight and the clones were transformed and expressed. Conformation of gene insertion was carried out via double EcoRI and KpnI digestion and single digestion of NdeI. Sequence was confirmed by sequencing.

Mutant fiber generation. Fiber gene on the fiber shuttle plasmid was mutated via quick-change protocol to generate isoleucine mutants of methionine 251 and 330. Their production was confirmed by sequencing analysis.

Generation of Ad backbone for fiber modification. To generate a unique restriction site within the Ad5 backbone, we designed unique 15 base pair inserts containing SmaI restriction site. The following oligos were ordered and used for this purpose, 5'-TACGCATTTAAATCGG-3' and 3'-GCGTAAATTTAGCCAT-5'. pTG3602 was partially digested using NdeI restriction enzyme for 45 minutes. The reaction was heat

inactivated after which the DNA was cleaned with clean DNA kit from Zymo research. Next the linker DNA and the cleaved pTG3602 were ligated overnight. The resultant product was transformed into DH10B cells and the clones analyzed by *SwaI* restriction enzyme. The clones that showed a single cut site when treated with *SwaI* were sent for sequencing. Sequencing results inconclusive.

References and notes

1. **A.C.; Baker A.H.; Ylä-Herttuala S, T. M. P. P. H. L. K. J. K. H. M. O. R. J. L. O. T. A.-M. N. A. N.** 2002. Peptide-Retargeted Adenovirus Encoding a Tissue Inhibitor of Metalloproteinase-1 Decreases Restenosis after Intravascular Gene Transfer. *Mol Ther* **6**:306-312.
2. **Abdulghani, J., and W. S. El-Deiry.** 2010. TRAIL receptor signaling and therapeutics. *Exp Opin Ther Targ.* **14**:1091-1108.
3. **Agard, N. J., J. M. Baskin, J. A. Prescher, A. Lo, and C. R. Bertozzi.** 2006. A Comparative Study of Bioorthogonal Reactions with Azides. *ACS Chem. Biol.* **1**:644-648.
4. **Agard, N. J., and C. R. Bertozzi.** 2009. Chemical Approaches To Perturb, Profile, and Perceive Glycans. *Acct. Chem. Res.* **42**:788-797.
5. **Agard, N. J., J. A. Prescher, and C. R. Bertozzi.** 2004. A Strain-Promoted [3 + 2] Azide−Alkyne Cycloaddition for Covalent Modification of Biomolecules in Living Systems. *J. Am. Chem. Soc.* **126**:15046-15047.
6. **Alemaný, R.** 2009. Designing adenoviral vectors for tumor-specific targeting. *Methods in Molecular Biology* **542**:57-74.
7. **Alemaný, R., C. Balague, and D. T. Curiel.** 2000. Replicative adenoviruses for cancer therapy. *Nat Biotech* **18**:723-727.
8. **Arrowsmith, J.** 2011. Trial watch: Phase III and submission failures: 2007–2010. *Nat Rev Drug Discov* **10**:87-87.

9. **Asada, T.** 1974. Treatment of human cancer with mumps virus. *Cancer* **34**:1907-1926.
10. **Banerjee, P. S., P. Ostapchuk, P. Hearing, and I. Carrico.** 2010. Chemoselective Attachment of Small Molecule Effector Functionality to Human Adenoviruses Facilitates Gene Delivery to Cancer Cells. *J. Am. Chem. Soc.* **132**:13615-13617.
11. **Banerjee, P. S., P. Ostapchuk, P. Hearing, and I. S. Carrico.** 2011. Unnatural Amino Acid Incorporation onto Adenoviral (Ad) Coat Proteins Facilitates Chemoselective Modification and Retargeting of Ad Type 5 Vectors. *J. Virol.* **85**:7546-7554.
12. **Banerjee, P. S., E. S. Zuniga, I. Ojima, and I. S. Carrico.** 2011. Targeted and armed oncolytic adenovirus via chemoselective modification. *Bioorganic & Medicinal Chemistry Letters* **In Press, Corrected Proof**.
13. **Baskin, J. M., K. W. Dehnert, S. T. Laughlin, S. L. Amacher, and C. R. Bertozzi.** 2010. Visualizing enveloping layer glycans during zebrafish early embryogenesis. *Proc. Natl. Acad. Sci. USA* **107**:10360-10365.
14. **Baskin, J. M., J. A. Prescher, S. T. Laughlin, N. J. Agard, P. V. Chang, I. A. Miller, A. Lo, J. A. Codelli, and C. R. Bertozzi.** 2007. Copper-free click chemistry for dynamic in vivo imaging. *Proc. Natl. Acad. Sci. USA* **104**:16793-16797.
15. **Beatty, K. E., J. D. Fisk, B. P. Smart, Y. Y. Lu, J. Szychowski, M. J. Hangauer, J. M. Baskin, C. R. Bertozzi, and D. A. Tirrell.** 2010. Live-Cell

- Imaging of Cellular Proteins by a Strain-Promoted Azide–Alkyne Cycloaddition. *ChemBioChem* **11**:2092-2095.
16. **Beatty, K. E., and D. A. Tirrell.** 2008. Two-color labeling of temporally defined protein populations in mammalian cells. *Bioorg. Med. Chem. Letts.* **18**:5995-5999.
 17. **Belousova, N., V. Krendelchtchikova, D. T. Curiel, and V. Krasnykh.** 2002. Modulation of Adenovirus Vector Tropism via Incorporation of Polypeptide Ligands into the Fiber Protein. *J. Virol.* **76**:8621-8631.
 18. **Blanche, F., B. Cameron, S. Somarriba, L. Maton, A. Barbot, and T. Guillemin.** 2001. Stabilization of Recombinant Adenovirus: Site-Directed Mutagenesis of Key Asparagine Residues in the Hexon Protein. *Anal. Biochem.* **297**:1-9.
 19. **Botchkina, G., E. Zuniga, M. Das, Y. Wang, H. Wang, S. Zhu, A. Savitt, R. Rowehl, Y. Leyfman, J. Ju, K. Shroyer, and I. Ojima.** 2010. New-generation taxoid SB-T-1214 inhibits stem cell-related gene expression in 3D cancer spheroids induced by purified colon tumor-initiating cells. *Mol Cancer* **9**:192.
 20. **Boyce, M., I. S. Carrico, A. S. Ganguli, S.-H. Yu, M. J. Hangauer, S. C. Hubbard, J. J. Kohler, and C. R. Bertozzi.** 2011. Metabolic cross-talk allows labeling of O-linked β -N-acetylglucosamine-modified proteins via the N-acetylgalactosamine salvage pathway. *Proc. Natl. Acad. Sci. USA* **108**:3141-3146.
 21. **Bruckman, M. A., G. Kaur, L. A. Lee, F. Xie, J. Sepulveda, R. Breitenkamp, X. Zhang, M. Joralemon, T. P. Russell, T. Emrick, and Q. Wang.** 2008.

- Surface Modification of Tobacco Mosaic Virus with “Click” Chemistry.
ChemBioChem **9**:519-523.
22. **Butkinaree, C., K. Park, and G. W. Hart.** 2010. O-linked [beta]-N-acetylglucosamine (O-GlcNAc): Extensive crosstalk with phosphorylation to regulate signaling and transcription in response to nutrients and stress. *Biochimica et Biophysica Acta (BBA) - General Subjects* **1800**:96-106.
 23. **Campos, S. K., M. B. Parrott, and M. A. Barry.** 2004. Avidin-based Targeting and Purification of a Protein IX-modified, Metabolically Biotinylated Adenoviral Vector. *Mol Ther* **9**:942-954.
 24. **Carlo-Stella, C., C. Lavazza, A. Locatelli, L. Viganò, A. M. Gianni, and L. Gianni.** 2007. Targeting TRAIL Agonistic Receptors for Cancer Therapy. *Clin Canc Res.* **13**:2313-2317.
 25. **Carrico, Z. M., D. W. Romanini, R. A. Mehl, and M. B. Francis.** 2008. Oxidative coupling of peptides to a virus capsid containing unnatural amino acids. *Chem. Commun.*:1205-1207.
 26. **Cauet, G., J.-M. Strub, E. Leize, E. Wagner, A. V. Dorselaer, and M. Lusky.** 2005. Identification of the Glycosylation Site of the Adenovirus Type 5 Fiber Protein. *Biochem.* **44**:5453-5460.
 27. **Cavazzana-Calvo, M., S. Hacein-Bey, G. d. S. Basile, F. Gross, E. Yvon, P. Nusbaum, F. Selz, C. Hue, S. Certain, J.-L. Casanova, P. Bousso, F. L. Deist, and A. Fischer.** 2000. Gene Therapy of Human Severe Combined Immunodeficiency (SCID)-X1 Disease. *Science* **288**:669-672.

28. **Chang, P. V., J. A. Prescher, M. J. Hangauer, and C. R. Bertozzi.** 2007. Imaging Cell Surface Glycans with Bioorthogonal Chemical Reporters. *J. Am. Chem. Soc.* **129**:8400-8401.
29. **Chartier, C., E. Degryse, M. Gantzer, A. Dieterle, A. Pavirani, and M. Mehtali.** 1996. Efficient generation of recombinant adenovirus vectors by homologous recombination in *Escherichia coli*. *J. Virol.* **70**:4805-4810.
30. **Chen, S. Y., X. R. Zhao, J. Y. Chen, J. Chen, L. Kuznetsova, S. S. Wong, and I. Ojima.** 2010. Mechanism-Based Tumor-Targeting Drug Delivery System. Validation of Efficient Vitamin Receptor-Mediated Endocytosis and Drug Release. *Bioconjugate Chemistry* **21**:979-987.
31. **Cheong, S. C., Y. Wang, J. H. Meng, R. Hill, K. Sweeney, D. Kirn, N. R. Lemoine, and G. Hallden.** 2008. E1A-expressing adenoviral E3B mutants act synergistically with chemotherapeutics in immunocompetent tumor models. *Cancer Gene Therapy* **15**:40-50.
32. **Christoph, V., and K. Stefan.** 2004. Adenoviral vectors for gene transfer and therapy. *J. Gene Med.* **6**:S164-S171.
33. **Cook, B. N., and C. R. Bertozzi.** 2002. Chemical approaches to the investigation of cellular systems. *Bioorg. Med. Chem.* **10**:829-840.
34. **Cornish, V. W., D. R. Benson, C. A. Altenbach, K. Hideg, W. L. Hubbell, and P. G. Schultz.** 1994. Site-specific incorporation of biophysical probes into proteins. *Proc. Natl. Acad. Sci. USA* **91**:2910-2914.

35. **Cowie, D. B., Cohen, G.N.** 1957. Biosynthesis by *Escherichia coli* of active altered proteins containing selenium instead of sulphur. *Biochim. Biophys. Acta.* **26**:252-261.
36. **Crowe, J., H. Dobeli, R. Gentz, E. Hochuli, D. Stüber, and K. Henco.** 1994. 6xHis-Ni-NTA Chromatography as a Superior Technique in Recombinant Protein Expression/Purification, p. 371-387, vol. 31.
37. **David T, C.** 1999. Strategies to Adapt Adenoviral Vectors for Targeted Delivery. *Ann. N Y Acad. Sci.* **886**:158-171.
38. **de Graaf, A. J., M. Kooijman, W. E. Hennink, and E. Mastrobattista.** 2009. Nonnatural Amino Acids for Site-Specific Protein Conjugation. *Bioconj. Chem.* **20**:1281-1295.
39. **Dedkova, L. M., N. E. Fahmi, S. Y. Golovine, and S. M. Hecht.** 2003. Enhanced d-Amino Acid Incorporation into Protein by Modified Ribosomes. *J. Am. Chem. Soc.* **125**:6616-6617.
40. **Dehnert, K. W., B. J. Beahm, T. T. Huynh, J. M. Baskin, S. T. Laughlin, W. Wang, P. Wu, S. L. Amacher, and C. R. Bertozzi.** 2011. Metabolic Labeling of Fucosylated Glycans in Developing Zebrafish. *ACS Chem. Biol.* **6**:547-552.
41. **Dhar, S., Z. Liu, J. r. Thomale, H. Dai, and S. J. Lippard.** 2008. Targeted Single-Wall Carbon Nanotube-Mediated Pt(IV) Prodrug Delivery Using Folate as a Homing Device. *J. Am. Chem. Soc.* **130**:11467-11476.
42. **Di Paolo, N. C., S. Tuve, S. Ni, K. E. Hellström, I. Hellström, and A. Lieber.** 2006. Effect of Adenovirus-Mediated Heat Shock Protein Expression and

- Oncolysis in Combination with Low-Dose Cyclophosphamide Treatment on Antitumor Immune Responses. *Canc. Res.* **66**:960-969.
43. **Dias, W. B., and G. W. Hart.** 2007. O-GlcNAc modification in diabetes and Alzheimer's disease. *Mol. BioS.* **3**:766-772.
44. **Dieterich, D. C., J. J. L. Hodas, G. Gouzer, I. Y. Shadrin, J. T. Ngo, A. Triller, D. A. Tirrell, and E. M. Schuman.** 2010. In situ visualization and dynamics of newly synthesized proteins in rat hippocampal neurons. *Nat Neurosci* **13**:897-905.
45. **Dobbelstein, M.** 2003. Viruses in therapy--royal road or dead end? *Virus Research* **92**:219-221.
46. **Dock, G.** 1904. Rabies virus vaccination in a patient with cervical carcinoma. *Am. J. Med. Sci.*:563.
47. **Dong, S., L. Merkel, L. Moroder, and N. Budisa.** 2008. Convenient syntheses of homopropargylglycine. *J. Pep. Sci.* **14**:1148-1150.
48. **Doronin, K., E. V. Shashkova, S. M. May, S. E. Hofherr, and M. A. Barry.** 2009. Chemical Modification with High Molecular Weight Polyethylene Glycol Reduces Transduction of Hepatocytes and Increases Efficacy of Intravenously Delivered Oncolytic Adenovirus. *Human Gene Ther.* **20**:975-988.
49. **Douglas, J. T., B. E. Rogers, M. E. Rosenfeld, S. I. Michael, M. Feng, and D. T. Curiel.** 1996. Targeted gene delivery by tropism-modified adenoviral vectors. *Nat. Biotech.* **14**:1574-1578.

50. **Dube, D. H., and C. R. Bertozzi.** 2005. Glycans in cancer and inflammation [mdash] potential for therapeutics and diagnostics. *Nat Rev Drug Discov* **4**:477-488.
51. **Dube, D. H., and C. R. Bertozzi.** 2003. Metabolic oligosaccharide engineering as a tool for glycobiology. *Curr. Op. Chem. Biol.* **7**:616-625.
52. **Fabry, C. M. S., M. Rosa-Calatrava, J. F. Conway, C. Zubieta, S. Cusack, R. W. H. Ruigrok, and G. Schoehn.** 2005. A quasi-atomic model of human adenovirus type 5 capsid. *EMBO J* **24**:1645-1654.
53. **Fabry, C. M. S., M. Rosa-Calatrava, C. Moriscot, R. W. H. Ruigrok, P. Boulanger, and G. Schoehn.** 2009. The C-Terminal Domains of Adenovirus Serotype 5 Protein IX Assemble into an Antiparallel Structure on the Facets of the Capsid. *J. Virol.* **83**:1135-1139.
54. **Falschlehner, C., T. M. Ganten, R. Koschny, U. Schaefer, and H. Walczak.** 2009. TRAIL and Other TRAIL Receptor Agonists as Novel Cancer Therapeutics, p. 195-206. *In* I. S. Grewal (ed.), *Therapeutic Targets of the TNF Superfamily*, vol. 647. Springer New York.
55. **Finlay, D., R. D. Richardson, L. K. Landberg, A. L. Howes, and K. Vuori.** 2010. Novel HTS Strategy Identifies TRAIL-Sensitizing Compounds Acting Specifically Through the Caspase-8 Apoptotic Axis. *PLoS ONE* **5**:e13375.
56. **Flavell, R. R., and T. W. Muir.** 2008. Expressed Protein Ligation (EPL) in the Study of Signal Transduction, Ion Conduction, And Chromatin Biology. *Accts. of Chem. Res.* **42**:107-116.

57. **Fox, J. D., K. M. Routzahn, M. H. Bucher, and D. S. Waugh.** 2003. Maltodextrin-binding proteins from diverse bacteria and archaea are potent solubility enhancers. *FEBS Letters* **537**:53-57.
58. **Friedmann, T.** 1989. Progress toward human gene therapy. *Science* **244**:1275-1281.
59. **Furter, R.** 1998. Expansion of the genetic code: Site-directed p-fluorophenylalanine incorporation in *Escherichia coli*. *Protein Sci* **7**:419-426.
60. **Ghosh, D., and M. A. Barry.** 2005. Selection of Muscle-Binding Peptides from Context-Specific Peptide-Presenting Phage Libraries for Adenoviral Vector Targeting. *J. Virol.* **79**:13667-13672.
61. **Glasgow, J. N., M. Everts, and D. T. Curiel.** 2006. Transductional targeting of adenovirus vectors for gene therapy. *Cancer Gene Ther.* **13**:830-844.
62. **Goetz, C., and M. Gromeier.** Preparing an oncolytic poliovirus recombinant for clinical application against glioblastoma multiforme. *Cytokine & Growth Factor Reviews* **21**:197-203.
63. **Guo, W., H. Zhu, L. Zhang, J. Davis, F. Teraishi, J. A. Roth, C. Stephens, J. Fueyo, H. Jiang, C. Conrad, and B. Fang.** 2005. Combination effect of oncolytic adenovirotherapy and TRAIL gene therapy in syngeneic murine breast cancer models. *Cancer Gene Ther* **13**:82-90.
64. **Gupta, S. S., J. Kuzelka, P. Singh, W. G. Lewis, M. Manchester, and M. G. Finn.** 2005. Accelerated Bioorthogonal Conjugation: A Practical Method for the Ligation of Diverse Functional Molecules to a Polyvalent Virus Scaffold. *Bioconj. Chem.* **16**:1572-1579.

65. **Gupta, S. S., K. S. Raja, E. Kaltgrad, E. Strable, and M. G. Finn.** 2005. Chem. Comm.:4315-4317.
66. **H Schneider, M. G., C Mühle, P N Reynolds, A Knight, M Themis, J Carvajal, F Scaravilli, D T Curiel, N F Fairweather and C Coutelle.** 2000. Retargeting of adenoviral vectors to neurons using the HC fragment of tetanus toxin. Gene Therapy **7**:1584-1592.
67. **Hamdan, M., and P. G. Righetti.** 2002. Modern strategies for protein quantification in proteome analysis: Advantages and limitations. Mass Spect. Revs. **21**:287-302.
68. **Hang, H. C., and C. R. Bertozzi.** 2005. The chemistry and biology of mucin-type O-linked glycosylation. Bioorg. Med. Chem. **13**:5021-5034.
69. **Hart, G. W., C. Slawson, G. Ramirez-Correa, and O. Lagerlof.** 2011. Cross Talk Between O-GlcNAcylation and Phosphorylation: Roles in Signaling, Transcription, and Chronic Disease. Annu. Rev. Biochem. **80**:825-858.
70. **Hassan, M., S. R. Braam, and F. A. E. Kruyt.** 2006. Paclitaxel and vincristine potentiate adenoviral oncolysis that is associated with cell cycle and apoptosis modulation, whereas they differentially affect the viral life cycle in non-small-cell lung cancer cells. Cancer Gene Therapy **13**:1105-1114.
71. **He, T.-C., S. Zhou, L. T. da Costa, J. Yu, K. W. Kinzler, and B. Vogelstein.** 1998. A simplified system for generating recombinant adenoviruses. Proc. Natl. Acad. Sci. USA **95**:2509-2514.

72. **Hedley, S., J. Chen, J. Mountz, J. Li, D. Curiel, N. Korokhov, and I. Kovesdi.** 2006. Targeted and shielded adenovectors for cancer therapy. *Cancer Immunol. Immunother.* **55**:1412-1419.
73. **Henning, P., E. Lundgren, M. Carlsson, K. Frykholm, J. Johannisson, M. K. Magnusson, E. Tang, L. Franqueville, S. S. Hong, L. Lindholm, and P. Boulanger.** 2006. Adenovirus type 5 fiber knob domain has a critical role in fiber protein synthesis and encapsidation. *J. Gen. Virol.* **87**:3151-3160.
74. **Hohsaka, T., Y. Ashizuka, H. Taira, H. Murakami, and M. Sisido.** 2001. Incorporation of Nonnatural Amino Acids into Proteins by Using Various Four-Base Codons in an Escherichia coli in Vitro Translation System. *Biochem.* **40**:11060-11064.
75. **Huang, B., R. Sikorski, D. H. Kirn, and S. H. Thorne.** 2011. Synergistic anti-tumor effects between oncolytic vaccinia virus and paclitaxel are mediated by the IFN response and HMGB1. *Gene Ther* **18**:164-172.
76. **Huebner, R. J., Rowe, J.P., Schatten, W.E., Smith, R.R. and Thomas, L.B.** 1956. Studies on the use of viruses in the treatment of carcinoma of the cervix. *Cancer* **9**:1211-1218.
77. **Hutchison, C. A., S. Phillips, M. H. Edgell, S. Gillam, P. Jahnke, and M. Smith.** 1978. Mutagenesis at a specific position in a DNA sequence. *J. Biol. Chem.* **253**:6551-6560.
78. **Ibba, M., P. Kast, and H. Hennecke.** 2002. Substrate Specificity Is Determined by Amino Acid Binding Pocket Size in Escherichia coli Phenylalanyl-tRNA Synthetase. *Biochem.* **33**:7107-7112.

79. **Ingemarsdotter, C. K., S. K. Baird, C. M. Connell, D. Oberg, G. Hallden, and I. A. McNeish.** 2010. Low-dose paclitaxel synergizes with oncolytic adenoviruses via mitotic slippage and apoptosis in ovarian cancer. *Oncogene* **29**:6051-6063.
80. **Jacobs, C. L., S. Goon, K. J. Yarema, S. Hinderlich, H. C. Hang, D. H. Chai, and C. R. Bertozzi.** 2001. Substrate Specificity of the Sialic Acid Biosynthetic Pathway†. *Biochem.* **40**:12864-12874.
81. **Jogler, C., D. Hoffmann, D. Theegarten, T. Grunwald, K. Uberla, and O. Wildner.** 2006. Replication Properties of Human Adenovirus In Vivo and in Cultures of Primary Cells from Different Animal Species. *J. Virol.* **80**:3549-3558.
82. **Johnson, J. A., Y. Y. Lu, J. A. Van Deventer, and D. A. Tirrell.** 2010. Residue-specific incorporation of non-canonical amino acids into proteins: recent developments and applications. *Curr. Op. Chem. Biol.* **14**:774-780.
83. **Jung, Y., H.-J. Park, P.-H. Kim, J. Lee, W. Hyung, J. Yang, H. Ko, J.-H. Sohn, J.-H. Kim, Y.-M. Huh, C.-O. Yun, and S. Haam.** 2007. Retargeting of adenoviral gene delivery via Herceptin-PEG-adenovirus conjugates to breast cancer cells. *J. Control. Release* **123**:164-171.
84. **Kanai, R., H. Wakimoto, T. Cheema, and S. D. Rabkin.** 2010. Oncolytic herpes simplex virus vectors and chemotherapy: are combinatorial strategies more effective for cancer? *Future Oncol.* **6**:619-634.
85. **Kashentseva, E. A., J. T. Douglas, K. R. Zinn, D. T. Curiel, and I. P. Dmitriev.** 2009. Targeting of Adenovirus Serotype 5 Pseudotyped with Short Fiber from Serotype 41 to c-erbB2-Positive Cells using Bispecific Single-Chain Diabody. *J. Mol. Biol.* **388**:443-461.

86. **Kiick, K. L., E. Saxon, D. A. Tirrell, and C. R. Bertozzi.** 2002. Incorporation of azides into recombinant proteins for chemoselective modification by the Staudinger ligation. *Proc. Natl. Acad. Sci. USA* **99**:19-24.
87. **Kim, M., J. Liao, M. L. Dowling, K. R. Voong, S. E. Parker, S. Wang, W. S. El-Deiry, and G. D. Kao.** 2008. TRAIL Inactivates the Mitotic Checkpoint and Potentiates Death Induced by Microtubule-Targeting Agents in Human Cancer Cells. *Cancer Res.* **68**:3440-3449.
88. **Kirby, I., E. Davison, A. J. Beavil, C. P. C. Soh, T. J. Wickham, P. W. Roelvink, I. Kovesdi, B. J. Sutton, and G. Santis.** 2000. Identification of Contact Residues and Definition of the CAR-Binding Site of Adenovirus Type 5 Fiber Protein. *J. Virol.* **74**:2804-2813.
89. **Kirby, I., R. Lord, E. Davison, T. J. Wickham, P. W. Roelvink, I. Kovesdi, B. J. Sutton, and G. Santis.** 2001. Adenovirus Type 9 Fiber Knob Binds to the Coxsackie B Virus-Adenovirus Receptor (CAR) with Lower Affinity than Fiber Knobs of Other CAR-Binding Adenovirus Serotypes. *J. Virol.* **75**:7210-7214.
90. **Ko, D., L. Hawkins, and D.-C. Yu.** 2005. Development of transcriptionally regulated oncolytic adenoviruses. *Oncogene* **24**:7763-7774.
91. **Köhler, C., E. L. Sullivan, and U. L. RajBhandary.** 2004. Complete set of orthogonal 21st aminoacyl-tRNA synthetase-amber, ochre and opal suppressor tRNA pairs: concomitant suppression of three different termination codons in an mRNA in mammalian cells. *Nucleic Acids Res.* **32**:6200-6211.
92. **Krasnykh, V., I. Dmitriev, G. Mikheeva, C. R. Miller, N. Belousova, and D. T. Curiel.** 1998. Characterization of an Adenovirus Vector Containing a

- Heterologous Peptide Epitope in the HI Loop of the Fiber Knob. *J. Virol.* **72**:1844-1852.
93. **Kreppel, F., J. Gackowski, E. Schmidt, and K. Stefan.** 2005. Combined Genetic and Chemical Capsid Modifications Enable Flexible and Efficient De- and Retargeting of Adenovirus Vectors. *Mol. Ther.* **12**:107-117.
94. **Kreppel, F., and S. Kochanek.** 2007. Modification of Adenovirus Gene Transfer Vectors With Synthetic Polymers: A Scientific Review and Technical Guide. *Mol. Ther.* **16**:16-29.
95. **Kristi, L. K., C. M. v. H. Jan, and A. T. David.** 2000. Expanding the Scope of Protein Biosynthesis by Altering the Methionyl-tRNA Synthetase Activity of a Bacterial Expression Host13. *Angew. Chem. Int. Ed.* **39**:2148-2152.
96. **Kruyt, F. A. E., and D. T. Curiel.** 2002. Toward a New Generation of Conditionally Replicating Adenoviruses: Pairing Tumor Selectivity with Maximal Oncolysis. *Human Gene Ther* **13**:485-495.
97. **Kuznetsova, L., J. Chen, L. Sun, X. Y. Wu, A. Pepe, J. A. Veith, P. Pera, R. J. Bernacki, and I. Ojima.** 2006. Syntheses and evaluation of novel fatty acid-second-generation taxoid conjugates as promising anticancer agents. *Bioorganic & Medicinal Chemistry Letters* **16**:974-977.
98. **Kwon, I., K. Kirshenbaum, and D. A. Tirrell.** 2003. Breaking the Degeneracy of the Genetic Code. *J. Am. Chem. Soc.* **125**:7512-7513.
99. **Lam, J. T., G. J. Bauerschmitz, A. Kanerva, S. D. Barker, J. M. Straughn, M. Wang, M. N. Barnes, J. L. Blackwell, G. P. Siegal, R. D. Alvarez, D. T. Curiel, and A. Hemminki.** 2000. Replication of an integrin targeted

- conditionally replicating adenovirus on primary ovarian cancer spheroids. *Cancer Gene Ther* **10**:377-387.
100. **Lane, D. P., C. F. Cheok, and S. Lain.** 2010. p53-based Cancer Therapy. *Cold Spring Harbor Perspectives in Biology* **2**.
101. **Laughlin, S. T., N. J. Agard, J. M. Baskin, I. S. Carrico, P. V. Chang, A. S. Ganguli, M. J. Hangauer, A. Lo, J. A. Prescher, C. R. Bertozzi, and F. Minoru.** 2006. Metabolic Labeling of Glycans with Azido Sugars for Visualization and Glycoproteomics, p. 230-250, *Methods in Enzymol.*, vol. Volume 415. Academic Press.
102. **Laughlin, S. T., and C. R. Bertozzi.** 2009. In Vivo Imaging of *Caenorhabditis elegans* Glycans. *ACS Chem. Biol.* **4**:1068-1072.
103. **LeBlanc, H., D. Lawrence, E. Varfolomeev, K. Totpal, J. Morlan, P. Schow, S. Fong, R. Schwall, D. Sinicropi, and A. Ashkenazi.** 2002. Tumor-cell resistance to death receptor-induced apoptosis through mutational inactivation of the proapoptotic Bcl-2 homolog Bax. *Nat Med* **8**:274-281.
104. **Lech, P. J., and S. J. Russell.** 2010. Use of attenuated paramyxoviruses for cancer therapy. *Expert Rev. Vaccines* **9**:1275-1302.
105. **Li, X., Y. Liu, Y. Tang, P. Roger, M.-H. Jeng, and C. Kao.** 2010. Docetaxel increases antitumor efficacy of oncolytic prostate-restricted replicative adenovirus by enhancing cell killing and virus distribution. *J. Gene Med.* **12**:516-527.
106. **Li, Y. M., S. T. Song, Z. F. Jiang, Q. Zhang, Y. M. Qu, C. Q. Su, C. H. Zhao, Z. Q. Li, F. J. Ge, and Q. J. Qian.** 2007. Synergistic antitumor efficacy of

- oncolytic adenovirus combined with chemotherapy. *Chinese Journal of Cancer Research* **19**:76-81.
107. **Liu, T.-C., E. Galanis, and D. Kirn.** 2007. Clinical trial results with oncolytic virotherapy: a century of promise, a decade of progress. *Nat Clin Prac Oncol* **4**:101-117.
108. **Liu, Y., H. Wang, R. Yumul, W. Gao, A. Gambotto, T. Morita, A. Baker, D. Shayakhmetov, and A. Lieber.** 2009. Transduction of Liver Metastases After Intravenous Injection of Ad5/35 or Ad35 Vectors With and Without Factor X-Binding Protein Pretreatment. *Human Gene Ther* **20**:621-629.
109. **Lo, H., C. Day, and M. Hung.** 2005. Cancer[hyphen (true graphic)]Specific Gene Therapy, p. 233-255. *In* M.-C. H. Leaf Huang and W. Ernst (ed.), *Advances in Genetics*, vol. Volume 54. Academic Press.
110. **Low, P. S., W. A. Henne, and D. D. Doorneweerd.** 2007. Discovery and Development of Folic-Acid-Based Receptor Targeting for Imaging and Therapy of Cancer and Inflammatory Diseases. *Acc. Chem. Res.* **41**:120-129.
111. **Low, P. S., and S. A. Kularatne.** 2009. Folate-targeted therapeutic and imaging agents for cancer. *Curr. Opin. Chem. Biol.* **13**:256-262.
112. **Luchansky, S. J., S. Goon, and C. R. Bertozzi.** 2004. Expanding the Diversity of Unnatural Cell-Surface Sialic Acids. *ChemBioChem* **5**:371-374.
113. **Luchansky, S. J., H. C. Hang, E. Saxon, J. R. Grunwell, C. Y. Danielle, D. H. Dube, and C. R. Bertozzi.** 2003. Constructing azide-labeled cell surfaces using polysaccharide biosynthetic pathways, p. 249-272, *Recognition of Carbohydrates*

- in Biological Systems Pt A: General Procedures, vol. 362. Academic Press Inc, San Diego.
114. **Luchansky, S. J., H. C. Hang, E. Saxon, J. R. Grunwell, C. Yu, D. H. Dube, C. R. Bertozzi, C. L. Yuan, and T. L. Reiko.** 2003. Constructing Azide-Labeled Cell Surfaces Using Polysaccharide Biosynthetic Pathways, p. 249-272, *Methods in Enzymol.*, vol. Volume 362. Academic Press.
 115. **Luchansky, S. J., K. J. Yarema, S. Takahashi, and C. R. Bertozzi.** 2003. GlcNAc 2-Epimerase Can Serve a Catabolic Role in Sialic Acid Metabolism. *J. Biol. Chem.* **278**:8035-8042.
 116. **Magnusson, M. K., S. S. Hong, P. Boulanger, and L. Lindholm.** 2001. Genetic Retargeting of Adenovirus: Novel Strategy Employing "Deknobbing" of the Fiber. *J. Virol.* **75**:7280-7289.
 117. **Magnusson, M. K. H., S.S.; Henning, P.; Boulanger, P.; Lindholm, L.** 2002. Genetic retargeting of adenovirus vectors: functionality of targeting ligands and their influence on virus viability. *J. Gene Med.* **4**:356-370.
 118. **Maizel, J. V., D. O. White, and M. D. Scharff.** 1968. The polypeptides of adenovirus. 1. Evidence for multiple protein components in the virion and a comparison of types 2, 7A, and 12. *Virology* **36**:115-125.
 119. **Manuel, A. F. V. G., and A. F. d. V. Antoine.** 2006. Adenovirus: from foe to friend. *Reviews in Medical Virology* **16**:167-186.
 120. **Marsh, M. P., S. K. Campos, M. L. Baker, C. Y. Chen, W. Chiu, and M. A. Barry.** 2006. Cryoelectron Microscopy of Protein IX-Modified Adenoviruses

- Suggests a New Position for the C Terminus of Protein IX. *J. Virol.* **80**:11881-11886.
121. **Mathis, J. M., M. A. Stoff-Khalili, and D. T. Curiel.** 2005. Oncolytic adenoviruses - selective retargeting to tumor cells. *Oncogene* **24**:7775-7791.
 122. **Matthews, Q., P. Yang, Q. Wu, N. Belousova, A. Rivera, M. Stoff-Khalili, R. Waehler, H.-C. Hsu, Z. Li, J. Li, J. Mountz, H. Wu, and D. Curiel.** 2008. Optimization of capsid-incorporated antigens for a novel adenovirus vaccine approach. *Virol. J.* **5**:98.
 123. **Matthews, Q. L.** 2010. Capsid-Incorporation of Antigens into Adenovirus Capsid Proteins for a Vaccine Approach. *Mol. Pharm.* **8**:3-11.
 124. **Misteli, T., and D. L. Spector.** 1997. Applications of the green fluorescent protein in cell biology and biotechnology. *Nat Biotech* **15**:961-964.
 125. **Mizuguchi, H., and T. Hayakawa.** 2004. Targeted Adenovirus Vectors. *Hum. Gene Ther.* **15**:1034-1044.
 126. **Monroe, J.** 2004, posting date. Viral Replication Cycle. James Madison University. [Online.]
 127. **Moran, E.** 1993. Interaction of adenoviral proteins with pRB and p53. *The FASEB Journal* **7**:880-885.
 128. **Morrison, J., S. S. Briggs, N. K. Green, C. Thoma, K. D. Fisher, S. Kehoe, and L. W. Seymour.** 2009. Cetuximab Retargeting of Adenovirus via the Epidermal Growth Factor Receptor for Treatment of Intraperitoneal Ovarian Cancer. *Human Gene Ther* **20**:239-251.

129. **Muir, T. W., D. Sondhi, and P. A. Cole.** 1998. Expressed protein ligation: A general method for protein engineering. *Proc. Natl. Acad. Sci. USA* **95**:6705-6710.
130. **Mullis, K. G., R. S. Haltiwanger, G. W. Hart, R. B. Marchase, and J. A. Engler.** 1990. Relative accessibility of N-acetylglucosamine in trimers of the adenovirus types 2 and 5 fiber proteins. *J. Virol.* **64**:5317-5323.
131. **Mulvihill, S., Warren, R., Venook, A., Adler, A., Randlev, B., Heise, C., and Kirm, D.** 2001. Safety and feasibility of injection with an E1B-55 kDa gene-deleted, replication-selective adenovirus (ONYX-015) into primary carcinomas of the pancreas: a phase I trial. *Gene Ther* **8**:308-315.
132. **Murakami, P., and M. T. McCaman.** 1999. Quantitation of Adenovirus DNA and Virus Particles with the PicoGreen Fluorescent Dye. *Anal. Biochem.* **274**:283-288.
133. **Myhre, S., P. Henning, M. Friedman, S. Stahl, L. Lindholm, and M. K. Magnusson.** 2008. Re-targeted adenovirus vectors with dual specificity; binding specificities conferred by two different Affibody molecules in the fiber. *Gene Ther* **16**:252-261.
134. **Nagano, S., J. Y. Perentes, R. K. Jain, and Y. Boucher.** 2008. Cancer cell death enhances the penetration and efficacy of oncolytic herpes simplex virus in tumors. *Cancer Research* **68**:3795-3802.
135. **Nemerow, G. R., L. Pache, V. Reddy, and P. L. Stewart.** 2009. Insights into adenovirus host cell interactions from structural studies. *Virology* **384**:380-388.

136. **Nettelbeck, D. M., D. W. Miller, V. Jerome, M. Zuzarte, S. J. Watkins, R. E. Hawkins, R. Muller, and R. E. Kontermann.** 2001. Targeting of Adenovirus to Endothelial Cells by a Bispecific Single-Chain Diabody Directed against the Adenovirus Fiber Knob Domain and Human Endoglin (CD105). *Mol Ther* **3**:882-891.
137. **Neumann, H., K. Wang, L. Davis, M. Garcia-Alai, and J. W. Chin.** 2010. Encoding multiple unnatural amino acids via evolution of a quadruplet-decoding ribosome. *Nature* **464**:441-444.
138. **Noren, C. J., S. J. Anthony-Cahill, M. C. Griffith, and P. G. Schultz.** 1989. A general method for site-specific incorporation of unnatural amino acids into proteins. *Science* **244**:182-188.
139. **O'Riordan, C. R., A. Lachapelle, C. Delgado, V. Parkes, S. C. Wadsworth, A. E. Smith, and G. E. Francis.** 1999. PEGylation of Adenovirus with Retention of Infectivity and Protection from Neutralizing Antibody in Vitro and in Vivo. *Hum. Gene Ther.* **10**:1349-1358.
140. **Oh, I. K., H. Mok, and T. G. Park.** 2006. Folate Immobilized and PEGylated Adenovirus for Retargeting to Tumor Cells. *Bioconj. Chem.* **17**:721-727.
141. **Ojima, I.** 2007. Guided Molecular Missiles for Tumor-Targeting Chemotherapy—Case Studies Using the Second-Generation Taxoids as Warheads. *Acc. Chem. Res.* **41**:108-119.
142. **Ojima, I., J. Chen, L. Sun, C. P. Borella, T. Wang, M. L. Miller, S. N. Lin, X. D. Geng, L. R. Kuznetsova, C. X. Qu, D. Gallager, X. R. Zhao, I. Zanardi, S. J. Xia, S. B. Horwitz, J. Mallen-St Clair, J. L. Guerriero, D. Bar-Sagi, J. M.**

- Veith, P. Pera, and R. J. Bernacki.** 2008. Design, synthesis, and biological evaluation of new-generation taxoids. *Journal of Medicinal Chemistry* **51**:3203-3221.
143. **Onimaru, M., K. Ohuchida, T. Egami, K. Mizumoto, E. Nagai, L. Cui, H. Toma, K. Matsumoto, M. Hashizume, and M. Tanaka.** 2010. Gemcitabine synergistically enhances the effect of adenovirus gene therapy through activation of the CMV promoter in pancreatic cancer cells. *Cancer Gene Ther* **17**:541-549.
144. **Onimaru, M., K. Ohuchida, E. Nagai, K. Mizumoto, T. Egami, L. Cui, N. Sato, J. Uchino, K. Takayama, M. Hashizume, and M. Tanaka.** 2010. Combination with low-dose gemcitabine and hTERT-promoter-dependent conditionally replicative adenovirus enhances cytotoxicity through their crosstalk mechanisms in pancreatic cancer. *Cancer Letters* **294**:178-186.
145. **Ottolino-Perry, K., J.-S. Diallo, B. D. Lichty, J. C. Bell, and J. Andrea McCart.** 2009. Intelligent Design: Combination Therapy With Oncolytic Viruses. *Mol Ther* **18**:251-263.
146. **Parker, N., M. J. Turk, E. Westrick, J. D. Lewis, P. S. Low, and C. P. Leamon.** 2005. Folate receptor expression in carcinomas and normal tissues determined by a quantitative radioligand binding assay. *Anal. Biochem.* **338**:284-293.
147. **Parr, M. J., Y. Manome, T. Tanaka, P. Wen, D. W. Kufe, W. G. Kaelin, and H. A. Fine.** 1997. Tumor-selective transgene expression in vivo mediated by an E2F-responsive adenoviral vector. *Nat Med* **3**:1145-1149.

148. **Parrott, M. B., K. E. Adams, G. T. Mercier, H. Mok, S. K. Campos, and M. A. Barry.** 2003. Metabolically Biotinylated Adenovirus for Cell Targeting, Ligand Screening, and Vector Purification. *Mol Ther* **8**:688-700.
149. **Parsons, J. F., G. Xiao, G. L. Gilliland, and R. N. Armstrong.** 1998. Enzymes Harboring Unnatural Amino Acids: Mechanistic and Structural Analysis of the Enhanced Catalytic Activity of a Glutathione Transferase Containing 5-Fluorotryptophan^{†,‡}. *Biochem.* **37**:6286-6294.
150. **Passer, B. J., P. Castelo-Branco, J. S. Buhrman, S. Varghese, S. D. Rabkin, and R. L. Martuza.** 2009. Oncolytic herpes simplex virus vectors and taxanes synergize to promote killing of prostate cancer cells. *Cancer Gene Ther* **16**:551-560.
151. **Pereboeva, L., S. Komarova, J. Roth, S. Ponnazhagan, and D. T. Curiel.** 2007. Targeting EGFR with metabolically biotinylated fiber-mosaic adenovirus. *Gene Ther* **14**:627-637.
152. **Pesonen, S., L. Kangasniemi, and A. Hemminki.** 2010. Oncolytic Adenoviruses for the Treatment of Human Cancer: Focus on Translational and Clinical Data. *Mol Pharm.* **8**:12-28.
153. **Pipkorn, R., W. Waldeck, B. Didinger, M. Koch, G. Mueller, M. Wiessler, and K. Braun.** 2009. Inverse-electron-demand Diels-Alder reaction as a highly efficient chemoselective ligation procedure: Synthesis and function of a BioShuttle for temozolomide transport into prostate cancer cells. *J. Pep. Sci.* **15**:235-241.

154. **Pratt, M. R., and C. R. Bertozzi.** 2005. Synthetic glycopeptides and glycoproteins as tools for biology. *Chem. Soc. Rev.* **34**:58-68.
155. **Prescher, J. A., and C. R. Bertozzi.** 2005. Chemistry in living systems. *Nat. Chem Biol.* **1**:13-21.
156. **Radhakrishnan, S., E. Miranda, M. Ekblad, A. Holford, M. T. Pizarro, N. R. Lemoine, and G. Hallden.** 2010. Efficacy of Oncolytic Mutants Targeting pRb and p53 Pathways Is Synergistically Enhanced When Combined with Cytotoxic Drugs in Prostate Cancer Cells and Tumor Xenografts. *Human Gene Therapy* **21**:1311-1325.
157. **Reddy, V. S., S. K. Natchiar, P. L. Stewart, and G. R. Nemerow.** 2010. Crystal Structure of Human Adenovirus at 3.5 Å Resolution. *Science* **329**:1071-1075.
158. **Rexroad, J., R. K. Evans, and C. R. Middaugh.** 2006. Effect of pH and ionic strength on the physical stability of adenovirus type 5. *J. Pharm. Sci.* **95**:237-247.
159. **Rexroad, J., T. T. Martin, D. McNeilly, S. Godwin, and C. R. Middaugh.** 2006. Thermal stability of adenovirus type 2 as a function of pH. *J. Pharm. Sci.* **95**:1469-1479.
160. **Rexroad, J., C. M. Wiethoff, A. P. Green, T. D. Kierstead, M. O. Scott, and C. R. Middaugh.** 2003. Structural stability of adenovirus type 5. *J. Pharm. Sci.* **92**:665-678.
161. **Rivera, A. A., J. Davydova, S. Schierer, M. Wang, V. Krasnykh, M. Yamamoto, D. T. Curiel, and D. M. Nettelbeck.** 2004. Combining high selectivity of replication with fiber chimerism for effective adenoviral oncolysis of CAR-negative melanoma cells. *Gene Ther* **11**:1694-1702.

162. **Rocconi, R. P., Z. B. Zhu, M. Stoff-Khalili, A. A. Rivera, B. Lu, M. Wang, R. D. Alvarez, D. T. Curiel, and S. K. Makhija.** 2007. Treatment of ovarian cancer with a novel dual targeted conditionally replicative adenovirus (CRAd). *Gynec Oncol.* **105**:113-121.
163. **Romanini, D. W., and M. B. Francis.** 2007. Attachment of Peptide Building Blocks to Proteins Through Tyrosine Bioconjugation. *Bioconj. Chem.* **19**:153-157.
164. **Ross, P. L., Y. N. Huang, J. N. Marchese, B. Williamson, K. Parker, S. Hattan, N. Khainovski, S. Pillai, S. Dey, S. Daniels, S. Purkayastha, P. Juhasz, S. Martin, M. Bartlet-Jones, F. He, A. Jacobson, and D. J. Pappin.** 2004. Multiplexed Protein Quantitation in *Saccharomyces cerevisiae* Using Amine-reactive Isobaric Tagging Reagents. *Mol. Cell. Prot.* **3**:1154-1169.
165. **Roth, J. A., and R. J. Cristiano.** 1997. Gene Therapy for Cancer: What Have We Done and Where Are We Going? *Journal of the National Cancer Institute* **89**:21-39.
166. **Russell-Jones, G., K. McTavish, J. McEwan, J. Rice, and D. Nowotnik.** 2004. Vitamin-mediated targeting as a potential mechanism to increase drug uptake by tumours. *J. Inorg. Biochem.* **98**:1625-1633.
167. **Russell, W. C.** 2009. Adenoviruses: update on structure and function. *J. Gen. Virol.* **90**:1-20.
168. **Rux, J. J., P. R. Kuser, and R. M. Burnett.** 2003. Structural and Phylogenetic Analysis of Adenovirus Hexons by Use of High-Resolution X-Ray

- Crystallographic, Molecular Modeling, and Sequence-Based Methods. *J. Virol.* **77**:9553-9566.
169. **Ryan, P. C., J. L. Jakubczak, D. A. Stewart, L. K. Hawkins, C. Cheng, L. M. Clarke, S. Ganesh, C. Hay, Y. Huang, M. Kaloss, A. Marinov, S. S. Phipps, P. S. Reddy, P. S. Shirley, Y. Skripchenko, L. Xu, J. P. Yang, S. Forry-Schaudies, and P. L. Hallenbeck.** 2004. Antitumor efficacy and tumor-selective replication with a single intravenous injection of OAS403, an oncolytic adenovirus dependent on two prevalent alterations in human cancer. *Cancer Gene Therapy* **11**:555-569.
170. **Saban, S. D., R. R. Nepomuceno, L. D. Gritton, G. R. Nemerow, and P. L. Stewart.** 2005. CryoEM Structure at 9 Å Resolution of an Adenovirus Vector Targeted to Hematopoietic Cells. *J. Mol. Biol.* **349**:526-537.
171. **Saban, S. D., M. Silvestry, G. R. Nemerow, and P. L. Stewart.** 2006. Visualization of α -Helices in a 6-Ångstrom Resolution Cryoelectron Microscopy Structure of Adenovirus Allows Refinement of Capsid Protein Assignments. *J. Virol.* **80**:12049-12059.
172. **Saks, M. E., J. R. Sampson, M. W. Nowak, P. C. Kearney, F. Du, J. N. Abelson, H. A. Lester, and D. A. Dougherty.** 1996. An Engineered *Tetrahymena* tRNA^{Gln} for in Vivo Incorporation of Unnatural Amino Acids into Proteins by Nonsense Suppression. *J. Biol. Chem.* **271**:23169-23175.
173. **San Martín, C., J. N. Glasgow, A. Borovjagin, M. S. Beatty, E. A. Kashentseva, D. T. Curiel, R. Marabini, and I. P. Dmitriev.** 2008. Localization

- of the N-Terminus of Minor Coat Protein IIIa in the Adenovirus Capsid. *J. Mol. Biol.* **383**:923-934.
174. **Sanger, F., S. Nicklen, and A. R. Coulson.** 1977. DNA sequencing with chain-terminating inhibitors. *Proc. Natl. Acad. Sci. USA* **74**:5463-5467.
175. **Satyam, A.** 2008. Design and synthesis of releasable folate-drug conjugates using a novel heterobifunctional disulfide-containing linker. *Bioorg. Med. Chem. Letts.* **18**:3196-3199.
176. **Saxon, E., and C. R. Bertozzi.** 2000. Cell Surface Engineering by a Modified Staudinger Reaction. *Science* **287**:2007-2010.
177. **Saxon, E., S. J. Luchansky, H. C. Hang, C. Yu, S. C. Lee, and C. R. Bertozzi.** 2002. Investigating Cellular Metabolism of Synthetic Azidosugars with the Staudinger Ligation. *J. Am. Chem. Soc.* **124**:14893-14902.
178. **Shashkova, E. V., S. M. May, and M. A. Barry.** 2009. Characterization of human adenovirus serotypes 5, 6, 11, and 35 as anticancer agents. *Virology* **394**:311-320.
179. **Singh, R., and K. Kostarelos.** 2009. Designer adenoviruses for nanomedicine and nanodiagnostics. *Trends Biotechnol.* **27**:220-229.
180. **Southam, C. M., and A. E. Moore.** 1952. Clinical studies of viruses as antineoplastic agents, with particular reference to egypt 101 virus. *Cancer* **5**:1025-1034.
181. **Sova, P., X.-W. Ren, S. Ni, K. M. Bernt, J. Mi, N. Kiviat, and A. Lieber.** 2004. A Tumor-Targeted and Conditionally Replicating Oncolytic Adenovirus Vector Expressing TRAIL for Treatment of Liver Metastases. *Mol Ther* **9**:496-509.

182. **Stevenson, M., A. B. H. Hale, S. J. Hale, N. K. Green, G. Black, K. D. Fisher, K. Ulbrich, A. Fabra, and L. W. Seymour.** 2007. Incorporation of a laminin-derived peptide (SIKVAV) on polymer-modified adenovirus permits tumor-specific targeting via α_6 -integrins. *Cancer Gene Ther* **14**:335-345.
183. **Stevenson, S., M. Rollence, B. White, L. Weaver, and A. McClelland.** 1995. Human adenovirus serotypes 3 and 5 bind to two different cellular receptors via the fiber head domain. *J. Virol.* **69**:2850-2857.
184. **Strable, E., D. E. Prasuhn, A. K. Udit, S. Brown, A. J. Link, J. T. Ngo, G. Lander, J. Quispe, C. S. Potter, B. Carragher, D. A. Tirrell, and M. G. Finn.** 2008. Unnatural Amino Acid Incorporation into Virus-Like Particles. *Bioconj. Chem.* **19**:866-875.
185. **Subramanian, I. V., S. Devineni, R. Ghebre, G. Ghosh, H. P. Joshi, Y. Jing, A. M. Truskinovsky, and S. Ramakrishnan.** 2011. AAV-P125A-endostatin and paclitaxel treatment increases endoreduplication in endothelial cells and inhibits metastasis of breast cancer. *Gene Ther* **18**:145-154.
186. **Suzuki, M., Y. Ito, H. E. Savage, Y. Husimi, and K. T. Douglas.** 2003. Intramolecular Fluorescent Resonance Energy Transfer (FRET) by BODIPY Chemical Modification of Cysteine-engineered Mutants of Green Fluorescent Protein. *Chem. Letts.* **32**:306-307.
187. **Tang, Y., P. Wang, J. A. Van Deventer, A. J. Link, and D. A. Tirrell.** 2009. Introduction of an Aliphatic Ketone into Recombinant Proteins in a Bacterial Strain that Overexpresses an Editing-Impaired Leucyl-tRNA Synthetase. *ChemBioChem* **10**:2188-2190.

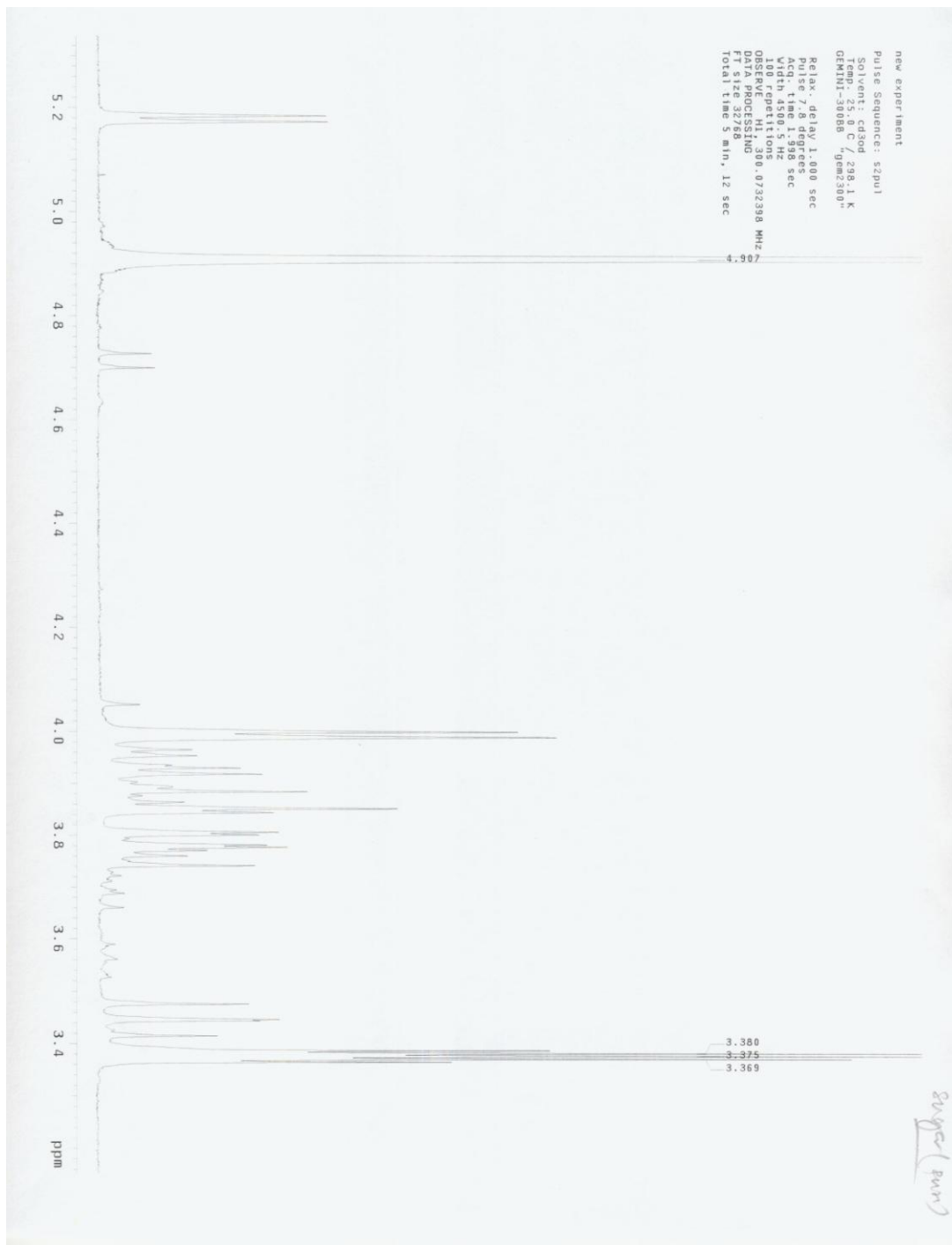
188. **Tang, Y., H. Wu, H. Ugai, Q. L. Matthews, and D. T. Curiel.** 2009. Derivation of a Triple Mosaic Adenovirus for Cancer Gene Therapy. *PLoS ONE* **4**:e8526.
189. **Tanrikulu, I. C., E. Schmitt, Y. Mechulam, W. A. Goddard, and D. A. Tirrell.** 2009. Discovery of *Escherichia coli* methionyl-tRNA synthetase mutants for efficient labeling of proteins with azidonorleucine in vivo. *Proc. Natl. Acad. Sci. USA* **106**:15285-15290.
190. **Tollefson, A. E., T. W. Hermiston, and W. S. Wold.** 1998. Preparation and Titration of CsCl-Banded Adenovirus Stock, p. 1-9, vol. 21.
191. **Tong, G. J., S. C. Hsiao, Z. M. Carrico, and M. B. Francis.** 2009. Viral Capsid DNA Aptamer Conjugates as Multivalent Cell-Targeting Vehicles. *J. Am. Chem. Soc.* **131**:11174-11178.
192. **Tseng, J. C., T. Granot, V. DiGiacomo, B. Levin, and D. Meruelo.** 2010. Enhanced specific delivery and targeting of oncolytic Sindbis viral vectors by modulating vascular leakiness in tumor. *Cancer Gene Ther* **17**:244-255.
193. **Varghese, R., Y. Mityas, P. L. Stewart, and R. Ralston.** 2004. Postentry Neutralization of Adenovirus Type 5 by an Antihexon Antibody. *J. Virol.* **78**:12320-12332.
194. **Vocadlo, D. J., H. C. Hang, E.-J. Kim, J. A. Hanover, and C. R. Bertozzi.** 2003. A chemical approach for identifying O-GlcNAc-modified proteins in cells. *Proc. Natl. Acad. Sci. USA* **100**:9116-9121.
195. **Vocadlo, D. J., H. C. Hang, E.-J. Kim, J. A. Hanover, and C. R. Bertozzi.** 2003. A chemical approach for identifying O-GlcNAc-modified proteins in cells. *Proc. Natl. Acad. Sci. USA* **100**:9116-9121.

196. **Vsevolod, V. R., G. G. Luke, V. F. Valery, and K. B. Sharpless.** 2002. A Stepwise Huisgen Cycloaddition Process: Copper(I)-Catalyzed Regioselective Ligation of Azides and Terminal Alkynes. *Angew. Chem. Int. Ed.* **41**:2596-2599.
197. **Waehler, R., S. J. Russell, and D. T. Curiel.** 2007. Engineering targeted viral vectors for gene therapy. *Nat. Rev. Genet.* **8**:573-587.
198. **Wang, L., J. Xie, and P. G. Schultz.** 2006. Expanding The Genetic Code. *Annu. Rev. Biophys. Biomol. Str.* **35**:225-249.
199. **Wang, Z., K. Park, F. Comer, L. C. Hsieh-Wilson, C. D. Saudek, and G. W. Hart.** 2009. Site-Specific GlcNAcylation of Human Erythrocyte Proteins. *Diabetes* **58**:309-317.
200. **Wang, Z., N. D. Udeshi, M. O'Malley, J. Shabanowitz, D. F. Hunt, and G. W. Hart.** 2010. Enrichment and Site Mapping of O-Linked N-Acetylglucosamine by a Combination of Chemical/Enzymatic Tagging, Photochemical Cleavage, and Electron Transfer Dissociation Mass Spectrometry. *Mol. Cell. Prot.* **9**:153-160.
201. **Wang, Z., N. D. Udeshi, C. Slawson, P. D. Compton, K. Sakabe, W. D. Cheung, J. Shabanowitz, D. F. Hunt, and G. W. Hart.** 2010. Extensive Crosstalk Between O-GlcNAcylation and Phosphorylation Regulates Cytokinesis. *Sci. Signal.* **3**:ra2-.
202. **Wickham, T. J., E. Tzeng, L. L. Shears, 2nd, P. W. Roelvink, Y. Li, G. M. Lee, D. E. Brough, A. Lizonova, and I. Kovesdi.** 1997. Increased in vitro and in vivo gene transfer by adenovirus vectors containing chimeric fiber proteins. *J. Virol.* **71**:8221-8229.

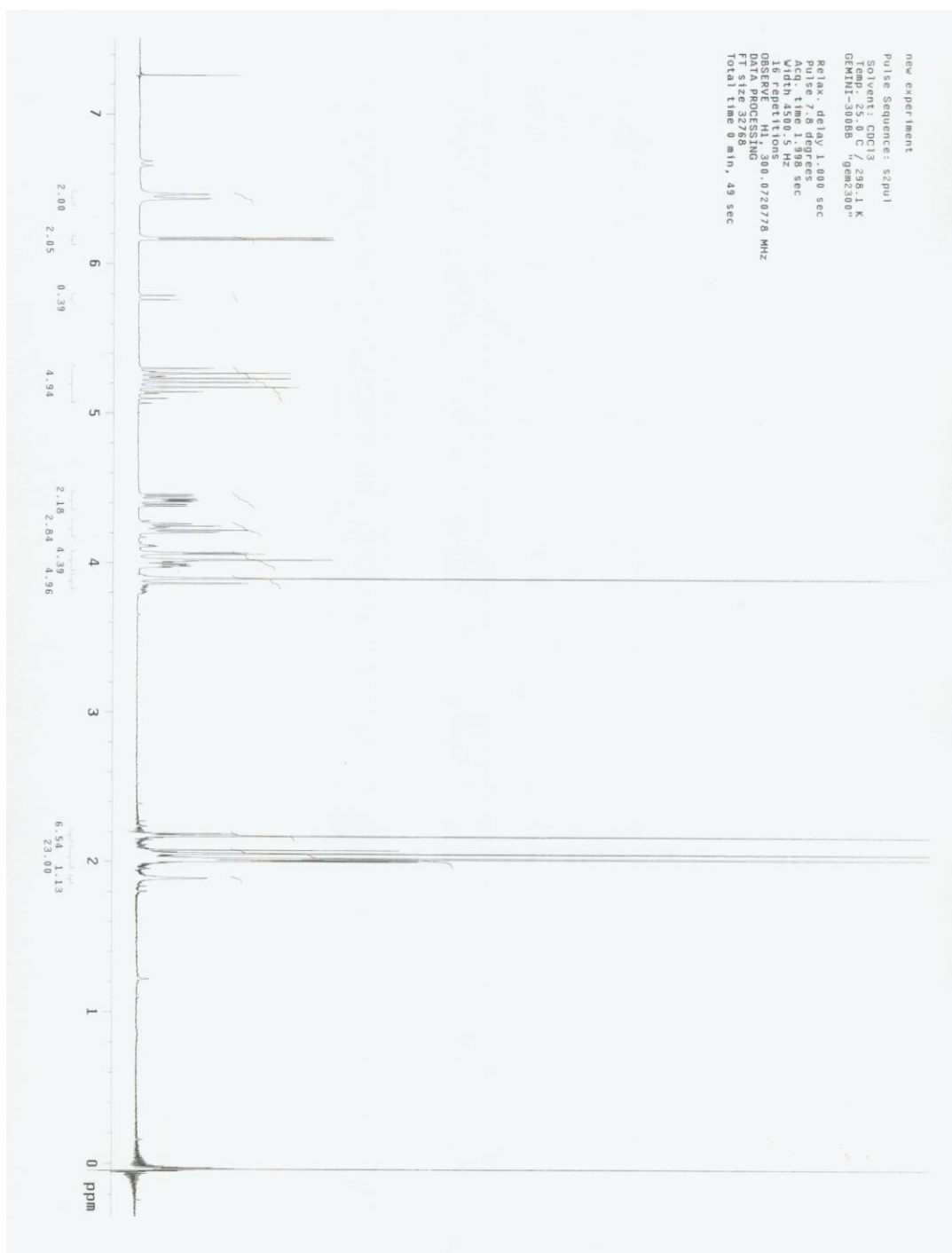
203. **Williams, D. A., and C. Baum.** 2003. MEDICINE: Gene Therapy--New Challenges Ahead. *Science* **302**:400-401.
204. **Wojciechowski, F., and C. J. Leumann.** 2011. Alternative DNA base-pairs: from efforts to expand the genetic code to potential material applications. *Chem. Soc. Rev.*
205. **Wu, E., L. Pache, D. J. Von Seggern, T.-M. Mullen, Y. Mityas, P. L. Stewart, and G. R. Nemerow.** 2003. Flexibility of the Adenovirus Fiber Is Required for Efficient Receptor Interaction. *J. Virol.* **77**:7225-7235.
206. **Wu, H., and D. T. Curiel.** 2008. Fiber-modified Adenoviruses for Targeted Gene Therapy, p. 113-132, *Gene Therapy Protocols*.
207. **Xia, W., and P. S. Low.** 2010. Folate-Targeted Therapies for Cancer. *J. Med. Chem.* **53**:6811-6824.
208. **Yamaguchi, H., C. T. Chen, C. K. Chou, A. Pal, W. Bornmann, G. N. Hortobagyi, and M. C. Hung.** 2010. Adenovirus 5 E1A enhances histone deacetylase inhibitors-induced apoptosis through Egr-1-mediated Bim upregulation. *Oncogene* **29**:5619-5629.
209. **Yamamoto, M., and D. T. Curiel.** 2009. Current Issues and Future Directions of Oncolytic Adenoviruses. *Mol. Ther.* **18**:243-250.
210. **Yarema, K. J., L. K. Mahal, R. E. Bruehl, E. C. Rodriguez, and C. R. Bertozzi.** 1998. Metabolic Delivery of Ketone Groups to Sialic Acid Residues. *J. Biol. Chem.* **273**:31168-31179.
211. **Young, T. S., and P. G. Schultz.** 2010. Beyond the Canonical 20 Amino Acids: Expanding the Genetic Lexicon. *J. Biol. Chem.* **285**:11039-11044.

212. **Yu, D. C., Y. Chen, J. Dilley, Y. H. Li, M. Embry, H. Zhang, N. Nguyen, P. Amin, J. Oh, and D. R. Henderson.** 2001. Antitumor synergy of CV787, a prostate cancer-specific adenovirus, and paclitaxel and docetaxel. *Cancer Research* **61**:517-525.
213. **Zaro, B. W., Y.-Y. Yang, H. C. Hang, and M. R. Pratt.** 2011. Chemical reporters for fluorescent detection and identification of O-GlcNAc-modified proteins reveal glycosylation of the ubiquitin ligase NEDD4-1. *Proc. Natl. Acad. Sci. USA* **108**:8146-8151.
214. **Zeidan, Q., Z. Wang, A. De Maio, and G. W. Hart.** 2010. O-GlcNAc Cycling Enzymes Associate with the Translational Machinery and Modify Core Ribosomal Proteins. *Mol. Biol. Cell* **21**:1922-1936.
215. **Zhang, J., N. Ramesh, Y. Chen, Y. H. Li, J. Dilley, P. Working, and D. C. Yu.** 2002. Identification of human uroplakin II promoter and its use in the construction of CG8840, a urothelium-specific adenovirus variant that eliminates established bladder tumors in combination with docetaxel. *Cancer Research* **62**:3743-3750.

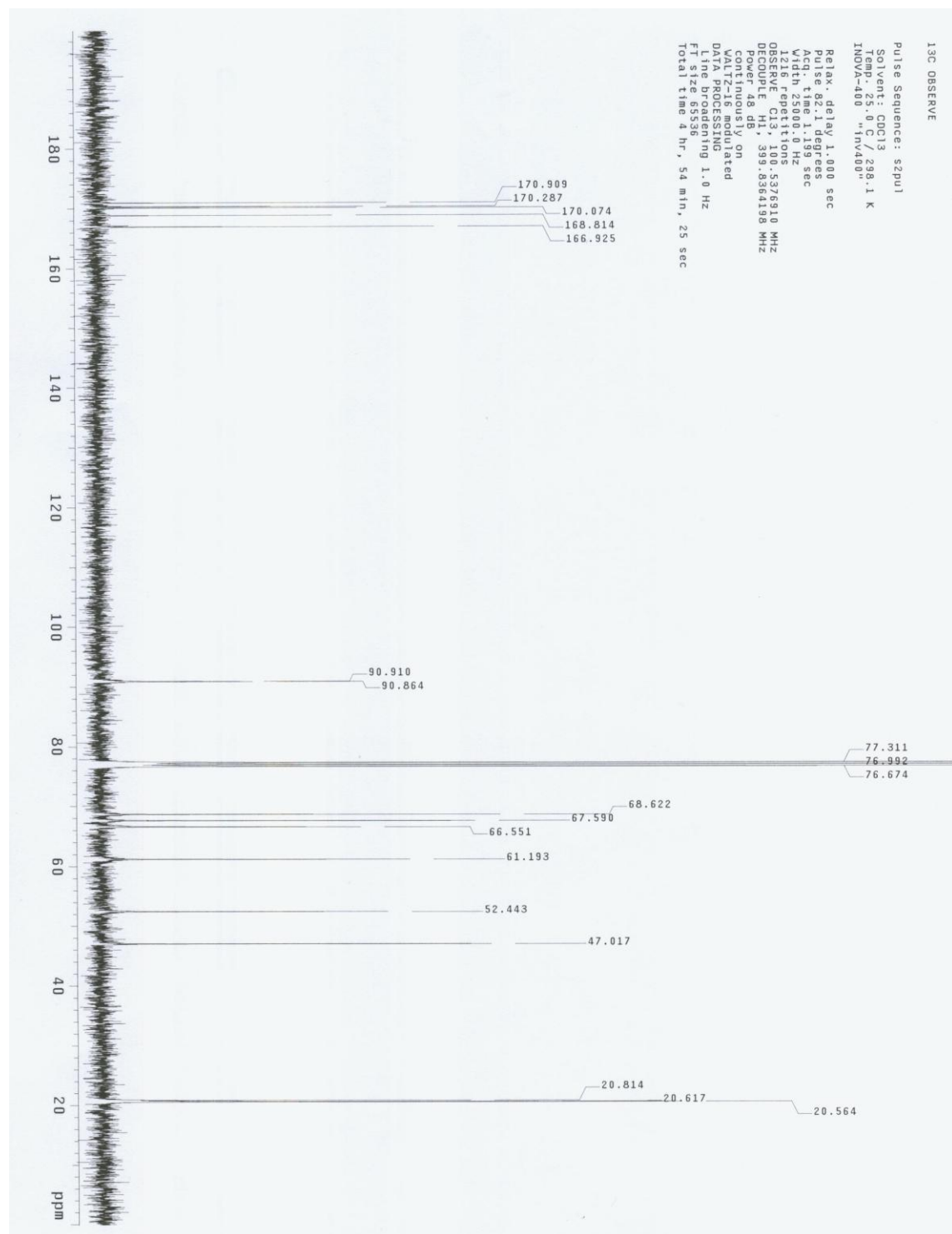
Appendix



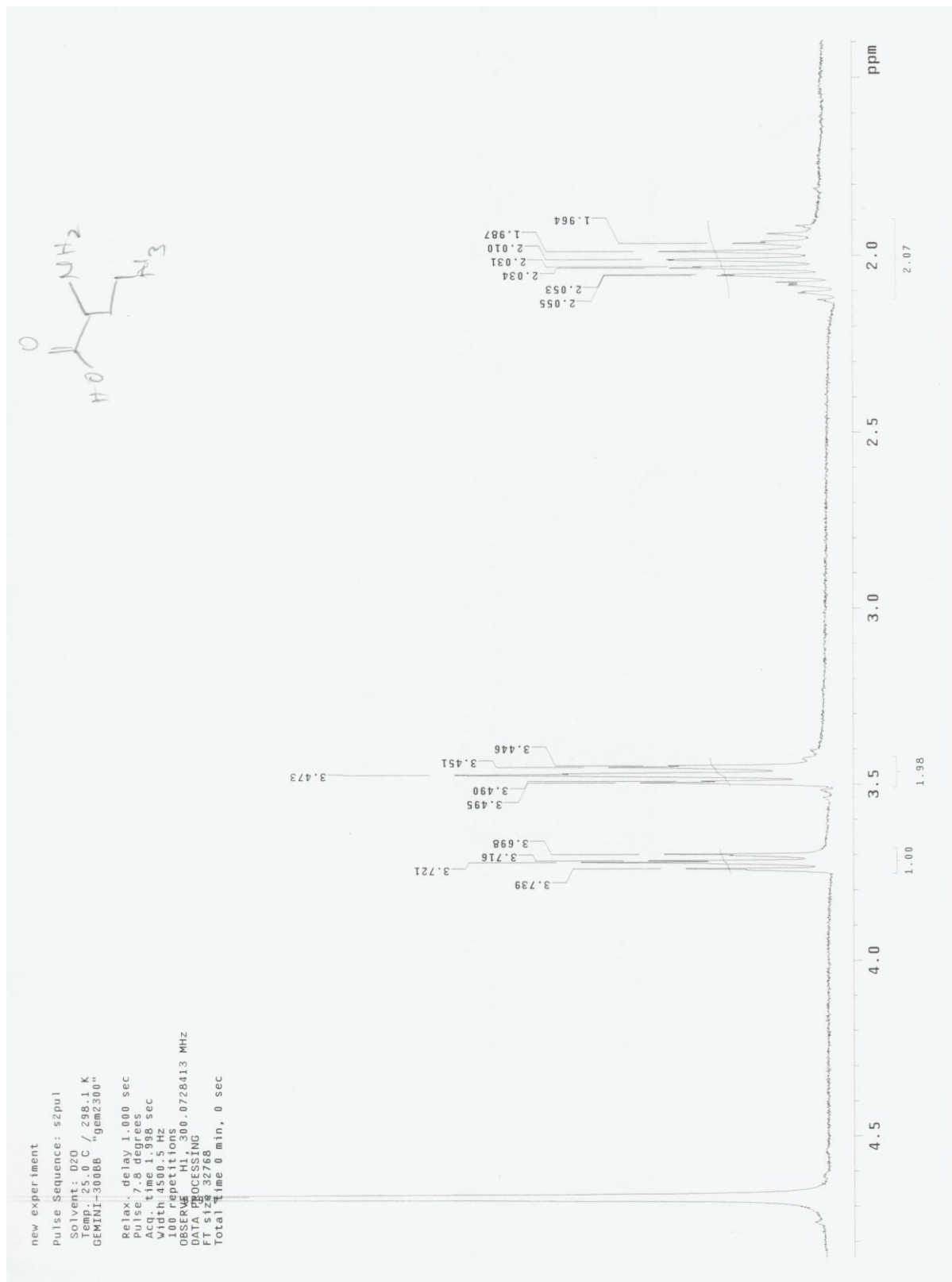
¹H NMR Spectra of N-azidoacetylgalactosamine



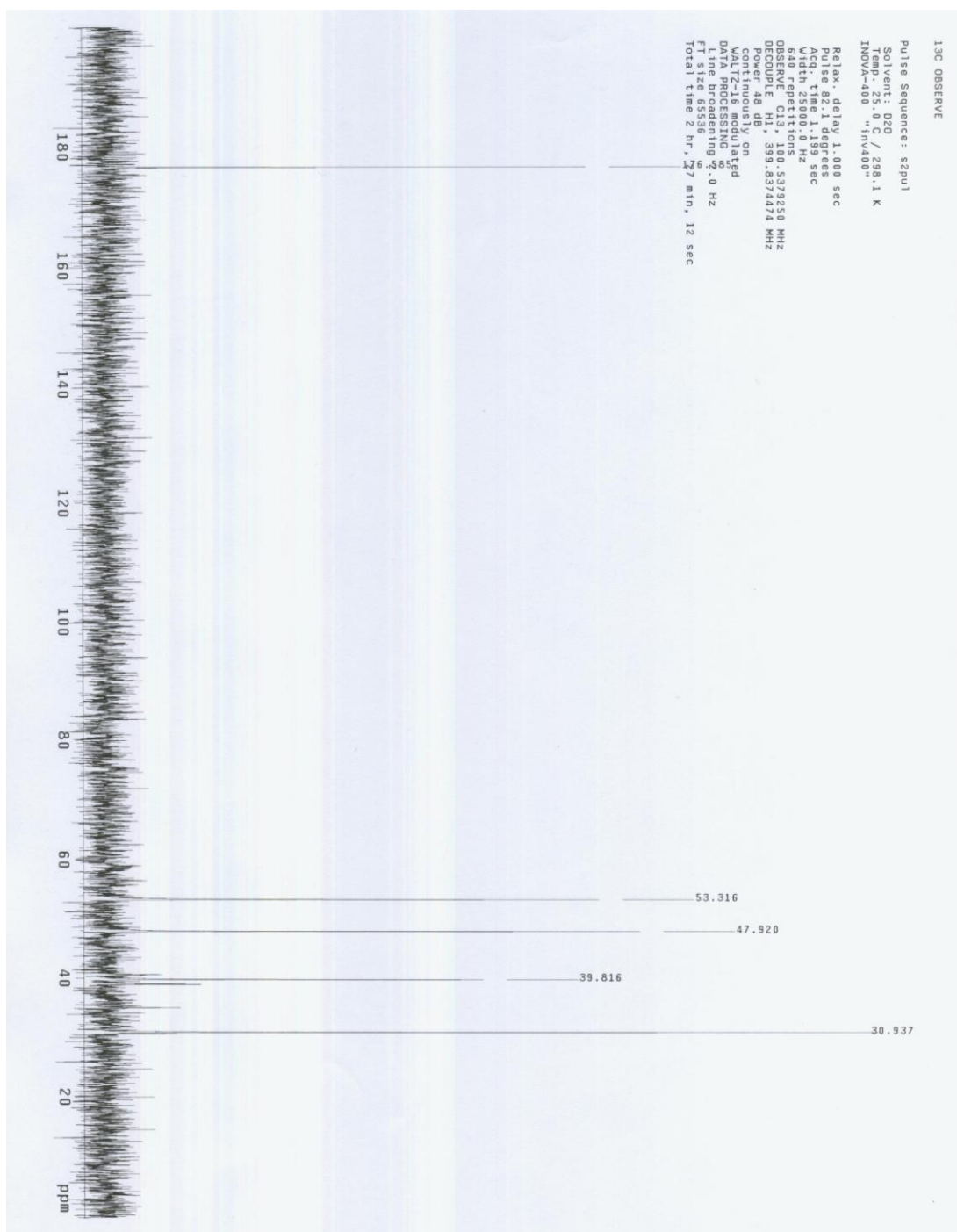
¹H NMR Spectra of 1,3,4,6-tetra-O-acetyl-N-azidoacetyl- α,β -D-galactosamine (per acetylated GalNAz)



^{13}C Spectra of 1,3,4,6-tetra-O-acetyl-N-azidoacetyl- α,β -D-galactosamine (per acetylated GalNAz)

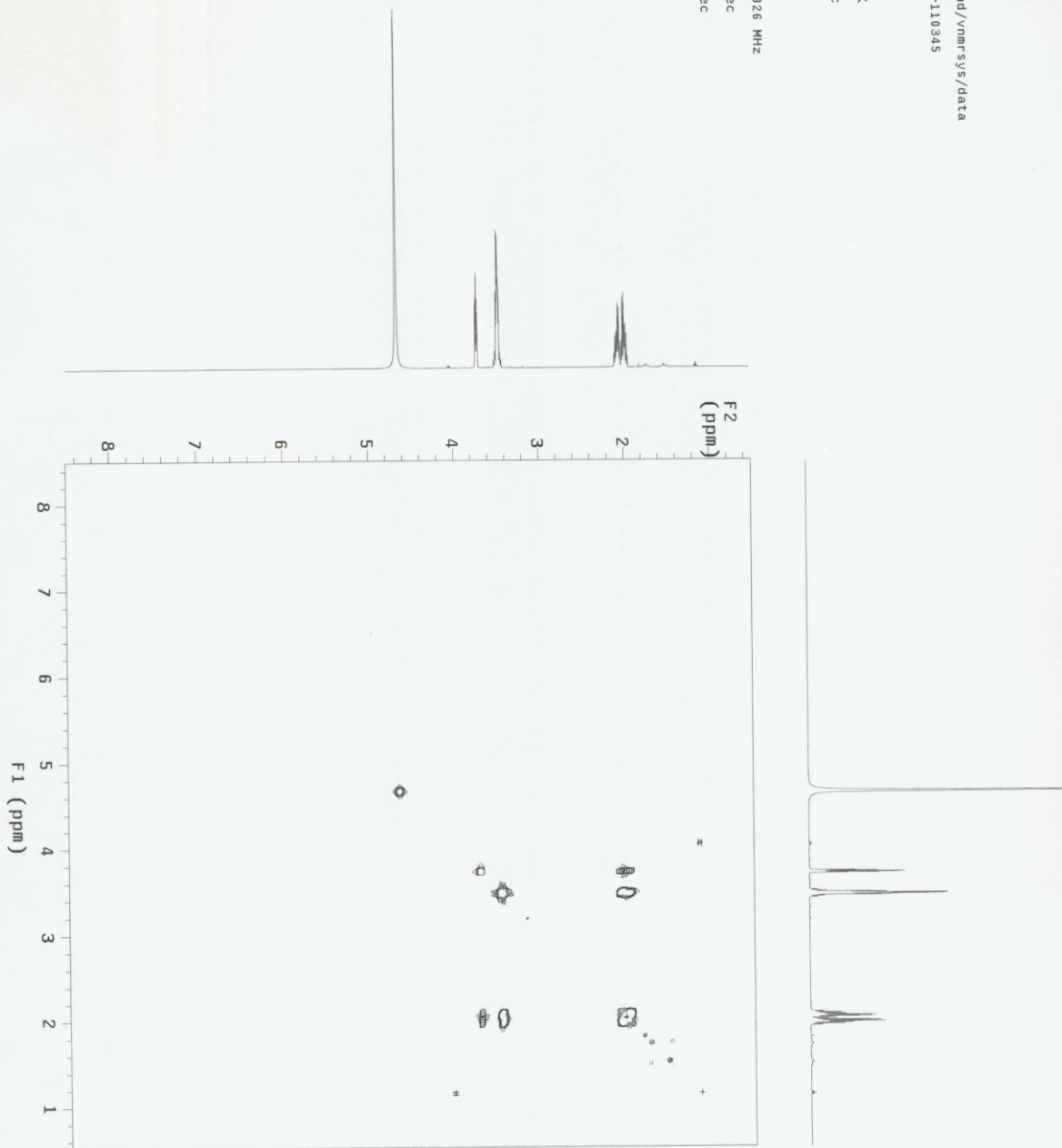


¹H NMR Spectra of Azidohomoalanine

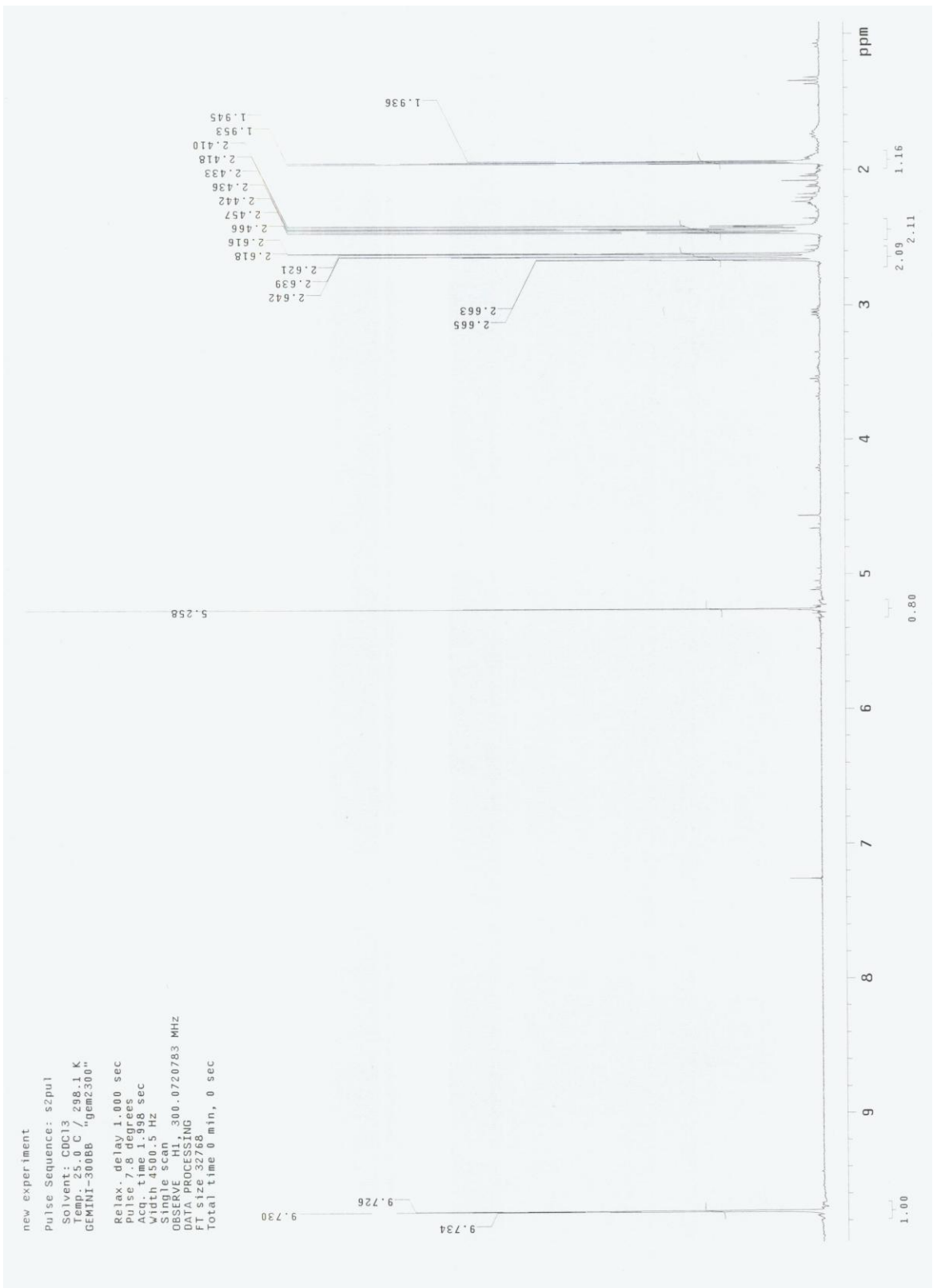


¹³C Spectra of azidohomoalanine

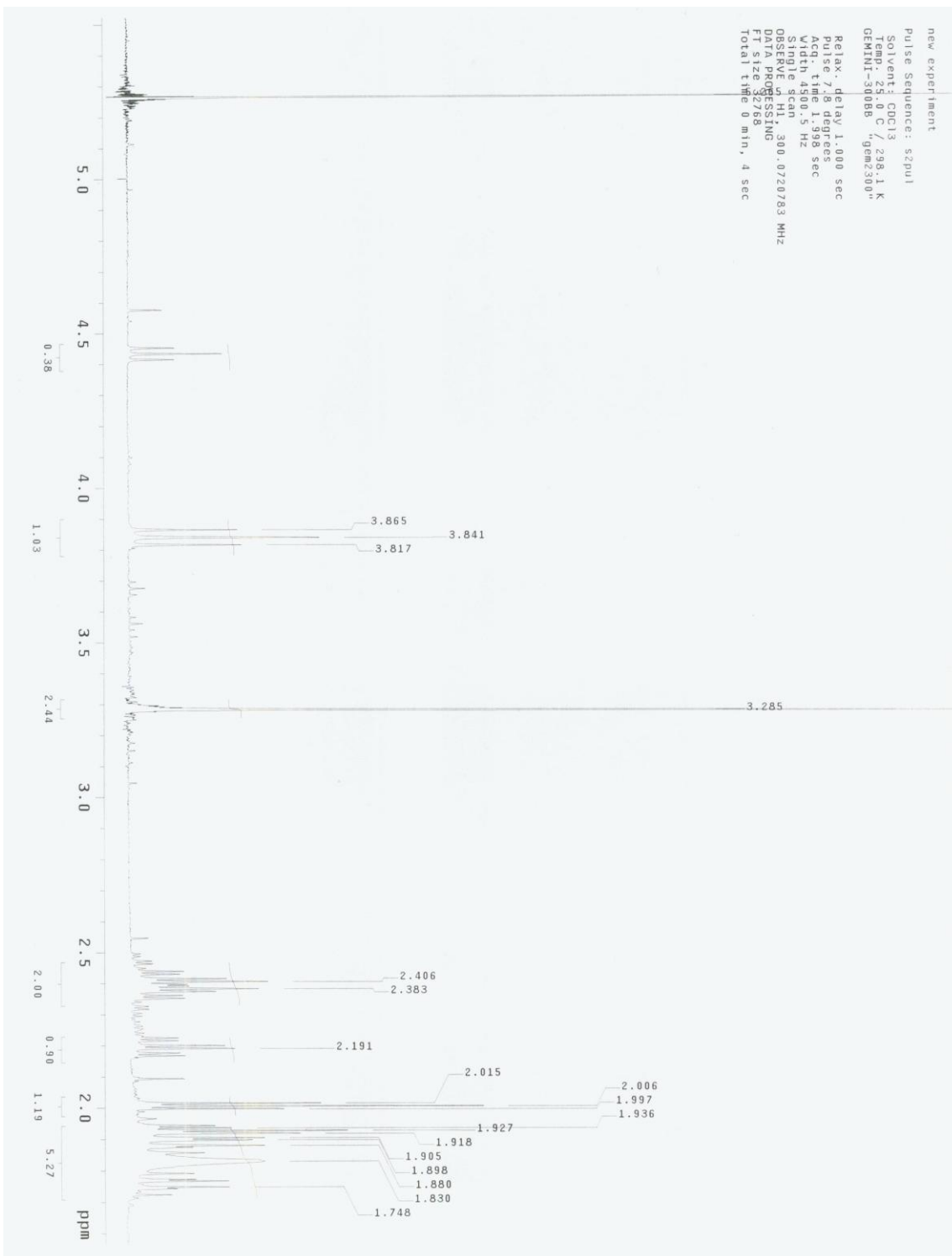
Data collected on:
inv500-inoava500
Archive directory:
/export/home/mfermand/vnmr/sys/data
Sample directory: 7-12-110945
mfermand_2007-07-12-110945
F1 file: gCOSY_01
Pulse Sequence: gCOSY
Solvent: D2O
Temp.: 25.0 C / 298.1 K
Relax. delay: 1.000 sec
Acq. time: 15.0 sec
Width: 3999.2 Hz
2D Width: 3999.2 Hz
4 repetitions
128 increments
OBSERVE H1, 499.8960928 MHz
DATA PROCESSING
Sq. sine bell 0.075 sec
F1 DATA PROCESSING
Sq. sine bell 1.024
F2 128 x 1024
Total time 10 min



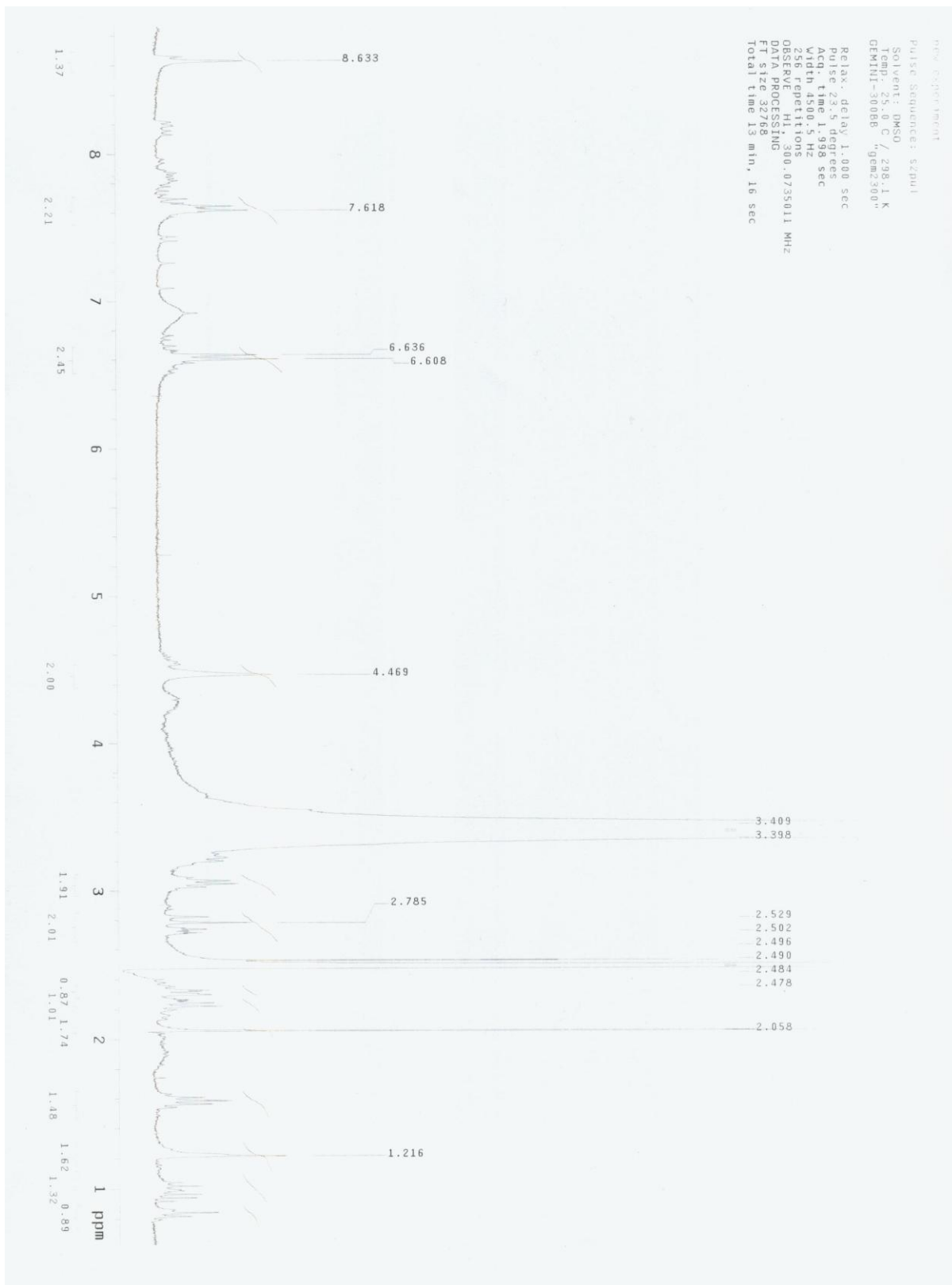
2D COSY Spectra of Azidohomoalanine



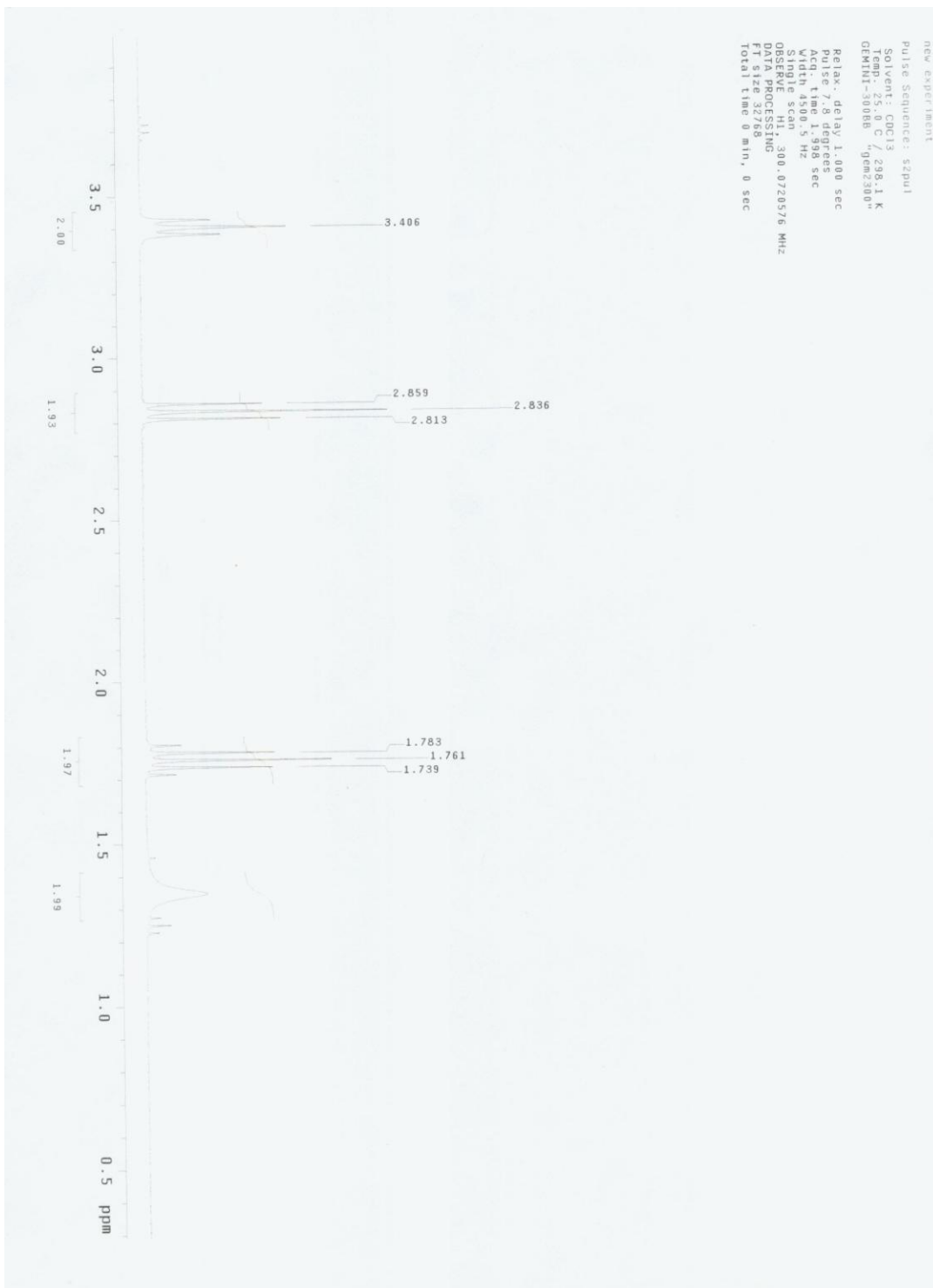
¹H NMR Spectra of 4-Pentynal



^1H NMR Spectra of Homopropargylglycine



¹H NMR Spectra of Alkyne-PEG-folate



^1H NMR Spectra of 3-azido-1-amino propane

Sequence Homology of Ad5 and Ad2 fiber proteins

```

Ad5 1 MKRARPSEDTFNPVYPYDTETGPPTVPFLTPPFVSPNGFQESPPGVLSLRLSEPLVTSNG 60
Ad2 1 MKRARPSEDTFNPVYPYDTETGPPTVPFLTPPFVSPNGFQESPPGVLSLRVSEPLDTSHG 60

Ad5 61 MLALKMGNGLSLDEAGNLTSQNVTTVSPPLKKTksNINLEISAPLTVTSEALTVAAAAPL 120
Ad2 61 MLALKMGSGLTLDKAGNLTSQNVTTVTQPLKKTksNISLDTSAPLITISGALTVATTAPL 120

Ad5 121 MVAGNTLTMQSQAPLTVHDSKLSIATQGPLTVSEGKLALQTSGLPLTTTDSSTLTITASPP 180
Ad2 121 IVTSGALSVQSQAPLTVQDSKLSIATKGPITVSDGKLALQTSAPLSGSDSDTLTVTASPP 180

Ad5 181 LTTATGSLGIDLKEPIYTQNGKLGKYGAPLHVTDLNTLTVATGPGVTINNTSLQTKVT 240
Ad2 181 LTTATGSLGINMEDPIYVNNKGIGIKISGPLQVAQNSDTLTVVTGPGVTVEQNSLRTKVA 240

Ad5 241 GALGFDSQGNMQLNVAGGLRIDSQNRRLILDVSYPFDAQNQLNLRGQGPLFINSAHNLD 300
Ad2 241 GAIGYDSSNMMEIKTGGGMRIN--NLLILDVDYPFDAQTKLRLKLGQGPLYINASHNLD 298

Ad5 301 INYNKGLYLFTASNNSKKLEVNLSAKGLMFDATAIAINAGDGLEF--GSLNAPNSNPLK 358
Ad2 299 INYNRGLYLFNASNNTKKLEVS IKKSSGLNFDNTAIAINAGKGLEFDTNTSESPDINPIK 358

Ad5 359 TKIGHGLEFDSNKAMVVKLGTGLSFDSTGAITVGNKNDKLT LWTPAPSPNCRLNAEKD 418
Ad2 359 TKIGSGIDYNENGAMITKLGAGLSFDNSGAITIGNKNDKLT LWTPDPSPNCRIHSDND 418

Ad5 419 AKLTLVLTKCGSQILATVSVLAVKGLAPISGTVQSAHLIIRFDENGVLNNSFLDPEYW 478
Ad2 419 CKFTLVLTKCGSQVLATVAALAVSGDLSSMTGTVASVSI FLRFDQNGVLMENSSLKHHY 478

Ad5 479 NFRNGDLTEGTAYTNAVGFMPNLSAYPKSHGKTAKSNIVSQVYLNKDGTKPVTLTITLNG 538
Ad2 479 NFRNGNSTNANPYTNAVGFMPNLLAYPKTQSQTAKNNIVSQVYLHGDGTKPMILTITLNG 538

Ad5 539 TQETGDTTP-SAYMSFSWDWSGHNYINEIFATSSYTF SYIAQE 581
Ad2 539 TSESTETSEVSTYSMSFTWSWESGKYTTETFATNSYTF SYIAQE 582

```

Identities = 405/584 (69%), Positives = 486/584 (83%), Gaps = 5/584 (1%)

Sequence homology of Ad5 and Ad2 fiber proteins. Conserved methionines are

highlighted. Unexposed: **turquoise**; exposed: **green**; no information: **pink**